Numerical Analysis of Optical Feedback Noise and Its Reduction in Semiconductor Lasers

Sazzad Muhammad Samaun Imran

July 2013

Doctoral Dissertation

Numerical Analysis of Optical Feedback Noise and Its Reduction in Semiconductor Lasers

Graduate School of
Natural Science & Technology
Kanazawa University

Major Subject: Division of Electrical Engineering
and Computer Science

Course: Electronic Science

School Registration No.: 1023112108

Name: Sazzad Muhammad Samaun Imran

Chief Advisor: Professor Minoru Yamada

Abstract

Semiconductor lasers play a central role in the growing world of optoelectronic technologies. A measure of the importance of this emerging optoelectronic technology is provided by the optical disc players, laser printers and the optical fiber communication system. But semiconductor lasers tend to be suffered by the optical feedback (OFB) noise caused by reflection of the output light at surface of the optical disc or the optical fiber. Hence, it is required to reveal the lower noise for the higher performance. This dissertation shows numerical simulations on the phenomena of the OFB noise, its suppression by the superposition of high frequency (HF) current and the condition at which the HF current is unable to suppress the noise.

We present an improved theoretical model to analyze dynamics and operation of semiconductor lasers under optical feedback. The model is based on a set of multimode rate equations in which the self and mutual gain saturation effects among lasing modes, re-injection of delayed feedback light reflected at surface of connecting optical device and Langevin noise sources for the intensity, phase and carrier fluctuations are taken into account. The proposed model is applied to 850nm GaAs lasers operating under optical feedback. Temporal variations of photon numbers, optical phases and electron density are traced by numerical calculation, and frequency spectra of intensity noise are determined by help of the fast Fourier transformation. Characteristics of the OFB noise are expressed in terms of the relative intensity noise (RIN).

The intensity noise of the semiconductor lasers consists of the quantum noise and the optical feedback noise. The quantum noise is generated by intrinsic property of the quantum mechanical fluctuation of the laser and very difficult to control in principle. On the other hand, numerical simulations based on our theoretical model confirmed that the OFB noise is classified into two types based on profiles of the frequency spectrum, where one is the low frequency type and another is the flat type. The low frequency type noise must be caused by the mode competition among the lasing modes in the solitary laser, and the flat type noise by the phase distortion between the internal reflected light and the external feedbacked light.

The output noise level of the laser is increased by 20dB or more as a result of the optical feedback and this excess noise degrades performance of the system. Superposition of high frequency current is used in this dissertation as a technique to suppress the OFB noise. The OFB noise is well suppressed by suitable selections of frequency and amplitude of the superposed current. The HF current modulates both electron number and photon number which works to change the operating state of the lasers from bi-stable to monostable, and stop mode hopping resulting in suppression of the OFB noise.

However, this technique is not effective when frequency of the HF current coincides with a rational number of the round trip time for the OFB. In that case, modulations of the electron number and the photon number are suppressed by the phase locking effect with undesirable phase relation and thus, the noise suppression effect does not work under this condition.

Generating mechanism of the optical feedback noise and its suppression by the superposition of high frequency current are explained in this dissertation with approximated but analytical equations. Excellent correspondence between previously obtained experimental data and simulation is also demonstrated.

Acknowledgement

All praises are for the One above all of us, the omnipresent God, for giving me the strength and courage and all the opportunities to finish my PhD successfully.

This dissertation would not have been possible without the guidance and the help of several individuals who in one way or another contributed and extended their valuable assistance in the preparation and completion of this study.

First and foremost, I would like to express the deepest appreciation to my chief advisor Professor Minoru Yamada for the continuous support of my PhD study and research, for his patience, motivation, enthusiasm and immense knowledge in semiconductor lasers, quantum physics, semiconductor optical amplifiers and many others. His guidance helped me in all the time of research and writing of this dissertation and other sub-theses. I could not have imagined having a better advisor and mentor for my PhD study.

Besides my chief advisor, I would like to thank Associate Professor Yuji Kuwamura for enlightening me some important parts of my research and the rest of my dissertation committee for their encouragement, insightful comments and wise questions.

I thank my fellow labmates in Optical Communication Lab, Kanazawa University for their useful discussion and helps, and for all the fun we have had in the last three years. I am also grateful to all my friends in Kanzawa or elsewhere in the world for their moral support and valuable advice without which it would be difficult for me to successfully finish my PhD study.

I also wish to thank all the support staffs of Kanazawa University for their sympathetic help in secretarial works during my staying in Japan.

I owe my loving thanks and sincere gratitude to all my family members and relatives, especially to my parents for supporting me throughout my life and the hardships they go through due to my research abroad.

I gratefully remember the administrative and moral support from my colleagues, students and staffs at the University of Dhaka, my parent organization in Bangladesh.

Lastly, the financial support of the Japanese Government through MEXT Scholarship is gratefully acknowledged.

List of Related Publications

The following papers are already published in journals and serve as the basis for this PhD dissertation.

[1] **S.M.S. Imran**, M. Yamada and Y. Kuwamura, "Theoretical analysis of the optical feedback noise based on multimode model of semiconductor lasers", IEEE J. Quantum Electron., vol. 48, issue 4, pp. 521-527, April 2012.

[2] **S.M.S. Imran** and M. Yamada, "Numerical analysis of suppression effects on optical feedback noise by superposition of high frequency current in semiconductor lasers", IEEE J. Quantum Electron., vol. 49, no. 2, pp. 196-204, February 2013.

Author of this dissertation has attended in the following international conferences and symposiums, and presented and shared there some research findings related to this PhD study.

[1] **S.M.S. Imran**, M. Yamada and Y. Kuwamura, "A theoretical analysis of the optical feedback noise based on multimode model of semiconductor lasers", PIERS Abstracts, Progress In Electromagnetics Research Symposium, pp. 604-605, 19-23 August 2012, Moscow, Russia.

[2] **S.M.S. Imran** and M. Yamada, "Numerical analysis of the noise reduction effect by superposition of high frequency current in semiconductor lasers", CLEO-PR & OECC/PS 2013, 30 June – 4 July, 2013, Kyoto International Conference Center, Kyoto, Japan. (Accepted)

Author has also presented the research data in the following domestic/ local conferences and symposiums.

[1] **S.M.S. Imran**, M. Yamada and Y. Kuwamura, "Theoretical analysis of the optical feedback noise based on multimode model of semiconductor lasers", Extended Abstract, The 34th International Symposium on Optical Communications, pp. 87, 21-23 August 2011, Kanazawa, Japan.

[2] **S.M.S. Imran**, M. Yamada and Y. Kuwamura, "An analysis of the optical feedback noise based on multimode model of semiconductor lasers", Speech 16p-F3-9, DVD 05-019, pp. 53, 59th Spring Meeting (annual conference/meeting of JSAP), 15-18 March 2012, Waseda University, Tokyo, Japan.

[3] **S.M.S. Imran** and M. Yamada, "Analysis of the optical feedback noise in semiconductor lasers under superposition of high frequency current", Extended Abstracts, The 35th International Symposium on Optical Communications 2012, pp. 36, 06-08 August 2012, Fujiyoshida, Japan.

[4] **S.M.S. Imran** and M. Yamada, "Numerical analysis of suppression effects on optical feedback noise by superposition of high frequency current in semiconductor lasers", Speech 29p-B4-14, DVD 05-030, pp. 51, 60th Spring Meeting (annual conference/meeting of JSAP), 27-30 March 2013, Kanagawa Institute of Technology, Tokyo, Japan.

[5] **S.M.S. Imran** and M. Yamada, "An analysis of noise reduction effect by superposition of high frequency current in semiconductor lasers", IEICE Technical Report, LQE2013-1 (2013-5), vol. 113, no. 49, pp. 1-6, 17 May 2013, Kanazawa University, Ishikawa, Japan.

List of Figures

Index

Chapter I: Introduction

Semiconductor laser was first invented in 1962 by Robert N. Hall [1]. Since then this is being used as principle device in all optical disc players, laser printers and most optical fiber communication systems. It is well known that optical feedback creates excess noise in semiconductor lasers. A variety of dynamical behaviors can be observed in semiconductor lasers with optical feedback and they have been investigated by many researchers for last three decades. In this context, this chapter reviews some major research articles on optical feedback noise in semiconductor lasers to briefly describe the progresses in this field. After that the significance of this PhD study is explained in succession with the previous research activities. Finally, outline of this dissertation is described.

1. Literature Review

M. Yamada and Y. Suematsu in their paper [2] discuss theoretically the condition for single longitudinal mode operation (SMO) of index guided semiconductor injection laser and a comparison with the experiment is done. Effects of the impurity concentration and the intraband relaxation, the spontaneous emission and the thermal resistance on longitudinal mode behavior are discussed. The conditions summarized for the SMO for GaAs lasers are: the dimension of the index-guiding waveguide must be set to cut off the higher order transverse modes; the spontaneous emission factor must be suppressed by decreasing the energy confinement in the active region; and the thermal resistance should be reduced to increase the stability of SMO at a fixed mode.

R. Lang and K. Kobayashi examine the influences of the externally reflected light on the static and dynamic behaviors of semiconductor laser [3]. Experimental observations with a GaAs/AlGaAs single mode laser are also presented with analysis based on a compound cavity laser model. It is demonstrated that the external feedback can make the injection laser multistable and cause hysteresis phenomena. It is reported that the multistability can show up more easily in semiconductor laser than in other lasers because of the strong dependence of the refractive index of the laser active region on the carrier density. The dynamic properties of semiconductor lasers are found to be affected by the interference effects in the compound cavity.

M. Yamada and Y. Suematsu analyze the gain suppression in injection lasers by taking into account the phase-synchronization effect, the intraband relaxation process and spatial diffusion of carriers [4]. They find that the excess gain suppression and the hysteresis phenomena are observable in lasers which have an undoped active region and well-designed index guiding structures. But the excess gain suppression is scarcely observed in lasers which have a heavily doped active region. Single longitudinal mode operation is not obtained in a strongly inhomogeneous laser in which the relaxation time is larger than $3x10^{-13}$

sec for strong nonuniformity across the spectral or energy distributions and the gain of some resonating modes is increased. When the relaxation time is smaller than $2x10^{-13}$ sec, the gain can be seen to be nearly homogeneous and the gain of nonoscillating modes is sufficiently suppressed because of the strong mode coupling effect. The authors also report from [5] that the gain of nonoscillating modes is suppressed more strongly than the oscillating mode in the lightly doped lasers.

Quantum noise in semiconductor lasers is one of the most important problems to be encountered in their applications. Y. Yamamoto in [6] describes quantum noise properties for semiconductor lasers through the use of four different theoretical formulations: the van der Pol equation; the Fokker-Planck equation; the rate equation; and the photon density matrix master equation. Theoretical formulations for AM noise (or intensity fluctuation) spectrum, photon number probability density, FM noise spectrum, instantaneous frequency probability density and power spectrum, that represent quantum noise characteristics for lasers, are derived. Formulas for the AM and FM noise spectra presented in this paper enable calculation of the signal-to-noise ratio and carrier-to-noise ratio degradation due to quantum noise. The paper clarifies that spontaneous emission coupled to a lasing mode is a direct origin of quantum noise.

In 1983 K. Vahala and A. Yariv present a semiclassical analysis of semiconductor laser noise which includes the carrier density as a dynamical variable and the carrier density dependence of the refractive index [7]. The treatment considers the effect of relaxation resonance in the power fluctuations spectrum of semiconductor lasers on the frequency fluctuations spectrum and field spectrum. Fluctuations of the field and the carrier density are driven by normalized Langevin forces. The authors investigate that carrier number fluctuations in the field spectrum result from the interactions of the carriers in the active region with other systems of particles. However, this analysis does not predict field spectrum linewidth broadening due to carrier number fluctuation in the active region.

The understanding of optical mode behavior and control of the oscillating mode in semiconductor injection lasers is a complicated but important problem for practical application of these devices. M. Yamada in [8] analyzes the oscillating transverse modes and longitudinal modes behavior based on the semiclassical method in which optical field is presented by Maxwell's equations and the lasing phenomenon is analyzed quantum mechanically using the density matrix formalism. This theoretical approach has been shown to provide excellent agreement for both small signal and saturated gain characteristics of these lasers for both lightly doped and p-type active regions without requiring the assumption of band tail states or violation of wavenumber conservation for optical transitions. The author also postulates the possibility of obtaining single longitudinal mode operation by utilization of the strong coupling effect when the transverse mode is well controlled by the laser stripe

structure. Some experimental results are also given in this paper to support his analyses.

K. Stubkjaer and M.B. Small experimentally investigate the feedback induced noise in index guided semiconductor lasers and report a reduction in feedback noise of 15-20 dB by direct modulation of the laser [9]. Excess noise is mainly caused by mode jumping which results from variations in the amplitude and phase of the reflected signal.

P. Spano *et al.* derive analytical expressions for the power spectral densities of intensity and frequency noise of single mode semiconductor laser in the presence of optical feedback [10]. They include gain and refractive index variation in the active layer due to any spontaneous emission process. They prove that the maximum attainable reduction of the low frequency part of the frequency noise spectrum, which is responsible for the linewidth, is independent from the linewidth enhancement factor. Furthermore, the use of a short external cavity causes a flattering of the frequency noise spectrum and a lowering of its amplitude as compared to that of the solitary laser.

K.E. Stubkjaer and M.B. Small in [11] present an experimental analysis of noise due to feedback into the semiconductor laser. The mechanism for noise reduction by current modulation is also demonstrated. The analysis includes the dependency of noise on output power level, proportion of the reflected light returned to the laser, external cavity length and modulation level. A noise reduction of as much as 20 dB is obtained by direct modulation of the laser in the frequency range of 50-200 MHz. They show that this reduction is correlated with the frequency modulation of the light output.

D. Marcuse in his first paper of a series devoted to theoretical studies of photon fluctuation in the light output of semiconductor injection lasers introduces the noise driven rate equations for a single-cavity laser, explains the method used for their numerical solution and discusses some approximate analytical results [12]. He outlines the derivation of the rate equations based on the theory of Langevin laser equations and collects the background material required for performing a computer simulation of the properties multimode, single-cavity lasers.

In [13] A. Ohishi *et al.* present a method of noise reduction by high-frequency (HF) superposition in single mode lasers. By this method, lasers show stable noise characteristics against ambient temperature variation or OFB. They develop a small packaged HF current source and apply to optical disc systems to suppress the excess noise induced by optical feedback.

Semiconductor injection lasers typically show mode hopping noise which accompanies unstable hopping phenomena among the oscillating longitudinal modes. In [14] M. Yamada theoretically analyzes the characteristics of the mode competition noise with the help of a perturbation approach. The source of the noise is supposed to be

fluctuations of the number of photons and electrons on optical emission and is amplified by optical gain. The noise becomes strongest when the lasing mode jump to another mode and the noise of total output power reduces when the laser is in pure single-mode operation or in stable multimode operation.

In [15] N. Schunk and K. Petermann estimate the effect of external feedback on a single-mode semiconductor laser by a numerical solution of the nonlinear rate equations. They distinguish three feedback regimes: in a regime I with low feedback the linewidth is broadened or narrowed depending on the feedback phase; in regime II with increasing feedback the laser locks to the mode with the maximum linewidth reduction; and in regime III the linewidth is drastically broadened which is also denoted as the coherence-collapse regime.

Dynamic equations for the injected carrier density and optical field are derived by M. Yamada based on density matrix formalism taking into account the nonlinear optical phenomena in semiconductor lasers [16]. Two kinds of nonlinear phenomena mentioned are – the beating vibration on spectral distribution of the injected carriers whose frequency range is limited by the intraband relaxation time, and the beating vibration of the injected carrier density whose frequency range is limited by the electron lifetime for band to band transition. The effects of these two phenomena on the saturated gain profile under a single-mode oscillation are derived which reveals the existence of an asymmetric property of the gain suppression effect.

M. Yamada and T. Higashi theoretically analyze, with support of experimental measurement, the mechanism of noise reduction method by superposition of high frequency (HF) current on the injection current based on mode competition theory in semiconductor injection laser [17]. The authors believe that multimode operation is not an essential condition to be free from the mode hopping phenomena. The results obtained are – superposition of HF current works to weaken the mode competition effect, noise reduction is most effective with modulation frequency near the resonance frequency and the noise reduction is more effective in the device having a higher thermal resistance.

Although the technique of high frequency injection (HFI) is popularly used to suppress the feedback induced RIN enhancement, the proper modulation frequency and depth must be chosen empirically. G.R. Gray *et al.* investigate this problem through computer simulations of the multimode stochastic rate equations [18]. They present a rate equation model that is capable of explaining why the RIN is increased and why this intensity noise can be avoided through high frequency injection. The authors conclude that the increase in RIN with OFB arises from deterministic chaos caused by the coupling of the laser to an external cavity and the effectiveness of the HFI technique to keep the RIN at low rests in its ability to suppress or delay the onset of the chaotic regions.

H. Kakiuchida and J. Ohtsubo explain the characteristics of the oscillation of a semiconductor laser in the presence of external optical feedback by the rate equations by considering multiple reflections of light in the external cavity [19]. They introduce the compound cavity model with the fact that the distance of the external reflector from the laser cavity is much smaller than the coherence length. The effects of the compound cavity result in an additional gain factor and a phase change in the rate equations. The oscillation characteristics are strongly dependent on the feedback intensity and the external cavity length. Despite the fact that the authors ignore mode competition in multimode oscillations, the theoretical results agree well with the experimental findings.

K. Petermann in [20] reviews mode-hopping phenomena, strong excess noise and chaotic behavior in the coherence collapse regime occurring in semiconductor lasers by considering short external resonators. The author mainly concentrates on the behavior of lasers due to weak optical feedback. He also gives guidelines for designing semiconductor lasers with high endurance against external optical feedback.

M. Yamada *et al.* and K. Matsuoka *et al.* report experimental evidence of two different types of mode competition phenomena in semiconductor lasers through characteristics on the noise spectrum [21], [22]. One is with competition among the internal cavity modes and the other is with competition among the external cavity modes which are built by the optical feedback. They also experimentally notice two different types of optical feedback noise – one was the low frequency type noise and the other was the flat type noise. However, the paper does not explain details of the operating conditions generating these excess noises.

K.I. Kallimani and M.J. O'Mahony present a study of the noise characteristics of semiconductor lasers with optical feedback and short external cavity length [23]. They use a unified rate equation model that is applied successfully to all the feedback regimes though the paper concentrates mainly on the moderate and strong feedback regimes. The rate equations include noise fluctuations for intensity, phase and carrier density but are only applicable for single mode emission. They conclude that weak feedback does not affect the frequency of relaxation oscillations, but the strong feedback results in significant reduction of the relaxation oscillation frequency.

One of the unstable features of the laser output is that the power drops with the frequency within the range of several to several tens of MHz known as low frequency fluctuations (LFF). Y. Takiguchi *et al.* experimentally investigate this LFF in semiconductor lasers with optical feedback for high frequency injection current modulation [24]. They observe synchronization of the modulation frequency at and very close to the external cavity mode. Low frequency fluctuation is not observed in this state. But the laser output power becomes unstable with an increase or decrease of the detuning from the external cavity mode frequency. LFF tends to be observed with a lower bias injection current.

M. Ahmed *et al.* report in [25] a self-contained numerical model to analyze the intensity and phase noise and broadening of the line shape in semiconductor lasers. A new systematic technique is devised to generate the correlated Langevin noise sources on the photon and carrier numbers as well as on the phase of the lasing field while keeping their auto- and cross-correlations satisfied. The authors examine the contributions of the carrier-number noise source to intensity and phase noise and found that the characteristics in the high-frequency regime are unaffected, while the RIN values are overestimated at low frequencies when the source is ignored.

In 2001 M. Yamada *et al.* report experimental characteristics of the optical feedback noise in semiconductor lasers under superposition of the high frequency (HF) current [26]. The feedback noise is mostly suppressed by superposition of high frequency current, but still remains when frequency of the HF current coincides with a rational number of the time period for the optical feedback. The authors qualitatively analyze such characteristic by the mode competition theory for the external cavity modes. They explain the noise reduction effect as shift of the operating point with the modulated components of the carrier density and photon numbers.

J.S. Lawrence and D.M. Kane reports a systematic experimental investigation into the nonlinear dynamic behavior of a directly modulated diode laser subject to strong external optical feedback as compared to the same laser subject to strong OFB which is phase modulated by an electro-optic modulator in the external cavity [27]. The output state for both types of modulation is dependent on the ratio of the modulation frequency to the external cavity resonant frequency and the modulation power. They observe eight distinct dynamic states, namely, conventional amplitude modulation; multimode – low-noise amplitude modulation; multimode – high-noise amplitude modulation; periodic limit-cycle operation; quasi-periodicity; chaos; low frequency fluctuations; and mode-locking. The modulation instability when induced by increased modulation at a frequency very close to the external cavity resonant frequency is shown to dynamically distinct for direct modulation.

In their paper [28] C. Serrat *et al.* analyze the dynamics and coherence properties of a multimode semiconductor laser with an external cavity of intermediate length by using numerical model of the temporal dynamics in semiconductor lasers. They qualitatively observe that the coherence time is degraded as the laser becomes more multimode. Their study is limited to a value of the injection current as twice the lasing threshold at a particular length of the external cavity.

S.G. Abdulrhmann *et al.* present an improved time-delay model to investigate the influence of strong OFB on the dynamics and operation of semiconductor lasers [29]. The single mode model is versatile and applicable under an arbitrary amount of OFB ranging from weak to very strong. The model considers multiple round trips of the lasing field in the

external cavity but does not consider the Langevin noise sources that induce spontaneous emission fluctuations in dynamics of the lasing modes. They classify the laser operation over wide ranges of the OFB and injection current to continuous wave under very weak optical feedback, chaos under moderate optical feedback and pulsation in the strong regime of OFB.

M. Ahmed and M. Yamada in [30] characterize the spectral line shape and the spectra of the RIN and frequency noise in five distinct operating regions – continuous wave, weak OFB-induced pulsation, period-doubling route-to-chaos, chaos or coherence collapse and strong OFB-induced pulsation. They generalize the simulation model of S.G. Abdulrhmann *et al.* in [29] which treats the optical feedback as a multiple round-trip time delay of the lasing field in the external cavity. However, their study is limited to single-mode model but is considering Langevin noise sources for photon number, phase and carrier density.

Reduction of intensity noise in semiconductor lasers is important subject to extend application range of the device. In 2006, M. Yamada *et al.* experimentally propose a novel scheme to reduce the optical feedback noise and the quantum noise [31]. They reduce the noise of InGaN blue-violet laser under optical feedback by applying electric feedback with is positive type at a high frequency and negative type for lower frequency range. Later the group refers the technique as EPNF (electric positive and negative feedback) method and compares the reduction ability of this method with that of the superposition of high frequency current [32]. They report the superiority of the EPNF method for quantum noise reduction noise due to the electric negative feedback.

In [33] M.C. Soriano *et al.* present their study on the influence of low-frequency current noise on a single-mode semiconductor laser subject to external optical cavity based on Lang-Kobayashi rate equations. The authors experimentally show that extra current noise and delayed optical feedback can modify the dynamical properties of single-mode semiconductor lasers. The modification of the dynamical properties is a linear superposition of the individual effects of the two.

S.M.S. Imran *et al.* analyze dynamics and operation of semiconductor laser under optical feedback based on a set of multimode rate equations for semiconductor lasers that includes nonlinear gain, re-injection of delayed feedback light and Langevin noise sources for the intensity and phase fluctuations [34]. The authors simulate the features of two types of intensity noise – the low frequency type and the flat type. They conclude that the low frequency type noise is caused by the mode hopping between bi-stable states and the flat type noise is caused by the phase distortion between the internal reflected light and the external feedbacked light.

Optical feedback causes chaotic dynamics associated with intermediate levels of OFB and greatly enhances the intensity noise. M. Ahmed *et al.* investigate control of this chaotic dynamics using time-delay

rate equation model including sinusoidal current modulation [35]. They found five distinct chaotic dynamic types, namely, continuous periodic signal, continuous periodic signal with relaxation oscillations, periodic pulse, periodic pulse with relaxation oscillations and periodic pulse with periodic doubling.

In [36] S.M.S. Imran and M. Yamada analyze mechanisms of the generation of the optical feedback noise and its suppression by the superposition of high frequency current. They explain, with approximated but analytical equations, the condition to suppress the OFB noise and present quantitative assessment for conditions unable to suppress optical feedback noise by HF current superposition. Highest OFB induced noise is caused by the mode hopping between bi-stable states. Superposition of high frequency current modulates both electron number and photon number that works to stop mode hopping resulting in suppression of the OFB noise. When frequency of the superposed HF current coincides with a rational number of external feedback frequency the modulations are suppressed by the phase locking effect and noise suppression effect does not work.

2. Significance of This Study

Semiconductor lasers are known to be very sensitive to output light when reflects from an external reflector and couples with the original field in the laser cavity. The dynamic behaviors of semiconductor lasers with optical feedback and their related topics have been investigated for last three decades. The phenomena still contain much of fundamental physics and the study is still under way.

This PhD study consists of two main parts, first part is the analysis of the optical feedback (OFB) noise and second part is the reduction of OFB noise by superposition of high frequency (HF) current. An improved theoretical model has been formulated that can numerically simulate generation of the OFB noise and its suppression by the superposition of HF current. The model is based on a set of multimode rate equations that include nonlinear gain, Langevin noise sources for photon number, phase and carrier density, the OFB and the HF superposition.

Theoretical analyses of the optical feedback noise in semiconductor lasers are classified into three groups. First one is the small signal analysis representing dynamic behaviors on frequency domain where the Langevin noise sources are taken into account [37], [38]. Dynamic effects of semiconductor lasers based on differential analysis of the rate equations using the Langevin method to determine laser's relative intensity noise (RIN) has been presented in [38]. The effects of optical feedback on the quantum mechanical amplitude noise properties of laser have also been described in [23] and [39]. However, effects of the OFB on the mode competition have been first analyzed in [14]. The second group is the single mode model, where time delay of the feedbacked light is taken into

account with or without introduction of the Langevin noise sources [10], [15], [30], [40]. Generation of chaotic phenomena by the OFB was well explained by this model. H. Haken has proposed some theoretical models for single mode lasers based on instability hierarchies of laser light, i.e., chaos and routes to chaos, using semiclassical approach [40]. This second model is effective to apply on the DFB (distributed feedback) laser or laser with DBR (distributed Bragg reflector) mirrors which are also called the dynamically single mode lasers used in the high capacity optical communication systems. The third group is the multimode model which counts the mode competition phenomena among the lasing modes in the solitary laser, but has not counted the Langevin noise sources yet [41].

Model used in this study is an extension of the third group. We start with a set of multimode rate equations for a solitary laser, where effects of the OFB are taken into account as delayed light. Additionally, the Langevin noise sources caused with photon generation are taken into account. Introduction of the noise sources is essential to show the noise characteristics.

Superposition of high-frequency (HF) current is the most popularly used method to suppress OFB noise. The OFB noise is well suppressed by suitable selections of frequency and amplitude of the superposed current. However, M. Yamada *et al.* experimentally report that the OFB noise is not suppressed when frequency of the superposed current and round-trip frequency of the OFB are in relation of rational numbers [26]. They give a theoretical analysis on this problem based on mode competition phenomena among external cavity modes which are built in the space between laser front facet and the reflecting point of OFB. Since this analysis is based on small signal approximation, quantitative assessment for conditions unable to suppress OFB noise is difficult.

Our proposed model allows numerical simulations of the generation of OFB noise and its suppression by the superposition of HF current. Hence, conditions unable to suppress the OFB noise are evidently shown and explained based on approximated but analytical equations. Some published experimental results are also presented and compared with simulation data to support the accuracy of the model.

3. Dissertation Outline

This PhD dissertation consists of five different chapters, namely, introduction, noise in semiconductor lasers, theoretical model of analysis, results and discussion, and conclusion.

Chapter I: Introduction starts with the brief description of some published research papers on noise analysis of semiconductor lasers with optical feedback, noise suppression by superposition of high frequency current and their related topics. Then the background of this PhD study or the significance has been presented in continuation with the previous investigations and reported results.

First part of Chapter II: Overview of Semiconductor Lasers briefly describes fundamental structure and operating mechanism of semiconductor lasers without introducing detail mathematics. Different types of noise in semiconductor lasers and their properties are explained in the second part. This chapter ends with brief description on some noise reduction methods.

Chapter III: Theoretical Model of Analysis deals with devising laser rate equations that are used for the modeling of semiconductor lasers with optical feedback noise and high frequency current modulation. We present detail steps to generate the rate equations for photon number, its phase and carrier numbers from the classical Maxwell's equations and quantum mechanical dynamic equation of the density matrix.

We present some numerically calculated data in Chapter IV: Simulation and Results Discussion based on our theoretical model devised in Chapter III. First part of this chapter focuses on analysis of the optical feedback noise in semiconductor lasers. Then the second part describes mechanisms of noise reduction by superposition of high frequency current injection. Some peculiar features of this technique with detail analyses are also presented in this chapter.

The dissertation ends with Chapter V: Conclusion that gives some concluding remarks on the noise analysis and simulation results of semiconductor lasers under optical feedback. This chapter also comments on OFB noise reduction by superposition of high frequency current injection.

Chapter II: Overview of Semiconductor Lasers

This chapter explains basic noise characteristics of semiconductor lasers which will lead to both qualitative and quantitative understanding of the dynamics of optical feedback noise. Then we briefly describe some noise, especially the optical feedback noise, reduction techniques. But, at first we overview the fundamental structure and operating mechanism of semiconductor lasers.

1. Fundamentals of Semiconductor Lasers

1-a. Device Structure

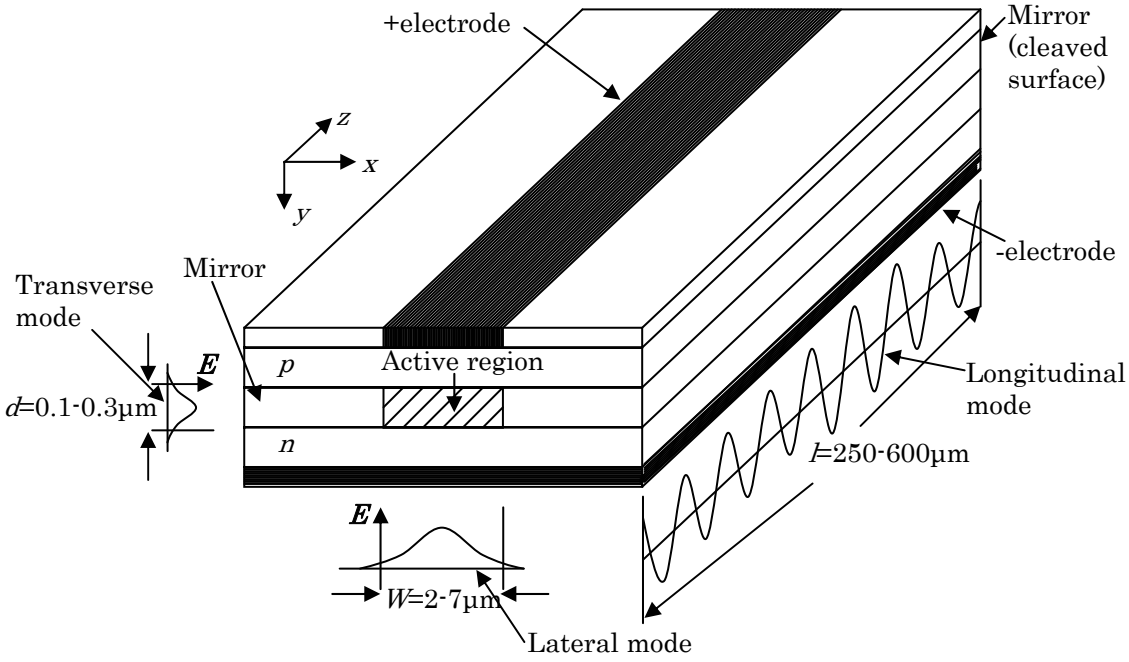

Fig. 2-1. Schematic structure of a semiconductor injection laser.

Semiconductor lasers are devices for oscillation or amplification of an optical wave based on stimulated emission of photons through optical transition of electrons in a semiconductor. It is composed of an active material which has optical gain and an optical resonator which feeds back lights by its reflectors. Fig. 2-1 shows a vastly simplified diagram of a semiconductor laser.

A semiconductor laser is usually fabricated with *p-i-n* semiconductor hetero junctions. Current, used to inject electrons and holes into the active region, is injected via two electrodes one of which is electrically connected to a heat sink. Lasing occurs in the active region between the electrodes. The optical wave propagates along the active region in the longitudinal z-direction. The optical resonator is formed by two parallel facets that are made by cleaving the substrate along crystal planes. Optical light is reflected back by these facet mirrors and forms a standing wave in the longitudinal direction. Typical sizes of the active

region are 0.01-0.3μm thick by 2-10μm wide by 250-600μm long. Several refinements may be incorporated into the laser to attain low threshold, continuous wave (CW) operation, operation at high temperature, narrow linewidth spectra or high output power [42].

1-b. Injection Mechanism

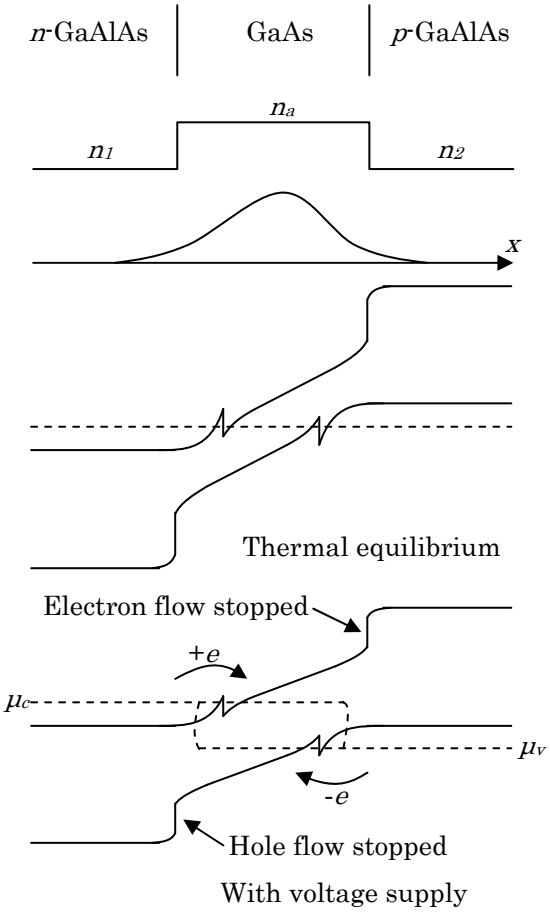

Fig. 2-2. Refractive index variation, optical field and potential barriers confinement, and energy band diagram of a DH laser.

Population inversion of a semiconductor laser is achieved with the structure of p-i-n junctions as illustrated in Fig. 2-2. The laser structure consists of an active layer of GaAs sandwiched between two cladding layers of $Al_xGa_{1-x}As$ with larger bandgap energy and has double heterojunctions (DH) [43]. The structure is fabricated by multilayer epitaxy on a GaAs substrate.

When voltage is applied from an external electric source, energy levels in the n-side are raised up and those in the p-side are brought down. Then the electrons and holes are injected into the active region from the n-side and p-side, respectively. Since the bandgaps of the connecting regions are higher than that in the active region, the injected carriers are well confined within the active layer at high densities without diffusion from the junctions.

When the injection current is low, the laser shows small output due to spontaneous emission only. When the injection current crosses the

threshold current level stimulated emission starts, spontaneous emission is amplified by the stimulated emission and optical output increases almost linearly with the injection current.

1-c. Laser Oscillation

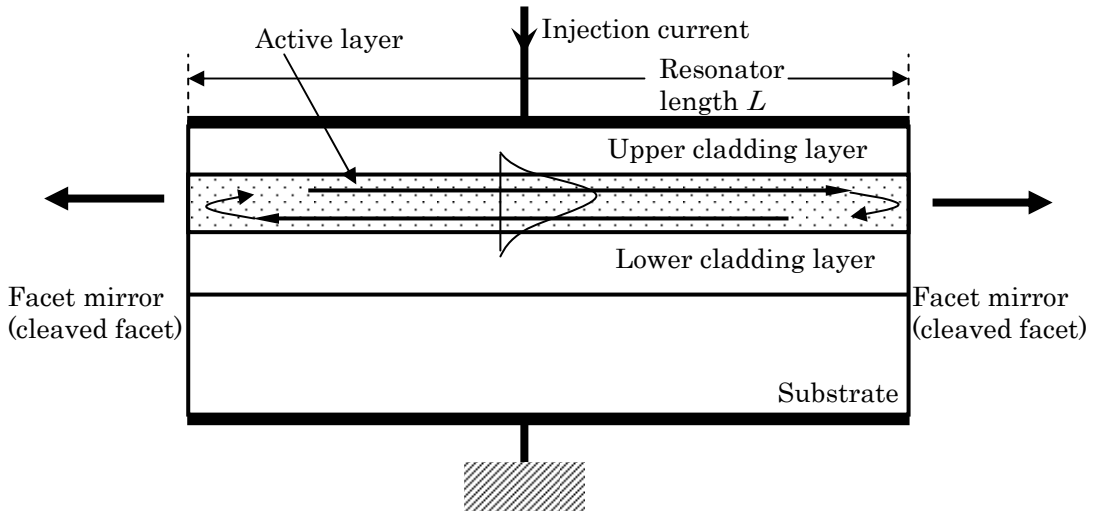

Fig. 2-3. Circulation of optical wave in semiconductor laser active region.

To implement a laser oscillator that generates a coherent optical wave, it is required to provide optical amplification with optical feedback. In semiconductor lasers, this is accomplished by cleaving the semiconductor crystal DH structure with the substrate to form a pair of facet mirrors perpendicular to the active layer. The optical wave undergoes amplification during circulation in the active region, as shown in Fig. 2-3.

Let R be the reflectivity of the facet mirrors, and L be the mirror separation; then the condition for the guided mode to recover its original intensity after a round trip is given by [43]

$$R^2\exp[2(\Gamma g - k)L]=1 \qquad (2\text{-}1)$$

where g is the amplification gain factor under the assumption that the optical wave is completely confined and propagates in the active layer, Γ the coefficient of reduction due to the penetration of the guided mode into the cladding layers, and k the factor representing the optical losses due to absorption and scattering caused by imperfection of the structure.

The condition for the wave to be superimposed with the same phase after the round trip is given by [43]

$$2L=m\lambda \qquad (\lambda=2c\pi/n_r\omega) \qquad (2\text{-}2)$$

where λ is the optical wavelength, c the light velocity in vacuum, ω the optical angular frequency, n_r the effective refractive index, and m an arbitrary integer. This is the condition for positive feedback.

An optical wave of wavelength satisfying Eq. (2-2) can resonate, since the wave is superimposed with the same phase after an arbitrary

number of round trips. When the injection current is increased and the effective gain for one of the resonant wavelengths reaches the value satisfying Eq. (2-1), optical power is accumulated and maintained in the resonator, and the power is emitted through the facet mirrors. This is the laser oscillation, i.e., lasing.

1-d. Lasing Modes

Properties of optical wave are characterized with the word mode. The mode of the optical wave generated by a laser is generally classified by transverse modes and longitudinal modes. The transverse mode (lateral mode) is the intensity distribution in the cross section normal to the optical axis (width direction x and thickness direction y in Fig. 2-1), is defined by the waveguide structure.

The longitudinal mode (axial mode), on the other hand, is defined by the distribution, along the direction of propagation (the optical axis, propagation direction z in Fig. 2-1), of the standing wave in the resonator. Each longitudinal mode corresponds to each integer m in Eq. (2-2) and constructs components with slightly different wavelengths.

The heterojunction of the active region is designed to achieve lower threshold current and suitable profile of the optical wave along thickness direction. The field distribution along the width direction is controlled with an artificially designed structure called the stripe structure. Hence, output optical wave spreads more widely along the thickness direction than the width direction. Also, direction of polarization is mostly characterized with the field distribution along the thickness direction.

Optical spectrum of output optical wave directly corresponds to the longitudinal mode. There are two cases of the spectrum – one is the single mode operation and another is the multimode operation.

Instability of the transverse mode gives rise to deterioration of the spatial coherence of the output wave and temporal coherence is degraded if several longitudinal modes oscillate simultaneously (multimode lasing) and/or there is fluctuation of modes.

In Fig. 2-1, optical field is confined in the active region and propagates along z-direction. The thickness of the active region is usually much smaller than the width w and is designed to obtain the lowest threshold current density [47], [48]. All higher order transverse modes along the y-direction are usually cut off with this optimum thickness.

2. Noise in Semiconductor Lasers

Noise problems in the semiconductor laser starts with the laser's invention [45]. Classification of noise in semiconductor lasers is based on either application of laser light as carrier of information transmission or generating mechanism of physical disturbance. Therefore, Noises related to semiconductor lasers are as follows.

(A) Based on application of the optical wave

(i) IM noise: intensity noise or intensity modulation noise where intensity of the optical wave is used as signal and the noise is due to fluctuation in amplitude of light.

(ii) FM noise: frequency modulation noise where frequency of phase of the optical wave is used as the signal and is caused due to fluctuation in frequency of light.

(B) Based on generating mechanism of physical disturbance

(a) Intrinsic noise, known as quantum noise or shot noise.

(b) External noise

(1) Optical feedback (OFB) noise

(i) Optical phase distortion: also known as coherent collapse or noise due to external mode competition.

(ii) Mode hopping noise: due to mode competition among internal lasing modes.

(2) Noise due to fluctuations in temperature, driving current and voltage. This type of noise is very low compared to the quantum noise and the optical feedback noise in semiconductor lasers.

2-a. Quantum Noise

As lasers are light emitting devices based on the optical transition of electrons, they inevitably involve a quantum noise problem [6], [43], [44]. Transition of one electron from conduction band to valence band induces one photon. This transition takes a finite time interval. Then both the photon number in the cavity and the electron density in the conduction band are not constant for time variation and must always have fluctuations. This type of intrinsic fluctuation is counted to be the quantum noise or the shot noise.

2-b. Optical Feedback Noise

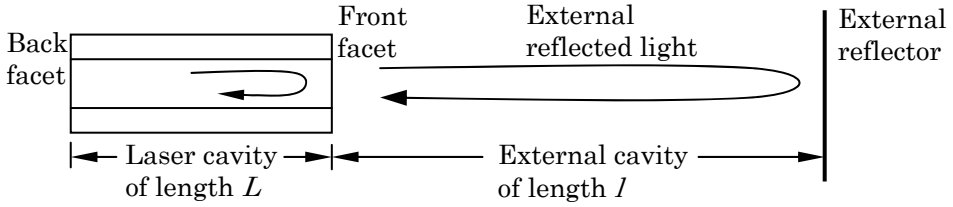

Fig. 2-4. Semiconductor laser with external reflector while connecting with other optical device.

When semiconductor laser is used as a light source connecting with other optical device, such as optical lens, optical fiber or optical detector, output light from the laser is reflected back from the optical device and re-injects into the laser. This optical feedback intricately changes light output characteristics of semiconductor laser according to the distance

between reflective external objects and the laser front facet, the feedback light intensity and driving conditions. As a result the laser reveals excess noise known as optical feedback noise or OFB noise [3], [46]. Generating mechanism of the OFB noise can be categorized as –

(i) Phase Distortion of Optical Light

This is also known as coherent collapse and sometimes explained in terms of mode competition among external cavity modes whose lasing frequency is decided by the space between the laser facet and the reflecting mirror [14], [21]. Phase of lasing light always fluctuates. Then phase of the re-injected light does not coincide with that of the oscillating light in the laser cavity. Such phase differences enhance fluctuation of the optical intensity through the laser polarization and in turn generate excess noise in laser output.

(ii) Mode Hopping Noise

The mode hopping noise results from the alternate oscillation of multiple modes with random durations. Since added optical waves by the internal reflection and the re-injected light have different phases, the equivalent reflection rate at the front facet has temporal variations, resulting in temporal variations of the threshold gain level for each lasing mode. Then depending upon the operation conditions, alteration of the oscillation between two modes takes place. Since total photon number is not constant during the mode hopping, laser shows large amount of noise called mode hopping noise. This mode hopping noise can be induced without optical feedback in some lasers having unstable transverse mode control property.

3. Noise Reduction in Semiconductor Lasers

In terms of generating mechanism and reduction principle, methods of noise reduction in semiconductor laser can be classified as follows.

(a) Optical isolator

(b) Electric negative feedback

(c) Self-pulsation laser

(d) Superposition of high frequency current

(e) Electric positive and negative feedback

3-a. Optical Isolator

External optical feedback induced noise can be eliminated by inserting a nonreciprocal isolator in the output beam path, since the isolator transmits only forward wave but block any reflected backward wave. This technique is practically used in optical fiber communication systems or optical measuring systems. But this method is not favored for

use in optical disc system for an optical isolator is very expensive and the size of the optical system increases.

3-b. Electric Negative Feedback

This method electrically compensates the fluctuation on the light emission. In this method we use electric negative feedback loop in which one part of the laser output is detected and electrically amplified with negative phase and then injected into the laser as injection current. Then the generated noise in the laser is suppressed to a level lower than the quantum noise limit.

The disadvantage of this method is that it requires an amplifier with sufficiently wide bandwidth. Also, the electric negative feedback is not so effective for reduction of the mode hopping noise.

3-c. Self-Pulsation Laser

In self-pulsation lasers, saturable absorbing region is put around the active region which speeds up the temporal variation of the photon number and thus output light reveals periodic pulsing variation with several hundred MHz even when the driving current is a regular DC current. Then dynamics of the resonance effect is continuously kept. Since electron density and photon numbers are vibrated with high frequency, self-pulsation lasers can avoid mode hopping noise induced by the optical feedback by releasing the coupling effect among the longitudinal modes [17].

Since the noise reduction is obtained automatically without any additional device the self-pulsation laser is suitable for application in the optical disc system. However, threshold current level in the self-pulsation laser has to be higher than that in the conventional laser because of the energy consumption in the saturable absorbing region.

3-d. Superposition of High Frequency Current

Superposition of HF current is the most popularly used method to reduce the optical feedback noise in semiconductor lasers. In this method, high frequency current with frequency of 100MHz to 1GHz is superposed on the injection current. Photon number and carrier density are modulated with modulation frequency of the superposed HF current and its harmonics, and thus operating point of the laser is shifted from bi-stable to stable multimode. Then the low frequency type optical feedback noise is reduced.

The most efficient frequency of the superposed current is the relaxation oscillation frequency, because photon numbers and electron density are mostly modulated at this frequency. As conventional semiconductor lasers are not designed for such higher frequency operation direct excitation with resonance frequency is difficult.

3-e. Electric Positive and Negative Feedback

While method (3-a) is effective only for suppressing the quantum noise, methods (3-c) and (3-d) are effective only for reducing optical feedback noise. Both quantum noise and optical feedback noise are suppressed over a frequency range of 100MHz by electric positive and negative feedback (EPNF) method [32]. Here an electric feedback loop from an optical detector to a laser is set with both electrically positive and negative phase relations [31]. Optical feedback noise is reduced by the positive feedback property and the quantum noise is suppressed by the negative feedback property.

Chapter III: Theoretical Model of Analysis

This chapter describes the theoretical model of semiconductor laser with optical feedback in detail that is used in our numerical simulation and analysis of noise. We also derive improved time-delay rate equations for the multimode model of semiconductor laser. First the rate equations for modal photon number, its phase and carrier number are generated for solitary laser. Then external optical feedback effect is introduced to the rate equations to analyze the OFB noise.

1. Manner of Analysis

The laser operation is based on interaction between electro-magnetic wave and electron-hole pairs in the semiconductor. The noise problem is understood as combined effect of fluctuations on optical absorption, stimulated emission and spontaneous emission. The manner of analysis taken here is semi-classical in which the optical wave is analyzed with the classical Maxwell's equations while spontaneous emission and noise are treated through the quantization of the optical wave.

We start with the classical Maxwell's equations to analyze the dynamics of the electromagnetic field. Dynamics of the carriers are represented as polarization, dielectric constant or conductivity, analyzed using density matrix and then introduced into the classical Maxwell's equations. Finally, electric field is transformed to photon number using quantization of the lasing field.

In this model of analysis, the modal behavior of longitudinal modes is analyzed considering a stable laser in which only fundamental transverse mode exists. Discussion of the transverse mode control is given in detail by M. Yamada in [8].

This model is also based on the assumption that spatial distribution of electron in the active region is uniform and the change of refractive index with carrier numbers is introduced through the linewidth enhancement factor.

2. Gain Coefficient

Optical wave in the semiconductor laser propagates along the active region and is reflected back by the front and back facet forming standing wave in the laser cavity as shown in Fig. 2-3. Suppose reflectivity of the front facet as R_f and that of the back fact as R_b. Maxwell's equations with respect to electric field $\vec{E}$, magnetic field $\vec{H}$, dielectric flux $\vec{D}$ and magnetic flux density $\vec{B}$ are,

$$\nabla \times \vec{H} = \frac{\partial \vec{D}}{\partial t} + \sigma \vec{E} \qquad (3\text{-}1)$$

$$\nabla \times \vec{E} = -\frac{\partial \vec{B}}{\partial t} \tag{3-2}$$

$$\nabla.\vec{E} = 0 \tag{3-3}$$

$$\nabla.\vec{B} = 0 \tag{3-4}$$

where, $\vec{D} = \varepsilon_0 \varepsilon_r \vec{E} + \vec{P}$ (3-5)

$$\vec{B} = \mu_0 \vec{H} \tag{3-6}$$

$\vec{P}$ = polarization formed by electron-hole pairs

ε_0 = dielectric constant in vacuum

μ_0 = permeability in vacuum

ε_r = relative dielectric constant of the laser material and

σ = conductivity causing loss in the laser cavity.

Taking curl of Eqn. (3-2)

$$\nabla \times \nabla \times \vec{E} = -\frac{\partial}{\partial t}\left(\nabla \times \vec{B}\right) = -\mu_0 \frac{\partial}{\partial t}\left(\nabla \times \vec{H}\right)$$

$$\Rightarrow \nabla.\nabla.\vec{E} - \nabla^2 \vec{E} = -\mu_0 \frac{\partial}{\partial t}\left[\frac{\partial \vec{D}}{\partial t} + \sigma \vec{E}\right]$$

$$\Rightarrow \nabla^2 \vec{E} = \mu_0 \frac{\partial^2 \vec{D}}{\partial t^2} + \mu_0 \sigma \frac{\partial \vec{E}}{\partial t}$$

$$= \mu_0 \frac{\partial^2}{\partial t^2}\left[\varepsilon_0 \varepsilon_r \vec{E} + \vec{P}\right] + \mu_0 \sigma \frac{\partial \vec{E}}{\partial t}$$

$$\Rightarrow \nabla^2 \vec{E} - \mu_0 \sigma \frac{\partial \vec{E}}{\partial t} - \mu_0 \varepsilon_0 \varepsilon_r \frac{\partial^2 \vec{E}}{\partial t^2} = \mu_0 \frac{\partial^2 \vec{P}}{\partial t^2} \tag{3-7}$$

Assuming $\vec{P} = 0$, $\sigma = 0$ and $\vec{E}(t) = \Phi_p(\vec{r}) \exp\left(j\omega_{0p} t\right)$ with characteristic angular frequency ω_{0p} in Eqn. (3-7),

$$\nabla^2 \vec{E} - \mu_0 \varepsilon_0 \varepsilon_r \frac{\partial^2 \vec{E}}{\partial t^2} = 0$$

$$\Rightarrow \exp\left(j\omega_{0p} t\right) \nabla^2 \Phi_p(\vec{r}) - \mu_0 \varepsilon_0 \varepsilon_r \Phi_p(\vec{r}) \exp\left(j\omega_{0p} t\right)\left(j\omega_{0p}\right)^2 = 0$$

$$\Rightarrow \nabla^2 \Phi_{0p}(\vec{r}) + \mu_0 \varepsilon_0 \varepsilon_r \omega_{0p}^2 \Phi_p(\vec{r}) = 0 \tag{3-8}$$

where $\Phi_p(\vec{r})$ is a field distribution function showing standing waves in the laser cavity. The distribution function is normalized to be unity in the whole cavity and maintains an orthonormal relation among the characteristic guided modes such that,

$$\int_0^L \int_{-\infty}^{+\infty} \int_{-\infty}^{+\infty} \Phi_p(\vec{r}) \Phi_q^*(\vec{r}) dx dy dz = \delta_{pq} \tag{3-9}$$

with p, q = 0, 1, 2, 3, . . . being the longitudinal mode numbers and L is the length of the laser.

The electric field $\vec{E}$ and the laser polarization $\vec{P}$ can be expanded as,

$$\vec{E} = \sum_p \overline{E}_p(t)\exp\{j\theta_p(t)\}\Phi_p(\vec{r})\exp(j\omega_p t) + c.c. \tag{3-10}$$

$$\vec{P} = \sum_p \overline{P}_p(t)\exp\{j\theta_p(t)\}\Phi_p(\vec{r})\exp(j\omega_p t) + c.c. \tag{3-11}$$

where, ω_p is the angular frequency of the lasing mode p

$\overline{E}_p(t)$, $\overline{P}_p(t)$ and $\theta_p(t)$ are the amplitude and phases of $\vec{E}$ and $\vec{P}$

$\widetilde{E}_p(t) = \overline{E}_p(t)\exp\{j\theta_p(t)\}$ is slowly time varying amplitude of the field

$\widetilde{P}_p(t) = \overline{P}_p(t)\exp\{j\theta_p(t)\}$ is also assumed to vary slowly with time.

$$\begin{aligned}
\nabla^2\vec{E} &= \nabla^2\left[\widetilde{E}_p(t)\Phi_p(\vec{r})\exp(j\omega_p t)\right] \\
&= \widetilde{E}_p(t)\exp(j\omega_p t)\nabla^2\Phi_p(\vec{r}) \\
&= \widetilde{E}_p(t)\exp(j\omega_p t)\{-\mu_0\varepsilon_0\varepsilon_r\omega_{0p}^2\Phi_p(\vec{r})\} \qquad \text{using Eqn. (3-8)} \\
&= -\mu_0\varepsilon_0\varepsilon_r\omega_{0p}^2\widetilde{E}_p(t)\Phi_p(\vec{r})\exp(j\omega_p t) \\
\Rightarrow \int(\nabla^2\vec{E})\Phi_p^*(\vec{r})\exp(-j\omega_p t)d^3\vec{r} & \\
&= -\int\varepsilon_0\varepsilon_r\mu_0\omega_{0p}^2\widetilde{E}_p(t)\Phi_p(\vec{r})\exp(j\omega_p t)\Phi_p^*(\vec{r})\exp(-j\omega_p t)d^3\vec{r} \\
&= -\varepsilon_0\varepsilon_r\mu_0\omega_{0p}^2\widetilde{E}_p(t) \qquad \text{using Eqn. (3-9)}
\end{aligned} \tag{3-12}$$

Temporal variation of the electric field can be written as,

$$\begin{aligned}
\frac{\partial\vec{E}}{\partial t} &= \frac{\partial}{\partial t}\left[\widetilde{E}_p(t)\Phi_p(\vec{r})\exp(j\omega_p t)\right] \\
&= \Phi_p(\vec{r})\exp(j\omega_p t)\frac{\partial\widetilde{E}_p}{\partial t} + \widetilde{E}_p(t)\Phi_p(\vec{r})\exp(j\omega_p t)(j\omega_p) \\
\Rightarrow \int\left(\frac{\partial\vec{E}}{\partial t}\right)\Phi_p^*(\vec{r})\exp(-j\omega_p t)d^3\vec{r} &= \frac{\partial\widetilde{E}_p}{\partial t} + j\omega_p\widetilde{E}_p(t)
\end{aligned} \tag{3-13}$$

$$\begin{aligned}
\frac{\partial^2\vec{E}}{\partial t^2} &= \frac{\partial}{\partial t}\left[\Phi_p(\vec{r})\exp(j\omega_p t)\frac{\partial\widetilde{E}_p(t)}{\partial t} + \widetilde{E}_p(t)\Phi_p(\vec{r})\exp(j\omega_p t)(j\omega_p)\right] \\
&= \Phi_p(\vec{r})\frac{\partial\widetilde{E}_p(t)}{\partial t}\exp(j\omega_p t)(j\omega_p) + \Phi_p(\vec{r})\exp(j\omega_p t)\frac{\partial^2\widetilde{E}_p(t)}{\partial t^2} \\
&\quad + \Phi_p(\vec{r})\exp(j\omega_p t)(j\omega_p)\frac{\partial\widetilde{E}_p(t)}{\partial t} + \widetilde{E}_p(t)\Phi_p(\vec{r})(j\omega_p)\exp(j\omega_p t)(j\omega_p) \\
\Rightarrow \int\frac{\partial^2\vec{E}}{\partial t^2}\Phi_p^*(\vec{r})\exp(-j\omega_p t)d^3\vec{r} &= \frac{\partial^2\widetilde{E}_p(t)}{\partial t^2} + 2j\omega_p\frac{\partial\widetilde{E}_p(t)}{\partial t} - \omega_p^2\widetilde{E}_p(t)
\end{aligned} \tag{3-14}$$

Similarly,

$$\int \frac{\partial^2 \vec{P}}{\partial t^2}.\Phi_p^*(\vec{r})\exp(-j\omega_p t)d^3\vec{r} = \frac{\partial^2 \tilde{P}_p(t)}{\partial t^2} + 2j\omega_p \frac{\partial \tilde{P}_p(t)}{\partial t} - \omega_p^2 \tilde{P}_p(t) \qquad (3\text{-}15)$$

By substituting Eqn. (3-10) and (3-11) into Eqn. (3-7), then multiplying by $\Phi_p^*(\vec{r})\exp(-j\omega_p t)$, taking integration within the laser cavity, using Eqn. (3-12)-(3-15), assuming $\overline{E}_p(t)$ as a real number and $\overline{P}_p(t)$ as a complex number, and using the approximations $\partial\tilde{E}_p/\partial t << |\omega_p \tilde{E}_p|$, $\partial\tilde{P}_p/\partial t << |\omega_p \tilde{P}_p|$, $\omega_p \approx \omega_{0p}$ and $\partial\theta_p/\partial t << \omega_p$ we obtain,

$$-\varepsilon_0\varepsilon_r\mu_0\omega_{0p}^2\tilde{E}_p(t) - \mu_0\sigma\left[\frac{\partial\tilde{E}_p(t)}{\partial t} + j\omega_p\tilde{E}_p(t)\right] - \varepsilon_0\varepsilon_r\mu_0\left[\frac{\partial^2\tilde{E}_p(t)}{\partial t^2} + 2j\omega_p\frac{\partial\tilde{E}_p(t)}{\partial t} - \omega_p^2\tilde{E}_p(t)\right] = \mu_0\left[\frac{\partial^2\tilde{P}_p(t)}{\partial t^2} + 2j\omega_p\frac{\partial\tilde{P}_p(t)}{\partial t} - \omega_p^2\tilde{P}_p(t)\right]$$

$$\Rightarrow -\varepsilon_0\varepsilon_r\mu_0\omega_{0p}^2\tilde{E}_p(t) - j\mu_0\sigma\omega_p\tilde{E}_p(t) - 2j\varepsilon_0\varepsilon_r\mu_0\omega_p\frac{\partial\tilde{E}_p(t)}{\partial t} + \varepsilon_0\varepsilon_r\mu_0\omega_p^2\tilde{E}_p(t) = -\mu_0\omega_p^2\tilde{P}_p(t)$$

$$\Rightarrow \varepsilon_0\varepsilon_r\mu_0\omega_{0p}^2\overline{E}_p(t)\exp\{j\theta_p(t)\} - j\mu_0\sigma\omega_p\overline{E}_p(t)\exp\{j\theta_p(t)\} - 2j\varepsilon_0\varepsilon_r\mu_0\omega_p\left[\exp\{j\theta_p(t)\}\right]\frac{\partial\tilde{E}_p(t)}{\partial t} + \overline{E}_p(t)\exp\{j\theta_p(t)\}j\frac{\partial\theta_p(t)}{\partial t} + \varepsilon_0\varepsilon_r\mu_0\omega_{0p}^2\overline{E}_p(t)\exp\{j\theta_p(t)\} = -\mu_0\omega_p^2\overline{P}_p(t)\exp\{j\theta_p(t)\}$$

$$\Rightarrow \frac{-j\varepsilon_0\varepsilon_r\mu_0\omega_{0p}^2}{2\varepsilon_0\varepsilon_r\mu_0\omega_p}\overline{E}_p(t) + \frac{\mu_0\sigma\omega_p}{2\varepsilon_0\varepsilon_r\mu_0\omega_p}\overline{E}_p(t) + \frac{\partial\tilde{E}_p(t)}{\partial t} + j\overline{E}_p(t)\frac{\partial\theta_p(t)}{\partial t} + \frac{j\varepsilon_0\varepsilon_r\mu_0\omega_p^2}{2\varepsilon_0\varepsilon_r\mu_0\omega_p}\overline{E}_p(t) = -\frac{j\mu_0\omega_p^2}{2\varepsilon_0\varepsilon_r\mu_0\omega_p}\overline{P}_p(t)$$

$$\Rightarrow \frac{\partial\overline{E}_p(t)}{\partial t} + j\left(\frac{\partial\theta_p(t)}{\partial t} + \frac{\omega_p^2}{2\omega_p} - \frac{\omega_{0p}^2}{2\omega_p}\right)\overline{E}_p(t) + \frac{\sigma}{2\varepsilon_0 n_r^2}\overline{E}_p(t) = -\frac{j\omega_p}{2\varepsilon_0 n_r^2}\overline{P}_p(t)$$

$$\Rightarrow \frac{\partial\overline{E}_p(t)}{\partial t} + j\left\{\frac{\partial\theta_p(t)}{\partial t} + (\omega_p - \omega_{0p})\right\}\overline{E}_p(t) + \frac{\sigma}{2\varepsilon_0 n_r^2}\overline{E}_p(t) = -\frac{j\omega_p}{2\varepsilon_0 n_r^2}\overline{P}_p(t) \qquad (3\text{-}16)$$

where $n_r = \sqrt{\varepsilon_r}$ is the refractive index in the active region and the susceptibility is defined as,

$$\chi = \overline{P}_p(t)/\overline{E}_p(t) = \mathrm{Re}\{\chi\} + j\,\mathrm{Im}\{\chi\} \qquad (3\text{-}17)$$

With susceptibility χ Eqn. (3-16) becomes,

$$\begin{aligned}
&\frac{\partial \overline{E}_p(t)}{\partial t} + j\left\{\frac{\partial \theta_p(t)}{\partial t} + \left(\omega_p - \omega_{0p}\right)\right\}\overline{E}_p(t) + \frac{\sigma}{2\varepsilon_0 n_r^2}\overline{E}_p(t) \\
&\qquad = -\frac{j\omega_p}{2\varepsilon_0 n_r^2}\left[\mathrm{Re}\{\chi\} + j\,\mathrm{Im}\{\chi\}\right]\overline{E}_p(t) \\
&\Rightarrow \frac{\partial \overline{E}_p(t)}{\partial t} - \frac{\omega_p}{2\varepsilon_0 n_r^2}\mathrm{Im}\{\chi\}\overline{E}_p(t) + \frac{\sigma}{2\varepsilon_0 n_r^2}\overline{E}_p(t) \\
&\quad + j\left\{\frac{\partial \theta_p(t)}{\partial t} + \left(\omega_p - \omega_{0p}\right) + \frac{\omega_p}{2\varepsilon_0 n_r^2}\mathrm{Re}\{\chi\}\right\}\overline{E}_p(t) = 0
\end{aligned} \tag{3-18}$$

Polarization $\overline{P}_p(t)$ is a function of injected carrier density N which is controlled by the injection current I and the field intensity $|E|^2$ in the laser cavity. Therefore,

$$\frac{\partial N}{\partial t} = U\left(N, |E|^2, I\right) \tag{3-19}$$

Consequently, equations for the field amplitude and phase can be expressed with the real and imaginary parts of Eqn. (3-18) as,

$$\begin{aligned}
\frac{\partial \overline{E}_p(t)}{\partial t} &= \left[\frac{\omega_p}{2\varepsilon_0 n_r^2}\mathrm{Im}\{\chi\} - \frac{\sigma}{2\varepsilon_0 n_r^2}\right]\overline{E}_p(t) \\
&= \frac{1}{2}\left(G_p - G_{th}\right)\overline{E}_p(t)
\end{aligned} \tag{3-20}$$

$$\frac{\partial \theta_p(t)}{\partial t} = \left(\omega_{0p} - \omega_p\right) - \frac{\omega_p}{2\varepsilon_0 n_r^2}\mathrm{Re}\{\chi\} \tag{3-21}$$

where the coefficient for the modal gain G_p is given by,

$$\begin{aligned}
G_p &= \frac{\omega_p}{\varepsilon_0 n_r^2}\mathrm{Im}\{\chi\} = \frac{\omega_p}{\varepsilon_0 n_r^2}\mathrm{Im}\left\{\overline{P}_p(t)/\overline{E}_p(t)\right\} \\
&= \frac{\omega_p}{\varepsilon_0 n_r^2}\frac{1}{\overline{E}_p(t).\Delta t}\mathrm{Im}\left\{\int_{t-\Delta t}^{t}\iint \vec{P}\Phi^*_p(\vec{r})\exp\left(-j\omega_p t\right)d^3\vec{r}\,dt\right\}
\end{aligned} \tag{3-22}$$

and the threshold gain coefficient G_{th} is expressed as,

$$\begin{aligned}
G_{th} &= \frac{\sigma}{\varepsilon_0 n_r^2} = \frac{1}{\varepsilon_0 n_r^2}\int \sigma\left|\Phi_p(\vec{r})\right|^2 d^3\vec{r} \quad \text{considering internal loss only} \\
&= \frac{c}{n_r}\left[k + \frac{1}{2L}\ln\frac{1}{R_f R_b}\right] \quad \text{considering mirror loss also.}
\end{aligned} \tag{3-23}$$

where k is the internal power loss coefficient, L is the resonator length, and R_f and R_b are the power reflectivity of front facet and back facet mirrors, respectively. Eqn. (3-23) is called the gain condition or amplitude condition for the lasing operation.

See Appendix-A for the detail derivation of Eqn. (3-23).

Eqn. (3-22) can be written in the form,

$$G_p = A_p - \sum_q B_{pq} \left| \overline{E}_q \right|^2 \tag{3-24}$$

Introducing an approximate formula for the linear gain peak A_p where the peak value of the linear gain varies linearly with carrier density and the spectrum around the gain peak can be approximated by a parabola, the first order linear gain coefficient can be approximated by,

$$A_p = \frac{a\xi}{V}\left[N - N_g - bV\left(\lambda_p - \lambda_0\right)^2\right] \tag{3-25}$$

where $\xi = \int \left|\Phi_p(\vec{r})\right|^2 d^3\vec{r}$ is the field confinement factor

a is the gradient of the gain peak

b is the curvature of the gain spectra in terms of wavelength

N_g is the carrier density at which the gain becomes zero

λ_p is the wavelength of mode p

λ_0 is the wavelength at gain peak

V is the volume of the laser active region, and

B_{pq} in Eqn. (3-24) is the nonlinear gain coefficient.

3. Rate Equation for Electron Density

The linear polarization of the laser, induced by the electric field, given by the quantum mechanics is,

$$P^{(1)} = N_t \sum_{b,a} \left(\rho_{ba}^{(1)} R_{ab} + \rho_{ab}^{(1)} R_{ba}\right) \tag{3-26}$$

where N_t is the total electron density in the conduction band b and valence band a, R_{mn} is the dipole moment and ρ_{mn} indicates the polarization in which the electron spreads over the energy levels $|m\rangle$ and $|n\rangle$.

If value of N or $\left(\rho_{bb}^{(0)} - \rho_{aa}^{(0)}\right)$, where ρ_{nn} indicates occupation probability of electron at the energy state $|n\rangle$, is time invariant then the linear susceptibility is obtained as,

$$\chi^{(1)}\left(\omega_p\right) = -\frac{N_t}{j\hbar\varepsilon_0} \sum_{b,a} \frac{\left|R_{ba}\right|^2 \left(\rho_{bb}^{(0)} - \rho_{aa}^{(0)}\right)}{j\left(\omega_p - \omega_{ba}\right) + \frac{1}{\tau_{in}}} \tag{3-27}$$

where ω_{ba} is angular frequency corresponding to the energy difference between energy level b in the conduction band and that of a in the valence band,

$$\omega_{ba} = \frac{W_b - W_a}{\hbar} = \frac{W_{ba}}{\hbar} > 0 \tag{3-28}$$

and τ_{in} is the effective intraband relaxation time related to the electron lifetime τ_s whose value is in the order of 10^{-9}s as,

$$\frac{1}{\tau_{in}} = \frac{1}{2}\left(\frac{1}{\tau_b} + \frac{1}{\tau_a}\right) + \frac{1}{\tau_s} \tag{3-29}$$

When the injected carrier density N increases from N_0 to $N_0+\Delta N$, change of the susceptibility can be given as

$$\chi^{(1)}(\omega_p, N_0 + \Delta N) = \chi^{(1)}(\omega_p, N_0) + \frac{\partial \chi^{(1)}(\omega_p)}{\partial N}\Delta N \tag{3-30}$$

Essentially, due to noise from spontaneous emission into the resonator modes, a free running single frequency laser has a certain finite linewidth. The increased linewidth results from a coupling between intensity and phase noise caused by a dependence of the refractive index on the carrier density in the semiconductor. The linewidth enhancement factor α is a proportionality factor relating the phase changes to the changes of amplitude gain.

$$\alpha = -\frac{\dfrac{\partial \operatorname{Re}\{\chi^{(1)}(\omega_p)\}}{\partial N}}{\dfrac{\partial \operatorname{Im}\{\chi^{(1)}(\omega_p)\}}{\partial N}} \tag{3-31}$$

$$\begin{aligned}\frac{\partial\{\chi^{(1)}(\omega_p)\}}{\partial N} &= \frac{\partial \operatorname{Re}\{\chi^{(1)}(\omega_p)\}}{\partial N} + j\frac{\partial \operatorname{Im}\{\chi^{(1)}(\omega_p)\}}{\partial N} \\ &= -\alpha\frac{\partial \operatorname{Im}\{\chi^{(1)}(\omega_p)\}}{\partial N} + j\frac{\partial \operatorname{Im}\{\chi^{(1)}(\omega_p)\}}{\partial N} \\ &= j(1 + j\alpha)\frac{\partial \operatorname{Im}\{\chi^{(1)}(\omega_p)\}}{\partial N}\end{aligned} \tag{3-32}$$

Imaginary part of the linear susceptibility at $N=N_0$ can be written in an approximated form with a coefficient κ as,

$$\begin{aligned}&\operatorname{Im}\{\chi^{(1)}(\omega_p, N_0)\} = \kappa\left[N_0 - N_g - b(\lambda_p - \lambda_0)^2\right] \\ &\Rightarrow \frac{\partial \operatorname{Im}\{\chi^{(1)}(\omega_p)\}}{\partial N} = \kappa\end{aligned} \tag{3-33}$$

$$\begin{aligned}\text{So, } \chi^{(1)}(\omega_p, N) &= \operatorname{Re}\{\chi^{(1)}(\omega_p, N_0)\} + j\operatorname{Im}\{\chi^{(1)}(\omega_p, N_0)\} + j(1 + j\alpha)\kappa.\Delta N \\ &= j\kappa\left[N_0 - N_g - b(\lambda_p - \lambda_0)^2\right] + \operatorname{Re}\{\chi^{(1)}(\omega_p, N_0)\} + j(1 + j\alpha)\kappa.\Delta N \\ &= j\kappa\left[(1 + j\alpha)N - N_g - b(\lambda_p - \lambda_0)^2\right] + \kappa.\Delta N_0 + \operatorname{Re}\{\chi^{(1)}(\omega_p, N_0)\} \\ &\approx j\kappa\left[(1 + j\alpha)N - N_g - b(\lambda_p - \lambda_0)^2\right]\end{aligned} \tag{3-34}$$

$\kappa.\Delta N_0 + \mathrm{Re}\{\chi^{(1)}(\omega_p, N_0)\}$ is the change of refractive index at saturation which is constant at threshold. So the term is neglected here as we are considering the beating vibration. The injected carrier density N for the zeroth order terms of the density matrix is defined by the following relation.

$$N = N_t \sum_b \left(\rho_{bb}^{(0)} - \tilde{\rho}_b\right)$$

$$= \frac{N_t}{2}\left\{\sum_b \left(\rho_{bb}^{(0)} - \tilde{\rho}_b\right) - \sum_a \left(\rho_{aa}^{(0)} - \tilde{\rho}_a\right)\right\}$$

$$\Rightarrow \frac{dN}{dt} = \frac{N_t}{2}\left(\sum_b \frac{d\rho_{bb}^{(0)}}{dt} - \sum_a \frac{d\rho_{aa}^{(0)}}{dt}\right)$$

$$= \frac{N_t}{2}\left[\sum_b \left\{\frac{\tilde{\tilde{\rho}}_b - \rho_{bb}^{(0)}}{\tau_b} + \frac{\tilde{\rho}_b - \rho_{bb}^{(0)}}{\tau_s} + \Lambda_b\right\} - \sum_a \left\{\frac{\tilde{\tilde{\rho}}_a - \rho_{aa}^{(0)}}{\tau_a} + \frac{\tilde{\rho}_a - \rho_{aa}^{(0)}}{\tau_s} + \Lambda_a\right\}\right]$$

$$= \frac{N_t}{2}\left[\sum_b \left\{\frac{\tilde{\tilde{\rho}}_b - \rho_{bb} + \rho_{bb}^{(2)}}{\tau_b} + \frac{\tilde{\rho}_b - \rho_{bb}^{(0)}}{\tau_s} + \Lambda_b\right\} - \sum_a \left\{\frac{\tilde{\tilde{\rho}}_a - \rho_{aa} + \rho_{aa}^{(2)}}{\tau_a} + \frac{\tilde{\rho}_a - \rho_{aa}^{(0)}}{\tau_s} + \Lambda_a\right\}\right]$$

$$= \frac{N_t}{2}\left[\sum_b \frac{\rho_{bb}^{(2)}}{\tau_b} - \sum_a \frac{\rho_{aa}^{(2)}}{\tau_a} + \sum_b \frac{\tilde{\tilde{\rho}}_b - \rho_{bb}}{\tau_b} - \sum_a \frac{\tilde{\tilde{\rho}}_a - \rho_{aa}}{\tau_a} + \sum_b \frac{\tilde{\rho}_b - \rho_{bb}^{(0)}}{\tau_s} - \sum_a \frac{\tilde{\rho}_a - \rho_{aa}^{(0)}}{\tau_s} + \Lambda_b - \Lambda_a\right] \quad (3\text{-}35)$$

If we assume spatially uniform electron distribution in the active region, then we have

$$\sum_b \frac{\rho_{bb} - \tilde{\tilde{\rho}}_b}{\tau_b} \approx \sum_a \frac{\rho_{aa} - \tilde{\tilde{\rho}}_a}{\tau_a} \approx 0 \quad (3\text{-}36)$$

Now Eqn. (3-35) can be approximately written as,

$$\frac{dN}{dt} \approx \frac{N_t}{2}\left(\sum_b \frac{\rho_{bb}^{(2)}}{\tau_b} - \sum_a \frac{\rho_{aa}^{(2)}}{\tau_a}\right) - \frac{N}{\tau_s} + \frac{I}{eV} \quad (3\text{-}37)$$

where I is the injection current density given by,

$$I = eN_t \int \sum_b \Lambda_b d^3\vec{r} = -eN_t \int \sum_a \Lambda_a d^3\vec{r} \quad (3\text{-}38)$$

The first order density matrix elements can be derived as,

$$\rho_{ab}^{(1)} = j\left(\rho_{bb}^{(0)} - \rho_{aa}^{(0)}\right)\frac{R_{ab}}{\hbar}\sum_p \frac{E_p \exp(j\omega_p t)}{j(\omega_p - \omega_{ba}) + \frac{1}{\tau_{in}}} \quad (3\text{-}39)$$

$$\rho_{ba}^{(1)} = \rho_{ab}^{(1)*} = j\left(\rho_{aa}^{(0)} - \rho_{bb}^{(0)}\right)\frac{R_{ba}}{\hbar}\sum_{p}\frac{E_p^{*}\exp\left(-j\omega_p t\right)}{j\left(\omega_{ba} - \omega_p\right) + \dfrac{1}{\tau_{in}}} \tag{3-40}$$

where the electric field of mode p in a laser cavity is expressed with the spatial distribution function $\Phi_p(\vec{r})$ as

$$E_p \exp\left(j\omega_p t\right) = \overline{E}_p(t)\Phi_p(\vec{r})\exp\left(j\omega_p t\right) \tag{3-41}$$

By Substituting Eqn. (3-39) and (3-40) into Eqn. (3-26) we get

$$\begin{aligned} P^{(1)} &= N_t \sum_{b,a}\left(\rho_{ba}^{(1)} R_{ab} + \rho_{ab}^{(1)} R_{ba}\right) \\ &= N_t \sum_{b,a}\left[j\left(\rho_{bb}^{(0)} - \rho_{aa}^{(0)}\right)\frac{\left|R_{ab}\right|^2}{\hbar}\sum_{p}\left\{\frac{E_p \exp\left(j\omega_p t\right)}{j\left(\omega_p - \omega_{ba}\right) + \dfrac{1}{\tau_{in}}} - \frac{E_p^{*}\exp\left(-j\omega_p t\right)}{j\left(\omega_{ba} - \omega_p\right) + \dfrac{1}{\tau_{in}}}\right\}\right] \\ &= \varepsilon_0 \sum_{p}\chi^{(1)}\left(\omega_p\right)E_p \exp\left(j\omega_p t\right) \end{aligned}$$

$$\Rightarrow \chi^{(1)}\left(\omega_p\right) = -\frac{N_t}{j\hbar\varepsilon_0}\sum_{b,a}\frac{\rho_{bb}^{(0)} - \rho_{aa}^{(0)}}{j\left(\omega_p - \omega_{ba}\right) + \dfrac{1}{\tau_{in}}}\left|R_{ba}\right|^2 \tag{3-42}$$

Again, using Eqn. (3-27) the second order density matrix elements can be derived as,

$$\rho_{bb}^{(2)} = -\frac{1}{\hbar^2}\left(\rho_{bb}^{(0)} - \rho_{aa}^{(0)}\right)\left|R_{ba}\right|^2 \sum_{p}\sum_{q}\left[\frac{E_p E_q^{*}\exp\left[j\left(\omega_p - \omega_q\right)t\right]}{\left\{j\left(\omega_p - \omega_{ba}\right) + \dfrac{1}{\tau_{in}}\right\}\left\{j\left(\omega_p - \omega_q\right) + \left(\dfrac{1}{\tau_b} + \dfrac{1}{\tau_s}\right)\right\}} + c.c.\right] \tag{3-43}$$

Derivations of Eqn. (3-39) and (3-43) from the dynamic equation of the density matrix are given in Appendix-B. From Eqn. (3-43) we get,

$$\frac{N_t}{j\varepsilon_0}\rho_{bb}^{(2)} = \sum_{p}\sum_{q}\left[\chi^{(1)}\left(\omega_p\right)\frac{E_p E_q^{*}\exp\left[j\left(\omega_p - \omega_q\right)t\right]}{\dfrac{1}{\tau_b} + \dfrac{1}{\tau_s}}\frac{1}{\hbar} + c.c.\right]$$

$$\Rightarrow \frac{N_t \rho_{bb}^{(2)}}{\tau_b} = \sum_{p}\sum_{q} j\frac{\varepsilon_0}{\hbar}\chi^{(1)}\left(\omega_p\right)E_p E_q^{*}\exp\left[j\left(\omega_p - \omega_q\right)t\right] + c.c. \tag{3-44}$$

Similarly,

$$\frac{N_t \rho_{aa}^{(2)}}{\tau_a} = -\frac{N_t \rho_{bb}^{(2)}}{\tau_b} = -\sum_{p}\sum_{q} j\frac{\varepsilon_0}{\hbar}\chi^{(1)}\left(\omega_p\right)E_p E_q^{*}\exp\left[j\left(\omega_p - \omega_q\right)t\right] + c.c. \tag{3-45}$$

Now, substituting Eqn. (3-34), (3-44) and (3-45) into Eqn. (3-37), dynamic equation for carrier density becomes,

$$\frac{dN}{dt} = -\sum_p \sum_q \frac{\varepsilon_0 \kappa}{\hbar} \left\{ \left[(1+j\alpha)N - N_g - b\left(\lambda_p - \lambda_0\right)^2 \right] E_p E_q^* \exp\left[j\left(\omega_p - \omega_q\right)t \right] + c.c. \right\} - \frac{N}{\tau_s} + \frac{I}{eV} \tag{3-46}$$

In terms of modal photon number S_p defined in Eqn. (3-49) and first order linear gain coefficient A_p defined in Eqn. (3-25) the dynamic equation for carrier number can be approximated from Eqn. (3-46) as

$$\frac{dN}{dt} = -\sum_p A_p S_p - \frac{N}{\tau_s} + \frac{I}{e} \tag{3-47}$$

The derivation of Eqn. (3-47) from Eqn. (3-46) is given in Appendix-C.

4. Rate Equation for Photon Number

Stored energy of optical wave in the cavity of semiconductor laser is calculated from Eqn. (3-10).

$$\begin{aligned} W &= \frac{1}{2}\iiint \left(\varepsilon E^2 + \mu_0 H^2\right) d^3\vec{r} = \iiint \varepsilon E^2 d^3\vec{r} \\ &= \varepsilon \iiint \sum_p \sum_q \left\{ \overline{E}_p(t)\Phi_p(\vec{r}) \exp\left(j\omega_p t\right) + c.c. \right\} \left\{ \overline{E}_q(t)\Phi_q(\vec{r}) \exp\left(j\omega_q t\right) + c.c. \right\} d^3\vec{r} \\ &= 2\varepsilon \iiint \sum_p \left|\overline{E}_p(t)\right|^2 \left|\Phi_p(\vec{r})\right|^2 d^3\vec{r} \\ &= 2\varepsilon \sum_p \left|\overline{E}_p(t)\right|^2 \qquad \left[\iint \left|\Phi_p(\vec{r})\right| d^3\vec{r} = 1\right] \\ &= \sum_p \left(S_p + \frac{1}{2} \right) \hbar\omega_p \end{aligned} \tag{3-48}$$

(This is postulated by quantization of the lasing field [25], [49])

$$\begin{aligned} &\Rightarrow \left|\overline{E}_p(t)\right| = \sqrt{\frac{S_p \hbar\omega_p}{2\varepsilon}} \\ &\Rightarrow \overline{E}_p(t) = \sqrt{\frac{S_p \hbar\omega_p}{2\varepsilon}} \exp\left(j\theta_p\right) \\ &\Rightarrow \left|\overline{E}_p(t)\right|^2 = \frac{\hbar\omega_p}{2\varepsilon} S_p \end{aligned} \tag{3-49}$$

Eqn. (3-20) gives variation of the absolute value of the electric field amplitude as,

$$\frac{d\left|\overline{E}_p(t)\right|}{dt} = \frac{1}{2\varepsilon}\left[\omega_p \,\mathrm{Im}\{\chi\} - \sigma\right] \left|\overline{E}_p(t)\right| \tag{3-50}$$

$$\frac{d\left|\overline{E}_p(t)\right|^2}{dt} = \frac{d\overline{E}_p(t)}{dt}\overline{E}_p^*(t) + \overline{E}_p(t)\frac{d\overline{E}_p^*(t)}{dt}$$
$$= 2\left|\overline{E}_p(t)\right|\frac{d\left|\overline{E}_p(t)\right|}{dt}$$
$$= \frac{1}{\varepsilon}\left[\omega_p \,\mathrm{Im}\{\chi\} - \sigma\right]\left|\overline{E}_p(t)\right|^2 \qquad (3\text{-}51)$$

Substituting Eqn. (3-49) into (3-51) gives variation of the photon number with gain coefficients defined in (3-22)-(3-25) as,

$$\frac{dS_p}{dt} = \left(G_p - G_{th}\right)S_p \qquad (3\text{-}52)$$

The amplification gain coefficient comes from stimulated emission by the semiconductor material in the active region. There is also spontaneous emission in the active region which is added to the photon rate equation (3-52) in a form independent from the photon number as,

$$\frac{dS_p}{dt} = \left(G_p - G_{th}\right)S_p + C_p \qquad (3\text{-}53)$$

where C_p indicates inclusion of the spontaneous emission into mode p.

5. Introducing Nonlinear Gain

We introduce laser polarization as P_{st} and spontaneous emission as P_{sp} to the Maxwell's wave equations. Then from Maxwell's wave equations we have [see Eqn. (3-7)],

$$\nabla^2\vec{E} - \mu\sigma\frac{\partial\vec{E}}{\partial t} - \mu\varepsilon\frac{\partial^2\vec{E}}{\partial t^2} = \mu\frac{\partial^2\vec{P}}{\partial t^2} \qquad (3\text{-}54)$$

and the electric field can be expanded with summed value of the guided modes as [see Eqn. 3-10],

$$\vec{E} = \sum_p \tilde{E}_p(t)\Phi_p(\vec{r})\exp\left(j\omega_p t\right) + c.c. \qquad (3\text{-}55)$$

with $\iiint\left|\Phi_p(\vec{r})\right|^2 d^3\vec{r} = 1$ [defined from Eqn. (3-9)] (3-56)

and $\vec{P} = P_{st} + P_{sp}$ (3-57)

Spatial distribution of the field is given by the relation [see Eqn. 3-8],

$$\left(\nabla^2 + \mu\varepsilon\omega_p^2\right)\Phi_p(\vec{r}) = 0 \qquad (3\text{-}58)$$

After some mathematical treatments we have the following equation [same as we have already derived Eqn. (3-20) and (3-22)],

$$\frac{\partial\overline{E}_p(t)}{\partial t} = -\frac{\sigma}{2\varepsilon}\overline{E}_p(t) - j\frac{\omega_p}{2\varepsilon}\frac{1}{\Delta t}\int_{t-\Delta t}^{t}\iint\vec{P}\Phi_p^*(\vec{r})\exp\left(-j\omega_p t\right)d^3\vec{r}\,dt \qquad (3\text{-}59)$$

Now the power variation in Eqn. (3-51) can be rewritten as,

$$\frac{\partial\left|\overline{E}_p(t)\right|^2}{\partial t} = -\frac{\sigma}{\varepsilon}\left|\overline{E}_p(t)\right|^2 + \mathrm{Im}\left\{\frac{\omega_p}{\varepsilon.\overline{E}_p(t)}\frac{1}{\Delta t}\int_{t-\Delta t}^{t}\int P_{st}\Phi^*_p(\vec{r})\exp\left(-j\omega_p t\right)d^3\vec{r}dt\right\}\left|\overline{E}_p(t)\right|^2 + \mathrm{Im}\left\{\frac{\omega_p}{\varepsilon}\frac{\overline{E}^*_p(t)}{\Delta t}\int_{t-\Delta t}^{t}\int P_{sp}\Phi^*_p(\vec{r})\exp\left(-j\omega_p t\right)d^3\vec{r}dt\right\} \tag{3-60}$$

By using quantized photon number defined in Eqn. (3-49) and using the gain coefficients defined in (3-22) and (3-23), Eqn. (3-60) is changed to the rate equation for the photon number introduced in Eqn. (3-53),

$$\frac{dS_p}{dt} = \left(G_p - G_{th}\right)S_p + C_p \tag{3-61}$$

with $C_p = \frac{2}{\hbar}\mathrm{Im}\left\{\frac{\overline{E}^*_p(t)}{\Delta t}\int_{t-\Delta t}^{t}\int P_{sp}\Phi^*_p(\vec{r})\exp\left(-j\omega_p t\right)d^3\vec{r}dt\right\}$ (3-62)

If we extend the perturbation expansion of the density matrix to count the saturation phenomena, the gain coefficient G_p counted up to the third order polarization is redefined from Eqn. (3-24) as,

$$G_p = G_p^{(1)} - \sum_q G^{(3)}_{p(q)}S_q \tag{3-63}$$

Here linear gain coefficient $G_p^{(1)}$ is same as A_p defined in Eqn. (3-25) without counting the saturation phenomena. To count the saturation phenomena we have to take into account the effect of other mode q to the linear gain coefficient through the beating vibration known as asymmetric gain saturation effect.

Now consider the linear gain coefficient given in Eqn. (3-22) or Eqn. (3-60)

$$\begin{aligned} G_p^{(1)} &= \mathrm{Im}\left\{\frac{\omega_p}{\varepsilon}\frac{1}{\overline{E}_p(t).\Delta t}\int_{t-\Delta t}^{t}\int P^{(1)}\Phi^*_p(\vec{r})\exp\left(-j\omega_p t\right)d^3\vec{r}dt\right\} \\ &= \mathrm{Im}\left\{\frac{\varepsilon_0\omega_p}{\varepsilon\Delta t}\int_{t-\Delta t}^{t}\int\sum_q \chi^{(1)}\left(\omega_q\right)\frac{\overline{E}_q}{\overline{E}_p}\Phi_q(\vec{r})\Phi^*_p(\vec{r})\exp\left\{j\left(\omega_q-\omega_p\right)t\right\}d^3\vec{r}dt\right\} \end{aligned} \tag{3-64}$$

If we restrict the existing modes to be two modes p and q, and express the linear susceptibility in the form of Eqn. (3-34), we have

$$G_p^{(1)} = \frac{\kappa\omega_p}{n_r^2\Delta t}\mathrm{Re}\int_{t-\Delta t}^{t}\left[\int\left\{(1+j\alpha)N - N_g - b\left(\lambda_p-\lambda_0\right)^2\right\}\left|\Phi_p(\vec{r})\right|^2 d^3\vec{r} + \int\left\{(1+j\alpha)N - N_g - b\left(\lambda_p-\lambda_0\right)^2\right\}\Phi_q(\vec{r})\Phi^*_p(\vec{r})\frac{\overline{E}_q}{\overline{E}_p}d^3\vec{r}\right]\exp\left\{j\left(\omega_q-\omega_p\right)t\right\}dt$$

If we substitute to this equation the varying electron density caused by the beating effect of

$$N = \overline{N} + \left\{N_1(x,y)\exp\left[j\left(\omega_q - \omega_p\right)t\right] + c.c.\right\}\cos\left\{\left(\beta_p - \beta_q\right)z\right\} \tag{3-65}$$

where $N_1(x,y)$ is derived in Appendix-D. By performing spatial integration along z-direction and taking time average with Δt, the linear gain becomes,

$$\begin{aligned}
G_p^{(1)} &= \xi a\left\{\overline{N} - N_g - b\left(\lambda_p - \lambda_0\right)^2\right\} \\
&\quad - \mathrm{Re}\left[\int_{-d/2}^{d/2}\int_{-W/2}^{W/2} \frac{(1+j\alpha)\dfrac{\kappa\omega_p}{n_r^2}\dfrac{\varepsilon_0\kappa}{\hbar L}\left(\overline{N} - N_g\right)\left|\overline{E}_q\right|^2\left|T(x,y)\right|^4}{-j\left(\omega_q - \omega_p\right) + \dfrac{1}{\tau_s} + \dfrac{2\varepsilon_0\kappa}{\hbar L}\left(\left|\overline{E}_p\right|^2 + \left|\overline{E}_q\right|^2\right)T(x,y)\right|^2} dxdy\right] \\
&= \xi a\left\{\overline{N} - N_g - b\left(\lambda_p - \lambda_0\right)^2\right\} - \mathrm{Re}\left[\frac{a^2}{2L}\frac{(1+j\alpha)\left(\overline{N} - N_g\right)S_q\dfrac{3\xi^2}{2dW}}{-j\left(\omega_q - \omega_p\right) + \dfrac{1}{\tau_s} + \dfrac{a}{L}\left(S_p + S_q\right)}\right] \\
&\approx \xi a\left\{\overline{N} - N_g - b\left(\lambda_p - \lambda_0\right)^2\right\} - \frac{3\xi^2 a^2}{4V}\frac{\alpha\left(\overline{N} - N_g\right)\left(\omega_p - \omega_q\right)}{\left(\omega_p - \omega_q\right)^2}S_q \\
&\approx \xi a\left\{\overline{N} - N_g - b\left(\lambda_p - \lambda_0\right)^2\right\} - \frac{3\xi^2 a^2}{4V}\frac{\alpha\left(\overline{N} - N_g\right)\left(\omega_p - \omega_q\right)}{\left(\omega_p - \omega_q\right)^2}S_q
\end{aligned} \tag{3-66}$$

$\int_{-d/2}^{d/2}\int_{-W/2}^{W/2}\left|T(x,y)\right|^4 dxdy$ and $\int_{-d/2}^{d/2}\int_{-W/2}^{W/2}\left|T(x,y)\right|^2 dxdy$ are also derived in appendix-D.

If we consider electron numbers instead of electron density the gain coefficient in Eqn. (3-66) becomes

$$\begin{aligned}
G_p^{(1)} &= \frac{\xi a}{V}\left\{\overline{N} - N_g - bV\left(\lambda_p - \lambda_0\right)^2\right\} - \frac{3\xi^2 a^2}{4V^2}\frac{\alpha\left(\overline{N} - N_g\right)\left(\omega_p - \omega_q\right)}{\left(\omega_p - \omega_q\right)^2}S_q \\
&\approx A_p - \frac{3\lambda_p^2}{8\pi c}\left(\frac{a\xi}{V}\right)^2\frac{\alpha\left(N - N_g\right)}{\lambda_q - \lambda_p}S_q \\
&\equiv A_p - H_{p(q)}S_q
\end{aligned} \tag{3-67}$$

where $H_{p(q)}$ is asymmetric nonlinear saturation gain defined as,

$$H_{p(q)} = \frac{3\lambda_p^2}{8\pi c}\left(\frac{a\xi}{V}\right)^2\frac{\alpha\left(N - N_g\right)}{\lambda_q - \lambda_p} \tag{3-68}$$

The saturation phenomena are taken into account with the higher order terms. However, examination up to third order term is enough to understand the most nonlinear effects in semiconductor lasers.

According to the perturbation expansion of the density matrix, third order polarization is given by,

$$\begin{aligned} P^{(3)} &= N_t \sum_{b,a} \left(\rho_{ba}^{(3)} R_{ab} + \rho_{ab}^{(3)} R_{ba} \right) \\ &= \varepsilon_0 \sum_p \sum_q \sum_r \chi^{(3)} \left(\omega_p, \omega_q, \omega_r \right) : \overline{E}_p \overline{E}_q \overline{E}_r \Phi_p(\vec{r}) \Phi_q(\vec{r}) \Phi_r(\vec{r}) \\ &\quad \exp\left\{ j \left(\omega_p + \omega_q + \omega_r \right) t \right\} \end{aligned} \tag{3-69}$$

From this third order polarization, the third-order gain coefficient of Eqn. (3-63) is defined by,

$$\begin{aligned} G_{p(q)}^{(3)} &= -\frac{\hbar \omega_p^2}{2\varepsilon_o n_r^3} \iiint \mathrm{Im}\left\{ \sum \chi^{(3)} \left(\omega_p, -\omega_q, \omega_q \right) \right\} \left| \Phi_p(\vec{r}) . \Phi_q(\vec{r}) \right|^2 d^3 \vec{r} \\ &\approx \frac{2aR_{cv}^2 \omega_p}{\left(1 + \delta_{p,q} \right) \varepsilon_0 n_r^2 \hbar \left[\left(\omega_p - \omega_q \right)^2 + \frac{1}{\tau_{in}^2} \right]} \int \left(N - N_s \right) \left| \Phi_p(\vec{r}) . \Phi_q(\vec{r}) \right|^2 d^3 \vec{r} \end{aligned} \tag{3-70}$$

where R_{cv} is the absolute value of the dipole moment.

When only two specific modes p and q exist, terms having the frequency combinations of $\left(\omega_q - \omega_q + \omega_p \right)$ and $\left(\omega_p - \omega_q + \omega_q \right)$ form the third-order gain coefficient for mode p. And $\int \left(N - N_s \right) \left| \Phi_p(\vec{r}) . \Phi_q(\vec{r}) \right|^2 d^3 \vec{r}$ is the difference of spatial distribution.

$$\int \left| \Phi_p(\vec{r}) \Phi_q(\vec{r}) \right|^2 d^3 \vec{r} = \frac{3\xi^2}{2dW} . \frac{1}{L} \left(1 + \frac{1}{2} \delta_{pq} \right) = \left(2 + \delta_{pq} \right) \frac{3\xi^2}{4V} \tag{3-71}$$

Eqn. (3-71) is derived from the spatial distribution of electric field with the cavity length L presented in Appendix-D.

Hence, for $p=q$ (in terms of carrier numbers)

$$\begin{aligned} G_{p(p)}^{(3)} &\approx \frac{2aR_{cv}^2 \omega_p \tau_{in}^2}{2\varepsilon_0 n_r^2 \hbar} \left(N - N_s \right) \frac{9\xi^2}{4V} . \frac{1}{V} \\ &= \frac{9}{4} \frac{\hbar \omega_p}{\varepsilon_0 n_r^2} \left(\frac{\xi \tau_{in}}{\hbar V} \right)^2 aR_{cv}^2 \left(N - N_s \right) \equiv B_p \end{aligned} \tag{3-72}$$

This is also known as self-saturation coefficient, and for $p \neq q$

$$\begin{aligned} G_{p(q)}^{(3)} &= \frac{2aR_{cv}^2 \omega_p \tau_{in}^2}{\varepsilon_0 n_r^2 \hbar \left\{ 1 + \tau_{in}^2 \left(\omega_p - \omega_q \right)^2 \right\}} \left(N - N_s \right) \frac{3\xi^2}{2V} . \frac{1}{V} \\ &= \frac{4}{3} \frac{B_p}{1 + \tau_{in}^2 \left(\omega_p - \omega_q \right)^2} \\ &= \frac{4}{3} \frac{B_p}{\left(\frac{2\pi c \tau_{in}}{\lambda_p^2} \right) \left(\lambda_p - \lambda_q \right)^2 + 1} \equiv G_{q(p)}^{(3)} \equiv D_{p(q)} \end{aligned} \tag{3-73}$$

which is known as cross-saturation coefficient.

Finally from the definitions of linear and nonlinear gain coefficients with taking into account the saturation effects, the gain coefficient G_p in Eqn. (3-63) becomes,

$$G_p = A_p - B_p S_p - \sum_{p \neq q} \left(D_{p(q)} + H_{p(q)} \right) S_q \tag{3-74}$$

The spontaneous emission from an electron-hole pair is generated by all possible optical fields surrounding the electron-hole pair. Only part of the spontaneous emission enters into the lasing mode p.

The stimulated emission is given with $A_p S_p$ in Eqn. (3-47), while an approximated expression of the gain is given in Eqn. (3-25). Therefore, terms $\xi a N S_p / V$ and $\xi a N_g S_p / V$ must correspond to the optical emission and the absorption, respectively. Then, the spontaneous emission entering into mode p must approximately be expressed with $\xi a N / V$.

If wavelength profile is taken into account with the half width of $\delta\lambda$, the spontaneous emission coefficient C_p in Eqn. (3-61) with Eqn. (3-62) becomes,

$$C_p = \frac{\xi a N / V}{\left[2\left(\lambda_p - \lambda_0 \right) / \delta\lambda \right]^2 + 1} \tag{3-75}$$

6. Introduction of the Noise Sources

Origin of the noise is the fluctuation on optical emission. To introduce the fluctuation in the classical Maxwell's wave equations let the polarization consists of the laser polarization P_{st} and the spontaneous polarization P_{sp} as has been introduced in Eqn. (3-57).

With this definition variation of the field amplitude is represented as,

$$\begin{aligned} \frac{\partial \overline{E}_p(t)}{\partial t} &= -\frac{\sigma}{2\varepsilon} \overline{E}_p(t) - j \frac{\omega_p}{2\varepsilon} \frac{1}{.\Delta t} \int_{t-\Delta t}^{t} \iint \left(P_{st} + P_{sp} \right) \Phi_p^*(\vec{r}) \exp\left(- j\omega_p t \right) d^3\vec{r} dt \\ &= -\frac{\sigma}{2\varepsilon} \overline{E}_p(t) - \frac{j\omega_p}{2n_r^2} \int \chi\left(\omega_p \right) \left| \Phi_p(\vec{r}) \right|^2 d^3\vec{r} \overline{E}_p(t) + U_p(t) \end{aligned} \tag{3-76}$$

where $P_{st} = \varepsilon_0 \sum_p \chi\left(\omega_p \right) \overline{E}_p(t) \Phi_p(\vec{r}) \exp\left(j\omega_p t \right) + c.c.$ is the laser polarization represented with laser susceptibility in which both linear and nonlinear effects are included, and $U_p(t)$ represents inclusion of the spontaneous emission.

$$U_p(t) = -\frac{j\omega_p}{2\varepsilon} . \frac{1}{\Delta t} \int_{t-\Delta t}^{t} \iint P_{sp} \Phi_p^*(\vec{r}) \exp\left(- j\omega_p t \right) d^3\vec{r} dt \tag{3-77}$$

If we put $\overline{E}_p(t) = \left| \overline{E}_p(t) \right| \exp\left\{ j\theta_p(t) \right\}$ in Eqn. (3-76) we get the following relation,

$$\frac{\partial \overline{E}_p(t)}{\partial t} = \frac{\partial \left|\overline{E}_p(t)\right|}{\partial t}\exp\left\{j\theta_p(t)\right\} + j\frac{\partial \theta_p(t)}{\partial t}\left|\overline{E}_p(t)\right|\exp\left\{j\theta_p(t)\right\}$$

$$= -\frac{\sigma}{2\varepsilon}\left|\overline{E}_p(t)\right|\exp\left\{j\theta_p(t)\right\} - j\frac{\omega_p}{2n_r^2}\int \chi(\omega_p)\left|\Phi_p(\vec{r})\right|^2 d^3\vec{r}\left|\overline{E}_p(t)\right|\exp\left\{j\theta_p(t)\right\} + U_p(t)$$

After multiplying the above equation with $\exp\{-j\theta_p(t)\}$ if we separate the real and imaginary parts then we get the relations,

$$\frac{\partial \left|\overline{E}_p(t)\right|}{\partial t} = -\frac{\sigma}{2\varepsilon}\left|\overline{E}_p(t)\right| + \frac{\omega_p}{2n_r^2}\mathrm{Im}\left\{\int \chi(\omega_p)\left|\Phi_p(\vec{r})\right|^2 d^3\vec{r}\left|\overline{E}_p(t)\right|\right\} + \mathrm{Re}\left\{U_p(t)\exp\left\{-j\theta_p(t)\right\}\right\}$$

$$\Rightarrow \frac{\partial \left|\overline{E}_p(t)\right|^2}{\partial t} = 2\left|\overline{E}_p(t)\right|\frac{d\left|\overline{E}_p(t)\right|}{dt}$$

$$= -\frac{\sigma}{\varepsilon}\left|\overline{E}_p(t)\right|^2 + \frac{\omega_p}{n_r^2}\mathrm{Im}\left\{\int \chi(\omega_p)\left|\Phi_p(\vec{r})\right|^2 d^3\vec{r}\left|\overline{E}_p(t)\right|^2\right\} + 2\left|\overline{E}_p(t)\right|\mathrm{Re}\left\{U_p(t)\exp\left\{-j\theta_p(t)\right\}\right\} \quad (3\text{-}78)$$

$$\text{and}\ \frac{\partial \theta_p(t)}{\partial t} = -\frac{\omega_p}{2n_r^2}\mathrm{Re}\left\{\int \chi(\omega_p)\left|\Phi_p(\vec{r})\right|^2 d^3\vec{r}\left|\overline{E}_p(t)\right|\right\} + \frac{1}{\left|\overline{E}_p(t)\right|}\mathrm{Im}\left\{U_p(t)\exp\left\{-j\theta_p(t)\right\}\right\} \quad (3\text{-}79)$$

By considering the inclusion of the spontaneous emission we can rewrite the relation between the square value of the electric field amplitude and photon number introduced in Eqn. (3-49) to be,

$$\frac{2\varepsilon}{\hbar\omega_p}\left|\overline{E}_p(t)\right|^2 = \begin{cases} S_p + 1 & \text{for optical emission} \\ S_p & \text{for optical absorption} \end{cases} \quad (3\text{-}80)$$

Then Eqn. (3-78) is rewritten as a rate equation by adding a source of fluctuation $F_{Sp}(t)$ to Eqn. (3-61) as

$$\frac{dS_p}{dt} = \left(G_p - G_{th}\right)S_p + C_p + F_{Sp}(t) \quad (3\text{-}81)$$

$$\text{where}\ F_{Sp}(t) = \frac{4\varepsilon}{\hbar\omega_p}\left|\overline{E}_p(t)\right|\mathrm{Re}\left\{U_p(t)\exp\left\{-j\theta_p(t)\right\}\right\} \quad (3\text{-}82)$$

By neglecting the effect of higher order polarizations on phase variation and using Eqn. (3-34) and (C-5) the temporal variation of phase in Eqn. (3-79) can be written as,

$$\frac{d\theta_p(t)}{dt} = \frac{\alpha a\xi}{2V}\left(N - \overline{N}\right) + F_{\theta p}(t) \quad (3\text{-}83)$$

where $\overline{N}$ is the time average value of the injected electron numbers and

$$F_{\theta p}(t) = \frac{1}{\left|\overline{E}_p(t)\right|}\mathrm{Im}\left\{U_p(t)\exp\left\{-j\theta_p(t)\right\}\right\} \quad (3\text{-}84)$$

The functions $F_{Sp}(t)$ and $F_{\theta p}(t)$ are Langevin noise sources. The mean values of these sources are zero, because the mean value of $U_p(t)$ is zero as follows.

$$\left\langle F_{Sp}(t)\right\rangle = \left\langle F_{\theta p}(t)\right\rangle = 0 \tag{3-85}$$

Auto-correlation or mutual correlation between the noise sources on the photon numbers of modes p and q are,

$$\left\langle F_{Sp}(t)F_{Sq}(t')\right\rangle = \left(\frac{4\varepsilon}{\hbar\omega_p}\right)^2 \left|\overline{E}_p(t)\right|^2 \left\langle \mathrm{Re}\left\{U_p(t)\exp\left\{-j\theta_p(t)\right\}\right\}\mathrm{Re}\left\{U_q(t')\exp\left\{-j\theta_q(t')\right\}\right\}\right\rangle$$

$$\Rightarrow V_{SpSp}\delta_{pq}\delta(t-t') = \left[\left\{\frac{\xi a}{V}\left(N+N_g\right)+G_{th}\right\}S_p + \frac{\xi aN}{V}\right]\delta_{pq}\delta(t-t') \tag{3-86}$$

This is for the statistical distribution of total photon number fluctuations due to electron transitions forms the Poisson's distribution. Then, correlated value for optical emission is same as total transition probability at steady state in Eqn. (3-81).

Sources of the photon fluctuation and phase fluctuation should be orthogonal with relation of

$$\left\langle \mathrm{Re}\left\{U_p(t)\exp\left\{-j\theta_p(t)\right\}\right\}\mathrm{Im}\left\{U_p(t)\exp\left\{-j\theta_p(t)\right\}\right\}\right\rangle = 0 \tag{3-87}$$

However, auto-correlation of the real and imaginary parts must be identical, because the fluctuation is caused by temporal random vibration.

$$\left\langle \mathrm{Re}^2\left\{U_p(t)\exp\left\{-j\theta_p(t)\right\}\right\}\right\rangle = \left\langle \mathrm{Im}^2\left\{U_p(t)\exp\left\{-j\theta_p(t)\right\}\right\}\right\rangle \tag{3-88}$$

Therefore, relation between noise sources of the photon number and the phase is,

$$\begin{aligned}\left\langle F_{\theta p}(t)F_{\theta q}(t')\right\rangle &= \frac{1}{\left|\overline{E}_p(t)\right|^2}\left\langle \mathrm{Im}\left\{U_p(t)\exp\left\{-j\theta_p(t)\right\}\right\}\mathrm{Im}\left\{U_q(t')\exp\left\{-j\theta_q(t')\right\}\right\}\right\rangle \\ &= \left(\frac{\hbar\omega_p}{4\varepsilon}\right)^2 \frac{1}{\left|\overline{E}_p(t)\right|^4}\left\langle F_{Sp}(t)F_{Sq}(t')\right\rangle \\ &= \frac{1}{4\left(S_p+1\right)^2}\left\langle F_{Sp}(t)F_{Sq}(t')\right\rangle \end{aligned} \tag{3-89}$$

Because $\left\langle \mathrm{Re}\left\{U_p(t)\exp\left\{-j\theta_p(t)\right\}\right\}\right\rangle$ and $\left\langle \mathrm{Im}\left\{U_p(t)\exp\left\{-j\theta_p(t)\right\}\right\}\right\rangle$ are orthogonal, cross-correlation of the fluctuation sources between photon number and phase is obviously zero.

$$\left\langle F_{Sp}(t)F_{\theta q}(t')\right\rangle = 0 \tag{3-90}$$

Variation of the electron density has been derived as variation of the diagonal elements of the density matrix. Hence, variation of the electron number N can simply be written by modification of Eqn. (3-47) by adding a fluctuating term $F_N(t)$.

$$\frac{dN}{dt} = -\sum_p A_p S_p - \frac{N}{\tau_s} + \frac{I}{e} + F_N(t) \tag{3-91}$$

The function $F_N(t)$ is the Langevin noise source on the carrier number and is mathematically characterized by

$$\langle F_N(t) \rangle = 0 \tag{3-92}$$

$$\langle F_N(t) F_N(t') \rangle = \left\{ \frac{\xi a}{V} (N + N_g) \sum_p S_p + \frac{N}{\tau_s} + \frac{I}{e} \right\} \delta(t - t') \tag{3-93}$$

The cross-correlation between photon number and electron number is picked up by counting common terms in Eqn. (3-81) and (3-91). Therefore, the cross-correlation is given by,

$$\langle F_{Sp}(t) F_N(t') \rangle = -\frac{\xi a}{V} \{ (N + N_g) S_p + N \} \delta(t - t') \tag{3-94}$$

The fluctuating source $F_{\theta p}(t)$ of the optical phase θ_p introduced in Eqn. (3-83) does not have any specific relation with the change of the photon number given in Eqn. (3-81). Therefore

$$\langle F_{\theta p}(t) F_N(t') \rangle = 0 \tag{3-95}$$

7. Introducing Optical Feedback Effect

The effect of optical feedback can be taken into account by two alternative methods. One is in the form of optical injection, where the time delay of the reflected light is taken into account [3], [50]-[52]. Another method takes into account the external cavity modes formed between the reflecting point and the front facets of the laser [14]. In our model, the OFB is counted as the time delay of the laser light at the front facet due to round trip in the external cavity.

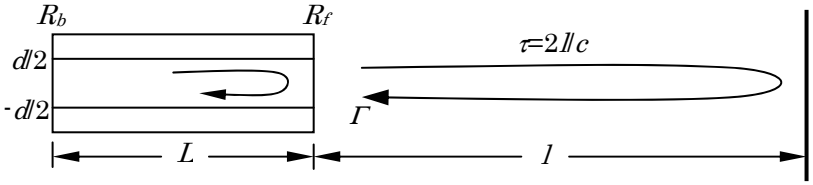

Fig. 3-1. Operation of a semiconductor laser under optical feedback.

Operation of a semiconductor laser under optical feedback is illustrated in Fig. 3-1 where an external reflector is located at a distance $l>>L$ from the laser front facet with reflectivity R_f. Ratio of the feedbacked light to the surface of the front facet is Γ. $(1-R_f)\eta\Gamma$ is power rate coupling to the lasing field in the laser active region, where η is a coupling coefficient from the feedbacked light to the active region. Time delay from the light output at the laser front facet to return back is

$$\tau = \frac{2l}{c} \tag{3-96}$$

The electric field in the laser is now presented in a form of the traveling wave as,

$$E(t,\vec{r}) = \sum_p \left\{ E_p^{(+)}(z,t)T(x,y)\exp\left(-j\beta_p z\right) + E_p^{(-)}(z,t)T(x,y)\exp\left\{-j\beta_p(L-z)\right\}\right\} + c.c. \tag{3-97}$$

Since the backward propagating component is given with summed value of directly reflected wave at the front facet and re-injected wave which travel out time τ after escapes out at the front facet,

$$\begin{aligned} E_p^{(-)}(L,t) &= \sqrt{R_f}\,E_p^{(+)}(L,t) + \left(1-R_f\right)\sqrt{\eta\Gamma}\exp\left(-j\omega_p\tau\right)E_p^{(+)}(L,t-\tau) \\ &= U_p\sqrt{R_f}\,E_p^{(+)}(L,t) \end{aligned} \tag{3-98}$$

where $E_p^{(+)}(L,t-\tau)$ is the amplitude of the forward wave at t-τ, $\exp\left(-j\omega_p\tau\right)$ is the phase delay of one time round trip and

$$\begin{aligned} U_p &= 1+\left(1-R_f\right)\sqrt{\frac{\eta\Gamma}{R_f}}\exp\left(-j\omega_p\tau\right)\frac{E_p^{(+)}(L,t-\tau)}{E_p^{(+)}(L,t)} \\ &= 1+\left(1-R_f\right)\sqrt{\frac{\eta\Gamma}{R_f}}\exp\left(-j\omega_p\tau\right)\frac{\left|\overline{E}_p^{(+)}(L,t-\tau)\right|}{\left|\overline{E}_p^{(+)}(L,t)\right|}\exp\left[j\left\{\theta_p(t-\tau)-\theta_p(t)\right\}\right] \\ &= 1+\left(1-R_f\right)\sqrt{\frac{\eta\Gamma}{R_f}}\exp\left(-j\omega_p\tau\right)\sqrt{\frac{S_p(t-\tau)}{S_p(t)}}\exp\left[j\left\{\theta_p(t-\tau)-\theta_p(t)\right\}\right] \\ &= \left|U_p\right|\exp(-j\varphi) \end{aligned} \tag{3-99}$$

$$\text{with } \varphi = -\tan^{-1}\frac{\mathrm{Im}U_p}{\mathrm{Re}U_p} + m\pi \qquad \left(-\pi \le \varphi \le \pi\right) \tag{3-100}$$

Now if we count the effect of optical feedback in changes of the threshold gain level and phase then from the laser oscillation condition we get the new forms of dynamic equations for photon number and phase in Eqn. (3-81) and (3-83) as

$$\frac{dS_p}{dt} = \left(G_p - G_{th} + \frac{c}{n_r L}\ln\left|U_p\right|\right)S_p + C_p + F_{Sp}(t) \tag{3-101}$$

$$\frac{d\theta_p(t)}{dt} = \frac{1}{2}\left[\frac{\alpha a\xi}{V}\left(N-\overline{N}\right) - \frac{c}{n_r L}\varphi\right] + F_{\theta p}(t) \tag{3-102}$$

Chapter IV: Simulation and Results Discussion

This chapter analyzes dynamics and operation of semiconductor lasers under optical feedback. First an improved set of rate equations are given formulated in Chapter III. After that we present some numerical data based on our proposed model and analyze the data with support of some previously obtained experimental measurement. Our analysis is broadly divided into two parts. In the first part we discuss about properties of the intensity noise induced by OFB in semiconductor lasers and the second part describes reduction mechanism of the OFB noise using superposition of high frequency current injection.

1. Improved Rate Equations

Operation of a semiconductor laser under optical feedback (OFB) is illustrated in Fig. 3-1. The cavity length and the effective refractive index of the laser are L and n_r, respectively. Distance between the laser and a reflecting mirror is l. Light emitted from the laser front facet with reflectivity R_f is assumed to travel single round-trip between the front facet and the external reflecting mirror with optical feedback ratio Γ, then re-injects into the laser cavity. The round-trip time is $\tau=2l/c$, where c is the speed of light in vacuum.

The multimode rate equations for the modal photon number $S_p(t)$, modal phase $\theta_p(t)$ and number of injected electrons $N(t)$ are derived in Chapter III which can be summarized as

$$\frac{dS_p}{dt} = \left(G_p - G_{tho} + \frac{c}{n_r L} \ln\left|U_p\right| \right) S_p + C_p + F_{Sp}(t) \tag{3-101}$$

$$\frac{d\theta_p(t)}{dt} = \frac{1}{2}\left[\frac{\alpha a \xi}{V}\left(N - \overline{N}\right) - \frac{c}{n_r L}\varphi \right] + F_{\theta p}(t) \tag{3-102}$$

$$\frac{dN}{dt} = -\sum_p A_p S_p - \frac{N}{\tau_s} + \frac{I}{e} + F_N(t) \tag{3-91}$$

where G_p is the gain of the mode p whose wavelength is λ_p.

G_{tho} is the threshold gain of the solitary laser.

U_p is a function counting contribution of the OFB to the instantaneous photon number $S_p(t)$ of the mode p.

These parameters are defined as

$$G_p = A_p - B_p S_p - \sum_{p \neq q}\left(D_{p(q)} + H_{p(q)}\right) S_q \tag{3-74}$$

$$G_{tho} = \frac{c}{n_r}\left[k + \frac{1}{2L}\ln\frac{1}{R_f R_b} \right] \tag{3-23}$$

$$U_p = 1 + (1 - R_f)\sqrt{\frac{\eta\Gamma}{R_f}}\exp(-j\omega_p\tau)\sqrt{\frac{S_p(t-\tau)}{S_p(t)}}\exp\left[j\{\theta_p(t-\tau) - \theta_p(t)\}\right]$$
$$= |U_p|\exp(-j\varphi) \tag{3-99}$$

$$\varphi = -\tan^{-1}\frac{\mathrm{Im}U_p}{\mathrm{Re}U_p} + m\pi \qquad (-\pi \le \varphi \le \pi) \tag{3-100}$$

Here, A_p is the linear gain, B_p is the coefficient of self-suppression, and $D_{p(q)}$ and $H_{p(q)}$ are the coefficients of symmetric gain saturation and asymmetric gain saturation, respectively. These coefficients are given by

$$A_p = \frac{a\xi}{V}\left[N - N_g - bV(\lambda_p - \lambda_0)^2\right] \tag{3-25}$$

$$B_p = \frac{9}{4}\frac{\hbar\omega_p}{\varepsilon_0 n_r^2}\left(\frac{\xi\tau_{in}}{\hbar V}\right)^2 aR_{cv}^2(N - N_s) \tag{3-72}$$

$$D_{p(q)} = \frac{4}{3}\frac{B_p}{\left(\frac{2\pi c\tau_{in}}{\lambda_p^2}\right)(\lambda_p - \lambda_q)^2 + 1} \tag{3-73}$$

$$H_{p(q)} = \frac{3\lambda_p^2}{8\pi c}\left(\frac{a\xi}{V}\right)^2\frac{\alpha(N - N_g)}{\lambda_q - \lambda_p} \tag{3-68}$$

In Eqn. (3-101),

a is the differential gain coefficient,

ξ is the field confinement factor,

V is the volume of the active region,

λ_0 is the peak wavelength and

$\delta\lambda$ is the half-width of spontaneous emission.

In Eqn. (3-102)

α is the linewidth enhancement factor and

$\overline{N}$ is the time average value of $N(t)$.

In Eqn. (3-91)

τ_s is the electron lifetime,

I is the injection current and

e is the electron charge.

In Eqn. (3-23)

k is the internal loss in the laser cavity.

In Eqn. (3-99)

η is the coupling coefficient into the active region,

Γ is the optical feedback ratio to the laser cavity,

$\omega_p = 2\pi c/\lambda_p$ is the angular frequency of mode p,

$\omega_p \tau$ is the phase delay of the field in the roundtrip time.

In Eqn. (3-25), (3-72), (3-73) and (3-68)

N_g is the electron number at transparency,

b is the width of the linear gain coefficient,

$\hbar$ is the reduced Planck constant,

$\omega = 2\pi c/\lambda_0$ is the central angular frequency,

τ_{in} is the intraband relaxation time,

R_{cv} is the dipole moment and

N_s is the electron number characterizing the self-suppression coefficient.

The central mode, p=0 with wavelength λ_0, is assumed to lie at the centre of the spectrum of gain. The wavelength of the other modes can be written as

$$\lambda_p = \lambda_0 + p\Delta\lambda = \lambda_0 + p\frac{\lambda_0^2}{2n_r L} \qquad p = 0,\pm1,\pm2,... \qquad (4\text{-}1)$$

The effect of high-frequency injection is included by modulating the injection current periodically with a modulation frequency f_M. The pumping term I in equation (3-91) then has to be replaced by

$$I = I_D + I_M \cos(2\pi f_M t) \qquad (4\text{-}2)$$

where I_D is the bias current,

I_M is the modulation current and

f_M is the frequency of sinusoidal modulation.

1-a. Constructing Langevin Noise Sources

Obtaining explicit forms for the functions $F_{Sp}(t)$, $F_{\theta p}(t)$ and $F_N(t)$ introduced in Eqn. (3-101), (3-102) and (3-91) respectively is necessary to perform numerical integration of the laser rate equations. Here, we demonstrate a general technique to simultaneously generate those cross-correlated noise sources.

To achieve the cross-correlations given in Eqn. (3-90), (3-94) and (3-95) we define here three new equations for photon number, phase and a variable $N + \sum_p K_p S_p$ (where K_p is real number) from the rate equations (3-101), (3-102) and (3-91) such as,

$$\frac{dS_p}{dt} = \left(G_p - G_{th} + \frac{c}{n_r L} \ln\left|U_p\right| \right) S_p + C_p + F_{Sp}(t) \tag{4-3}$$

$$\frac{d\theta_p(t)}{dt} = \frac{1}{2}\left[\frac{\alpha a \xi}{V}\left(N - \bar{N}\right) - \frac{c}{n_r L}\varphi \right] + F_{\theta p}(t) \tag{4-4}$$

$$\begin{aligned} \frac{d\left\{ N + \sum_p K_p S_p \right\}}{dt} &= \left[-\sum_p A_p S_p - \frac{N}{\tau_s} + \frac{I}{e} \right] \\ &\quad + \sum_p K_p \left[\left(G_p - G_{th} + \frac{c}{n_r L} \ln\left|U_p\right| \right) S_p + C_p \right] \\ &\quad + \left[F_N(t) + \sum_p K_p F_{Sp}(t) \right] \end{aligned} \tag{4-5}$$

When parameter K_p is defined from Eqn. (3-86) and (3-94) as

$$K_p = -\frac{V_{SpN}}{V_{SpSp}} = \frac{\frac{\xi a}{V}\left(N + N_g\right) + N}{\left\{ \frac{\xi a}{V}\left(N + N_g\right) + G_{th} \right\} S_p + \frac{\xi a N}{V}} \tag{4-6}$$

the noise functions $F_{Sp}(t)$, $F_{\theta p}(t)$ and $N + \sum_p K_p S_p$ become mutually orthogonal without cross-correlations among them so that we can define them independently. The noise sources are then expressed as,

$$F_{Sp}(t) = \sqrt{\frac{V_{SpSp}}{\Delta t}} . g_s \tag{4-7}$$

$$F_{\theta p}(t) = \sqrt{\frac{V_{SpSp}}{\Delta t}} \cdot \frac{1}{2\left(S_p + 1\right)} . g_\theta \tag{4-8}$$

$$F_N(t) + \sum_p K_p F_{Sp}(t) = \sqrt{\frac{V_{NN}(t) + \sum_p K_p V_{SpN}(t)}{\Delta t}} . g_N$$

$$\Rightarrow F_N(t) = \sqrt{\frac{V_{NN}(t) + \sum_p K_p V_{SpN}(t)}{\Delta t}} . g_N - \sum_p K_p F_{Sp}(t) \tag{4-9}$$

where the variances V_{SpSp}, V_{NN} and V_{SpN} are defined from Eqn. (3-86), (3-93) and (3-94) respectively as

$$V_{SpSp} = \left\{ \frac{\xi a}{V}\left(N + N_g\right) + G_{th} \right\} S_p + \frac{\xi a N}{V} \tag{4-10}$$

$$V_{NN} = \frac{\xi a}{V}\left(N + N_g\right) \sum_p S_p + \frac{N}{\tau_s} + \frac{I}{e} \tag{4-11}$$

$$V_{SpN} = -\frac{\xi a}{V}\left\{\left(N + N_g\right)S_p + N\right\} \tag{4-12}$$

with $\Delta t = t_{i+1} - t_i$ is the time interval between sampling time of t_{i+1} and t_i.

Here g_s, g_θ and g_N are three independent random numbers forming Gaussian probability distribution functions with zero mean values of $\langle g_s \rangle = \langle g_\theta \rangle = \langle g_N \rangle = 0$ and unity variances $\langle g_s^2 \rangle = \langle g_\theta^2 \rangle = \langle g_N^2 \rangle = 1$ for ensembles of time.

In Eqn. (4-7), (4-8) and (4-9) g_s, g_θ and g_N are independent random numbers given by [25]

$$-1 \le g_s \le 1,\ -1 \le g_\theta \le 1 \text{ and } -1 \le g_N \le 1, \tag{4-13}$$

1-b. Calculating Relative Intensity Noise

The intensity noise is the fluctuation in the photon number $S_p(t)$. RIN (Relative Intensity Noise) is evaluated from fluctuations $\delta S(t_i) = S(t_i) - \bar{S}$ of the total photon number $S(t_i) = \sum_p S_p(t_i)$ according to the definition of [12]

$$\begin{aligned} RIN &= \frac{1}{\bar{S}^2}\left\{\frac{1}{T}\int_0^T\left[\int_0^\infty \delta S(t)\delta S(t+\tau)\exp(j\omega\tau)d\tau\right]dt\right\} \\ &= \frac{1}{\bar{S}^2}\left\{\frac{1}{T}\left|\int_0^T \delta S(\tau)\exp(-j\omega\tau)d\tau\right|^2\right\} \end{aligned} \tag{4-14}$$

RIN is then computed directly from the obtained values of $S(t)$ by employing the fast Fourier transform (FFT) to integrate the discrete version of equation (4-14) as

$$RIN = \frac{1}{\bar{S}^2}\frac{\Delta t^2}{T}\left|FFT\left[\delta S(t_i)\right]\right|^2 \tag{4-15}$$

where T is the total time period of calculation and

$\bar{S} = \sum_p \bar{S}_p$ in which $\bar{S}_p$ is the time average photon number of $S_p(t)$.

The rate equations derived as Eqn. (3-101), (3-102) and (3-91) with modulation current given in Eqn. (4-2) can be used to obtain the RIN of the diode laser for the modulated signal in the presence of optical feedback by integrating them numerically and calculating the spectrum of intensity fluctuations.

In experiment, the individual modes are not distinguished. Rather, the system performance is governed by the total photon number [18]. The RIN for the total photon number with superposition of high frequency current is applied is therefore given by

$$RIN = \frac{\langle S_\Omega^2 \rangle}{|\bar{S}|^2} \qquad (4\text{-}16)$$

where S_Ω is calculated from the fluctuations $\delta S(t_i) = S(t_i) - \bar{S}$ of the total photon number $S(t_i) = \sum_p S_p(t_i)$ and $\bar{S}$ is the time average of the total photon number.

The values of intensity fluctuation for modulated signal are then computed in terms of RIN by using Eqn. (4-15).

2. Procedure of Numerical Calculation

Table 4.a: Values of the Simulation Parameters for 850nm GaAs Semiconductor Laser

Symbol	Definition	Value	Unit
a	tangential gain coefficient	2.75×10^{-12}	m^3s^{-1}
b	dispersion parameter of the linear gain spectrum	3×10^{19}	m^3A^{-2}
$\lvert R_{cv}\rvert^2$	squared absolute value of the dipole moment	2.8×10^{-57}	C^2m^2
$\Delta\lambda$	half-width of spontaneous emission	23	nm
α	Linewidth enhancement factor	2.6	-
ξ	confinement factor of field	0.2	-
τ_{in}	electron intraband relaxation time	0.1	ps
τ_S	average electron lifetime	2.79	ns
N_S	electron number characterizing non-linear gain	1.7×10^{8}	-
N_g	electron number at transparency	2.1×10^{8}	-
V	volume of the laser active region	100	μm^3
d	thickness of the laser active region	0.11	µm
L	length of the laser active region	300	µm
n_r	refractive index of laser active region	3.6	-
k	internal loss in the laser cavity	10	cm^{-1}
R_f	reflectivity of front facet	0.30	-
R_b	reflectivity of back facet	0.60	-

The proposed model is applied to 850nm GaAs lasers to investigate the effect of external optical feedback on the characteristics of intensity

noise in the lasers. The systems of rate equations (3-101), (3-102) and (3-91) are solved numerically by means of the fourth-order Runge-Kutta method [12], [53]. The time-step of integration is set as short as Δt=5ps. This short time step corresponds to a cutoff Fourier frequency of 100GHz that is high enough to guarantee fine resolution of the OFB-induced dynamics. Thirteen longitudinal modes are considered here in the calculation.

The distance to the reflecting mirror is L=12cm which corresponds to external cavity modes whose frequency spacing is $f_{ex}=1/\tau$=1.25GHz and L=15cm which corresponds to external cavity modes whose frequency spacing is $f_{ex}=1/\tau$=1GHz. For the coupling constant we have used η=0.02 to estimate the optical feedback ratio Γ.

The integration is first made without OFB for solitary laser from time t=0 until the round-trip time $t=\tau$. The calculated values of $S_p(t=0$ to $\tau)$ and $\theta_p(t=0$ to $\tau)$ of mode p are then stored for use as time delayed values $S_p(t-\tau)$ and $\theta_p(t-\tau)$, including OFB terms, for the rest of the calculations. Dynamics are examined after 0.5μs passed from t=0, which is long enough for the transients to be died out. The integration is then proceeded over a long time period of $T\geq$2μs, which can give intensity noise for $f\geq$250kHz. The RIN is then computed from the obtained values of $S(t_i)=\sum_p S_p(t_i)$ by employing the FFT to integrate Eqn. (4-15).

Note that noise on the calculated RIN spectrum is due to the finite duration of computed time resolved signal for our impossibility to simulate infinitely long laser outputs. To improve numerical accuracy, RIN spectra are smoothed by running an adjacent averaging of spectral components [53]. The numerical values of 850nm GaAs laser parameters, listed in Table 4-a, are employed in the calculations. Each of the independent Gaussian random variables g_s, g_θ and g_N are generated using Polar Rejection Method [54] and restricted the values between [-1, 1].

3. Analysis of OFB Noise

3-a. Noise Properties

First we show the results of applying our model to solitary laser, without any external feedback, to simulate the quantum noise. The results are plotted in Fig. 4-1 to investigate the effect of current injection on the characteristics of quantum noise. When the laser is in pure single-mode operation or in stable multimode operation, the noise coincides to the quantum noise obtained by D.E. McCumber in [44]. Noise with injection current below threshold is mainly caused by fluctuations of the electron density, not by fluctuations of the photons. The peak shown around the threshold current is attributed to the maximum contribution of the spontaneous emission to light amplification, which rapidly decreases above threshold compared with the contribution of the stimulated

emission [14].

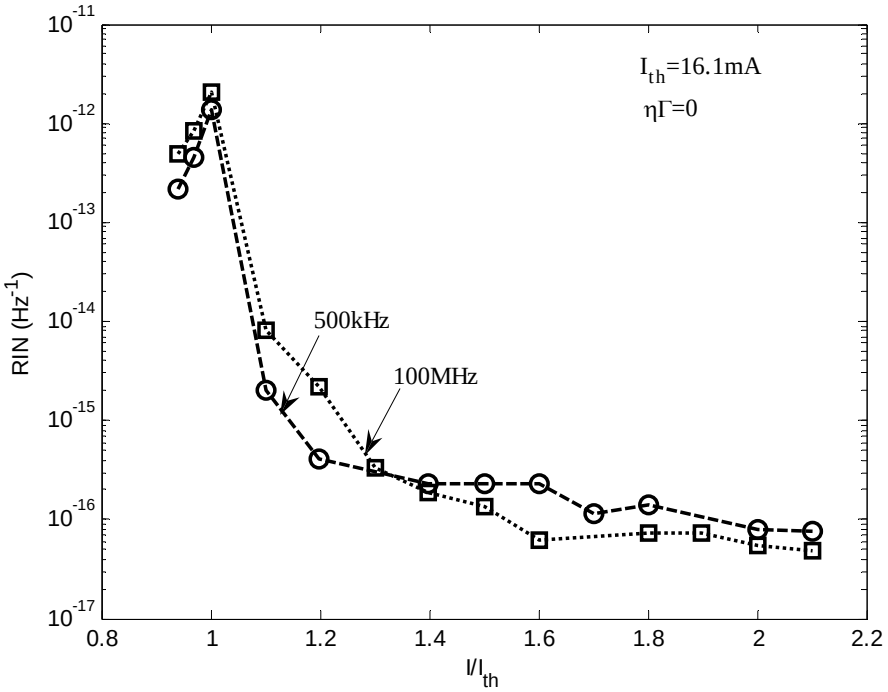

Fig. 4-1. The simulated characteristics of quantum noise with normalized current. The quantum noise reveals a peak value at the threshold current and reduces with increasing of the current.

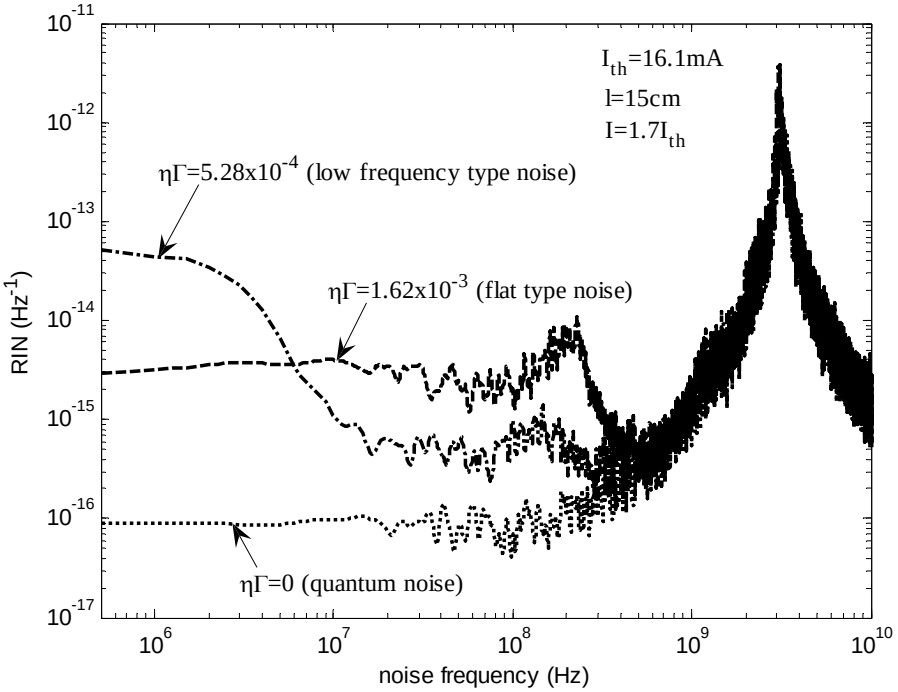

Fig. 4-2. The simulated spectra of RIN profiles for different OFB strengths. The OFB noise is classified into the low frequency type and the flat type based on noise frequency profile.

Optical feedback affects the noise and dynamics of laser in different ways depending on the strength of external feedback. Typical noise

spectra in the 850nm GaAs laser under the OFB are shown in Fig. 4-2. The noise level is around 10^{-16} Hz^{-1} when there is no feedback; that corresponds to the quantum noise of the solitary laser. By increasing $\eta\Gamma$, where $\eta\Gamma$ is the effective feedback ratio measuring the OFB strength, from 0 to $5.28\text{x}10^{-4}$ the RIN was increased in lower frequency region below 10MHz. We call here this type of noise to be low frequency type noise. When OFB strength was increased more, the RIN profile became flat for wide frequency range from very low frequency to several 100MHz. We call here this type of noise to be flat type noise.

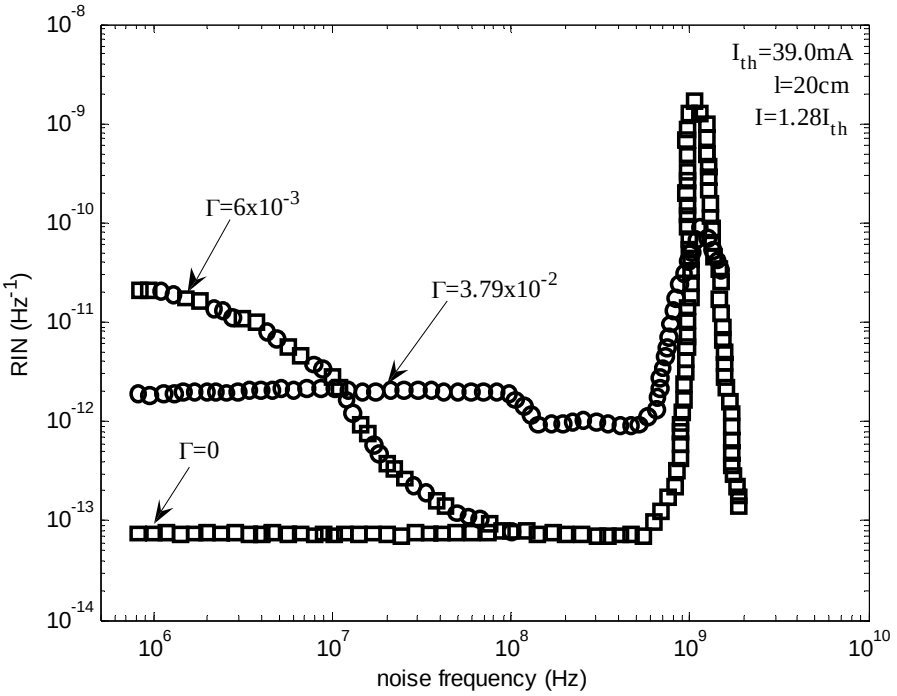

Fig. 4-3. Experimentally observed frequency spectra of the noise cited from Ref. [21].

The peak around at 3.2GHz in Fig. 4-2 indicates the relaxation oscillation. The beating signal $\Delta f=c/2l$ corresponding to the external modes must be Δf=1GHz with l=15cm, but is almost hidden in the broadened spectrum of the relaxation oscillation. The numerical results also show a secondary peak around at 250MHz for larger optical feedback. This peak must be a subharmonic of Δf.

Experimentally observed frequency spectra of the noise in 780nm HL7801E AlGaAs laser are cited in Fig. 4-3 from Ref. [21]. Experimental data are given with the Γ not $\eta\Gamma$ because determination of η in the experiment is difficult. We can find good correspondence between the simulated results in Fig. 4-2 and the experimental data in Fig. 4-3. Different feature between the theoretical calculation and the experimental data is on the height of the noise and the detailed profile. The data by the theoretical calculation show lower levels than those by experiment. The difference may be caused by different selection of parameters for the laser material and structure as well as additional fluctuation phenomena such as the electron diffusion and the inhomogeneous electron injection

mechanism in the real device [33].

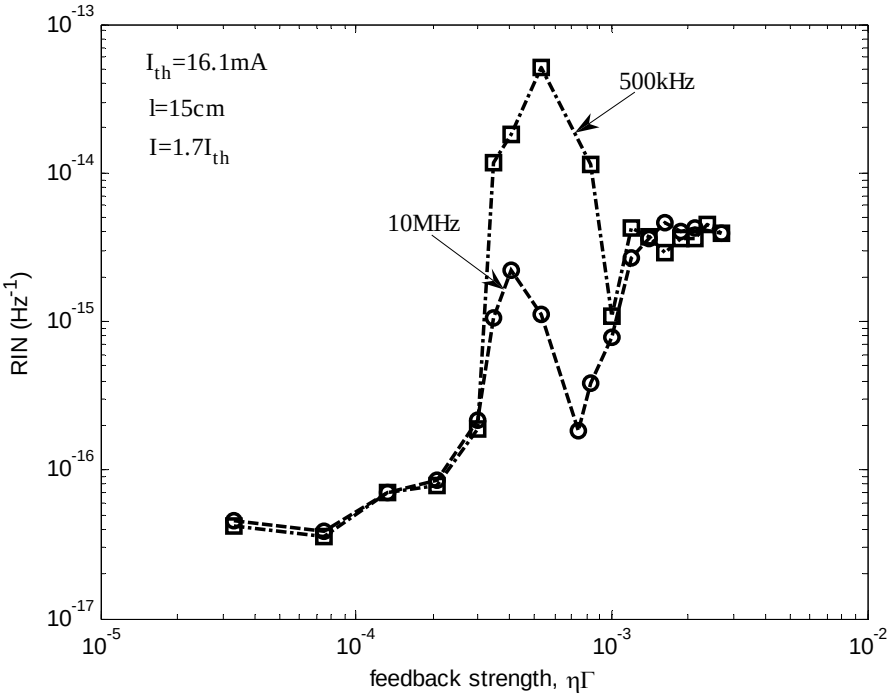

(a)

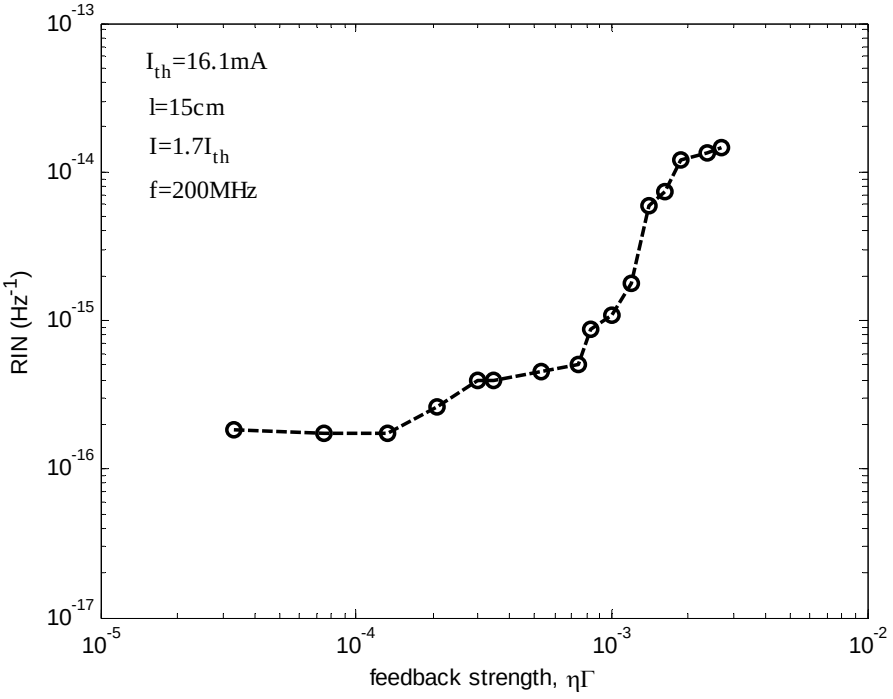

(b)

Fig. 4-4. Simulated results of the variation of the noise with feedback strength. (a) Low frequency type, (b) Flat type. The low frequency type noise reveals the maximum peak with certain feedback ratio.

Variations of the RIN with feedback strength are shown in Fig. 4-4(a) and 4-4(b), for *f*=500kHz and *f*=10MHz representing the low frequency type noise and for *f*=200MHz representing the flat type noise, respectively.

The RIN was increased with the feedback strength for ηI>7.41x10^{-4}. However, the RIN at 500kHz had a peak value at ηI≒5.28x10^{-4} and the RIN at 10MHz also shown a peak at around ηI≒4.04x10^{-4}. Experimental results of noise variations for f=500kHz and f=400MHz are also cited in Fig. 4-5 from Ref. [21] which show good correspondences to the numerical simulations.

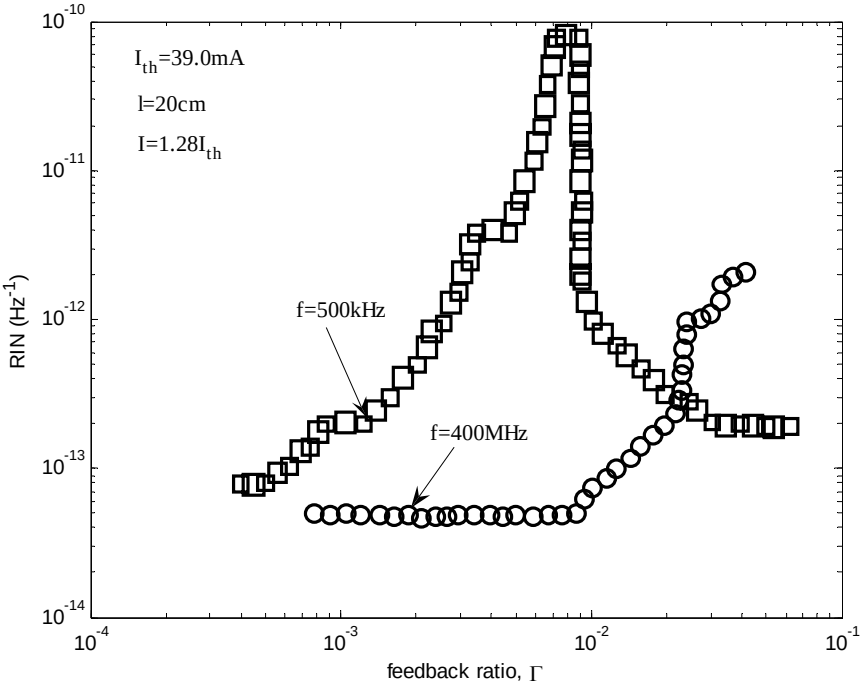

Fig. 4-5. Experimentally observed variation of the noise with the feedback ratio cited from Ref. [21].

3-b. Generation of OFB Noise

The temporal variations and time averaged profiles of the lasing modes are shown in Fig. 4-6 to 4-8. Fig. 4-6 is the case that the OFB is zero. The laser shows stable single mode operation with a dominant mode p=+1. The dominant mode has been shifted from p=0 to p=+1 by increase of the lasing power due to the asymmetric mutual-gain saturation. Other side modes are well suppressed lower than 1/100 of the dominant mode as shown in Fig. 4-6(b), achieving the low noise level corresponding to the quantum noise.

Fig. 4-7 is the case showing unstable mode hopping between p=+2 and +1 due to the OFB of ηI≒ 5.28x10^{-4} with which the RIN shows the highest value of the OFB noise in form of the low frequency type noise. All previous analyses based on the single mode model never reveal such low frequency type noise [15], [30]. This result gives clear evidence that the low frequency type noise is caused by the mode hopping phenomena among the lasing modes. The RIN becomes the highest when the mode hopping is the most unstable. We need to pay attention here that the time averaged modal spectrum looks like a multimode operation as shown in Fig. 4-7(b). However, this is not the true multimode operation but the

mode hopping phenomena between bi-stable states of the single mode operation with p=+2 or +1.

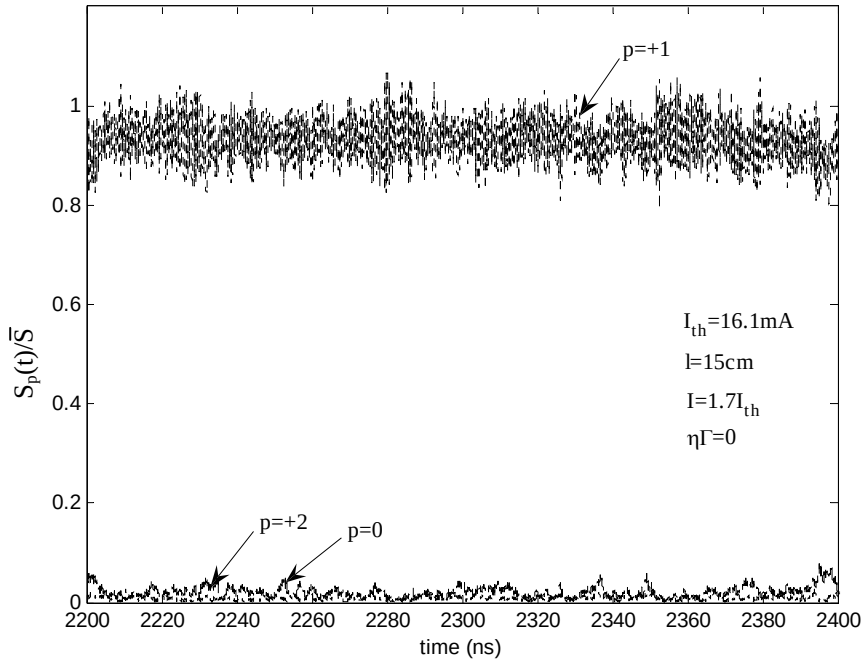

(a)

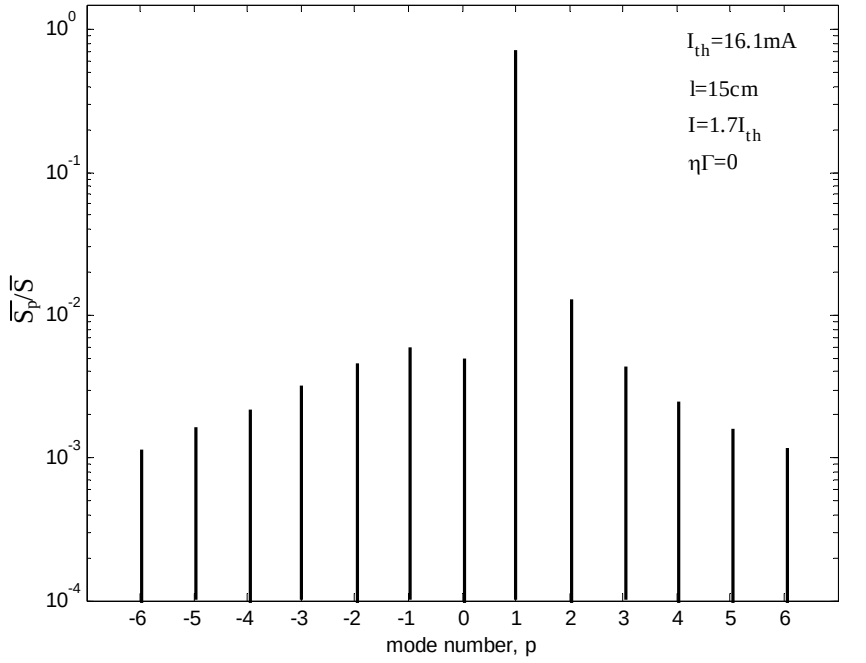

(b)

Fig. 4-6. Modal behavior without OFB. (a) Temporal variation of lasing modes. (b) Time-averaged modal spectrum. Stable single mode operation is achieved with low noise.

It has been well known that when the optical feedback noise raises up operation of the laser becomes unstable as firstly pointed out by Lang

and Kobayashi in [3]. This instability must come from the unstable mode hopping which start from $\eta\Gamma$= 3.46x10^{-4} in our calculation.

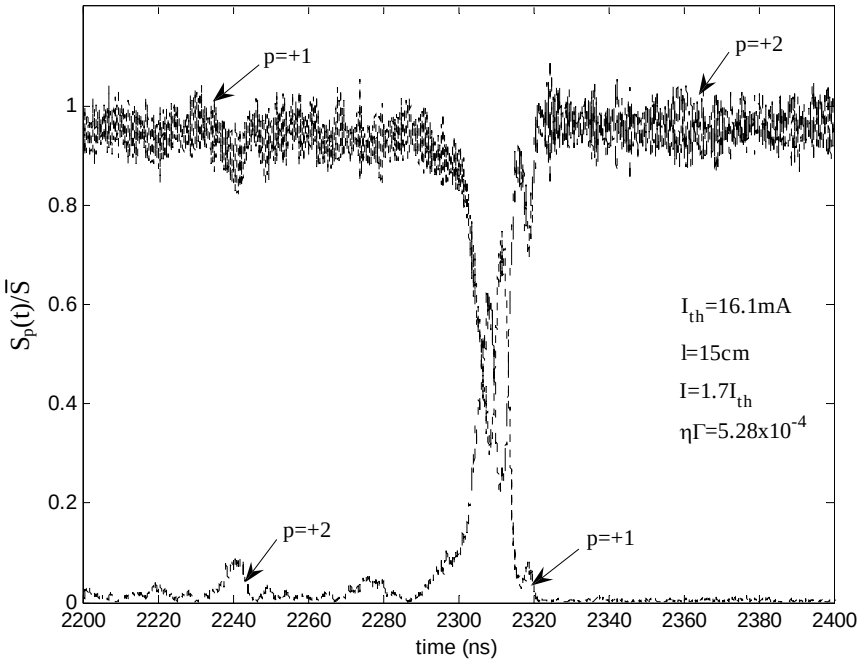

(a)

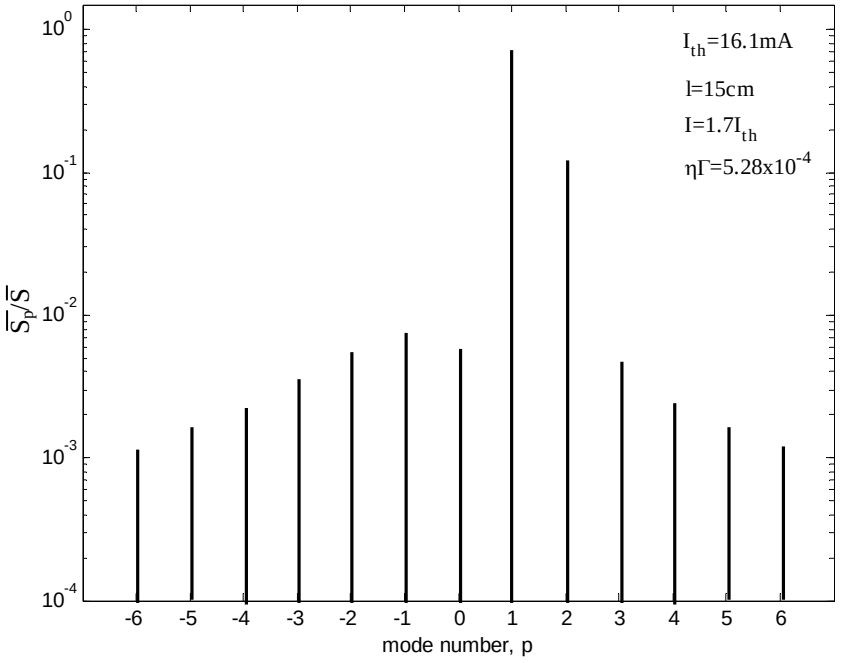

(b)

Fig. 4-7. Modal behavior when the RIN becomes the highest with form of the low frequency type noise by the OFB. (a) Temporal variation of lasing modes. (b) Time-averaged modal spectrum. The lasing modes show unstable mode hopping between p=+1 and +2.

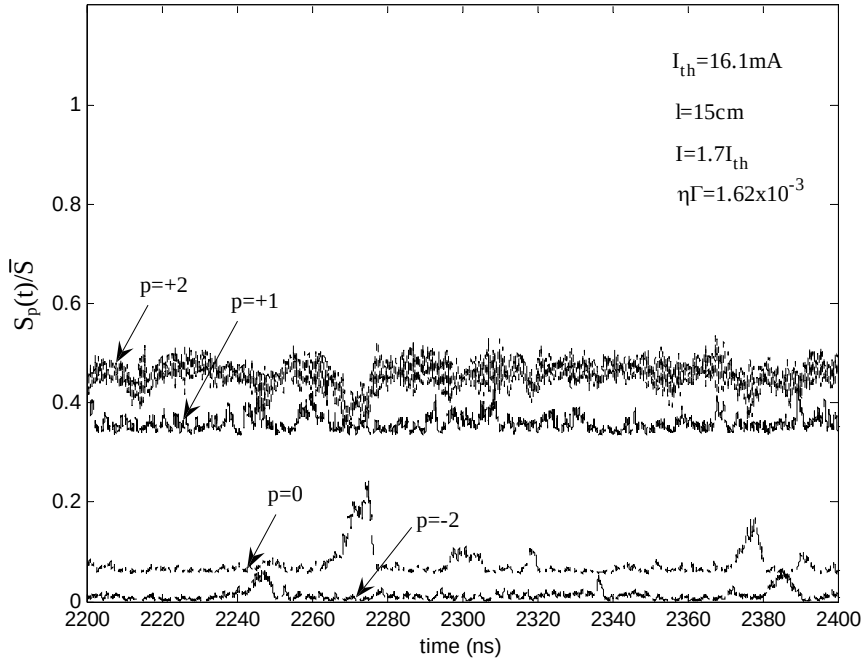

(a)

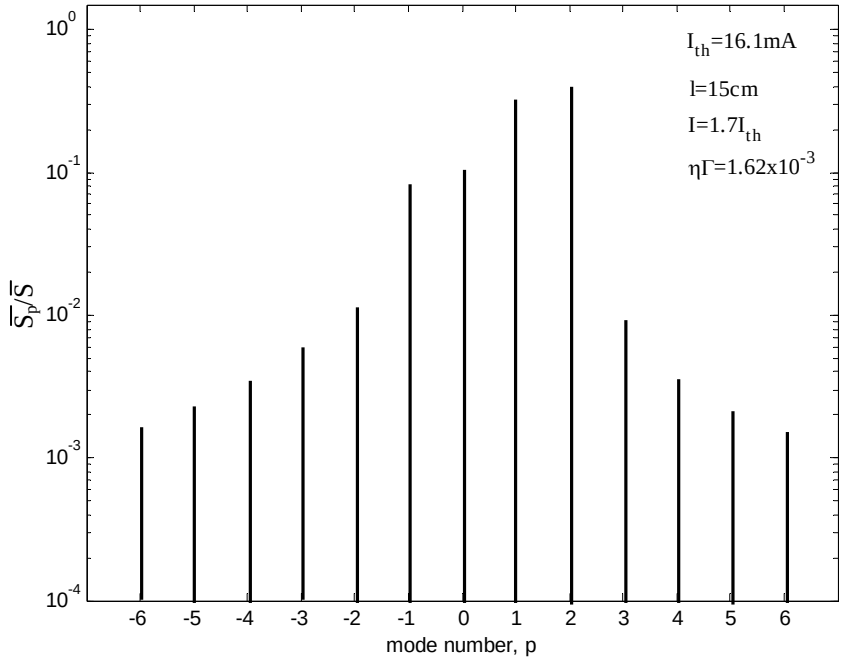

(b)

Fig. 4-8. Modal behavior with rather high OFB ratio. (a) Temporal variation of lasing modes. (b) Time-averaged modal spectrum. The operation changes to a stable multimode operation with reduction of the low frequency type noise, while the flat type noise increases with increase of the external optical feedback ratio.

By further increase of the OFB, the operation changes to a stable multimode operation, resulting in reduction of the low frequency type

noise. Fig. 4-8 is the case the OFB is rather high as $\eta I \fallingdotseq 1.62\text{x}10^{-3}$. Temporal variations of the lasing modes are stabilized as in Fig. 4-8(a) and the modal spectrum is spread to wider wavelength as in Fig. 4-8(b). The flat type noise increases with increase of the feedback ratio. Since the flat type noise is obtained even in the single mode model as reported in [15] and [30], generating mechanism of the flat type noise is independent from the mode competition phenomena among the lasing modes in the solitary laser. The flat type noise is explained in terms of the phase distortion of the lasing modes or mode competition among the external cavity modes.

The low frequency type noise must be caused by the mode competition among the lasing modes in the solitary laser [14], [55], and the flat type noise must be caused by the phase distortion between the internal reflected light and the external feed-backed light [15], [30]. Cause of the flat type noise is also explained in terms of mode competition among external modes whose lasing frequency is decided by the space between the laser facet and the reflecting mirror [14], [21].

3-c. Generating Mechanism of OFB Noise

From Eqn. (3-101) and (3-74), the variation of the photon number S_p of mode p can be written as,

$$\begin{aligned}\frac{dS_p}{dt} &= \left(G_p - G_{tho} + \frac{c}{n_r L}\ln\left|U_p\right| \right) S_p + C_p + F_{Sp}(t) \\ &= \left\{ A_p - B_p S_p - \sum_{p \neq q} \left(D_{p(q)} + H_{p(q)} \right) S_q - G_{tho} + M_p \right\} S_p + C_p + F_{Sp}(t)\end{aligned} \tag{4-17}$$

$$\text{where } M_p = \frac{c}{n_r L}\ln\left|U_p\right| \tag{4-18}$$

represents contribution of the OFB to the lasing mode p.

We can obtain a dynamic chart from Eqn. (4-17), as shown in Fig. 4-9, considering two modes p and q. Arrows in the figure indicate flow of the operating point. The lines L_p and L_q indicate conditions $dS_p/dt=0$ and $dS_q/dt=0$, respectively. Operation at steady state is at the point P or Q. If the operation is at P, the laser shows single mode operation with mode p. If the operation is at Q, the laser shows single mode operation with mode q. Selection of the operating point is decided with the initial condition. As found in this figure, the operating points form bi-stable state in a solitary semiconductor laser.

The fluctuating terms $F_{Sp}(t)$ and $F_{Sq}(t)$ give small movements around the steady point P and Q. Since fluctuations are involved in the photon numbers S_p and S_q, and the optical phases θ_p and θ_q, the OFB light has also fluctuations. The stronger the OFB, fluctuations in M_p and M_q become larger through the terms U_p and U_q defined in Eqn. (3-99). Then positions of the lines L_p and L_q move randomly, resulting in mode hopping between two operating points P and Q. Fig. 4-7(a) confirms mode hopping

between bi-stable states p=+1 (we may consider this as P) and p=+2 (we may consider this as Q). Since summed value of the photon number S_p+S_q is not constant during the mode hopping the laser reveals large variation on the output power.

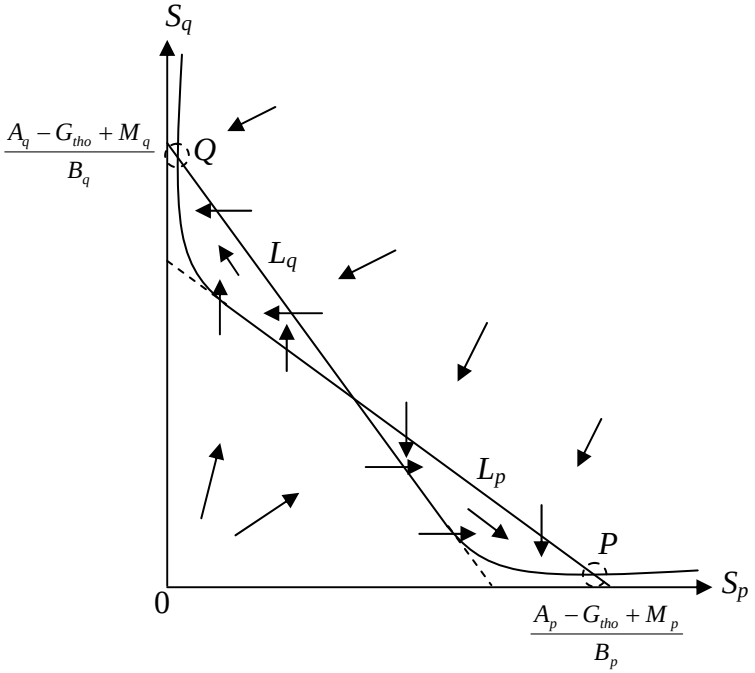

Fig. 4-9. Dynamic chart indicating mode competition phenomena between two lasing modes. When the OFB level increases the operating point jumps from P to Q or from Q to P.

4. Effect of Superposition of HF Current

4-a. Reduction of OFB Noise

Calculated examples of noise spectrum of the OFB noise and its suppression by superposition of HF current are shown in Fig. 4-10. The feedback distance is l=12cm which corresponds to a round trip time period of f_{ex}=1/τ=c/2l=1.25GHz. Feedback strength is I=2.45x10^{-3} by which the low frequency type noise is enhanced. Frequency of the superposed HF current is f_M=500MHz. Line spectrum in the figure indicates modulation of the photon number with the HF current and its higher harmonics. Quantum noise spectra are also shown for comparison. The noise is increased more than 20dB by the OFB, and is well suppressed by introduction of the superposition of HF current.

Dependency of suppressed noise level with the modulation depth of HF current is shown in Fig. 4-11. HF modulation of more than 30% is required to suppress the OFB noise in this numerical example.

Fig. 4-12 shows temporal variations of all lasing modes and the longitudinal mode spectrum with OFB and HF superposition. In that case, the lasing modes show stable multimode operation without any mode hopping. That is, the HF current changes the laser operation from bi-

stable state with random mode hopping to stable multimode operation and hence, reduces the low frequency type OFB noise.

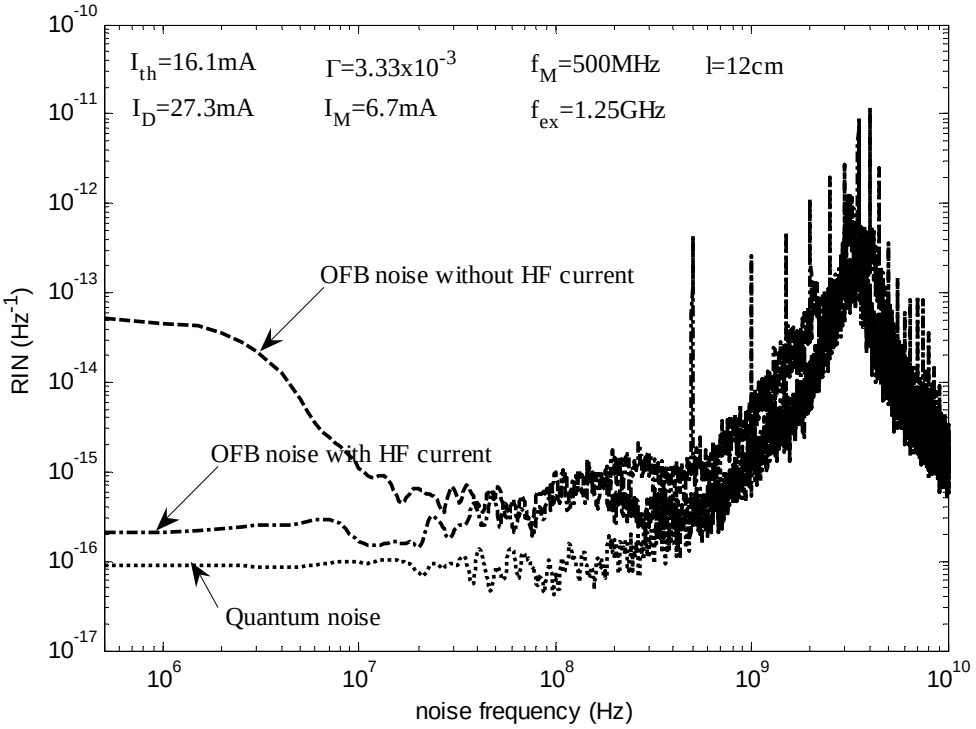

Fig. 4-10. The simulated spectra of RIN profiles of the OFB noise and suppressed noise by superposition of HF current.

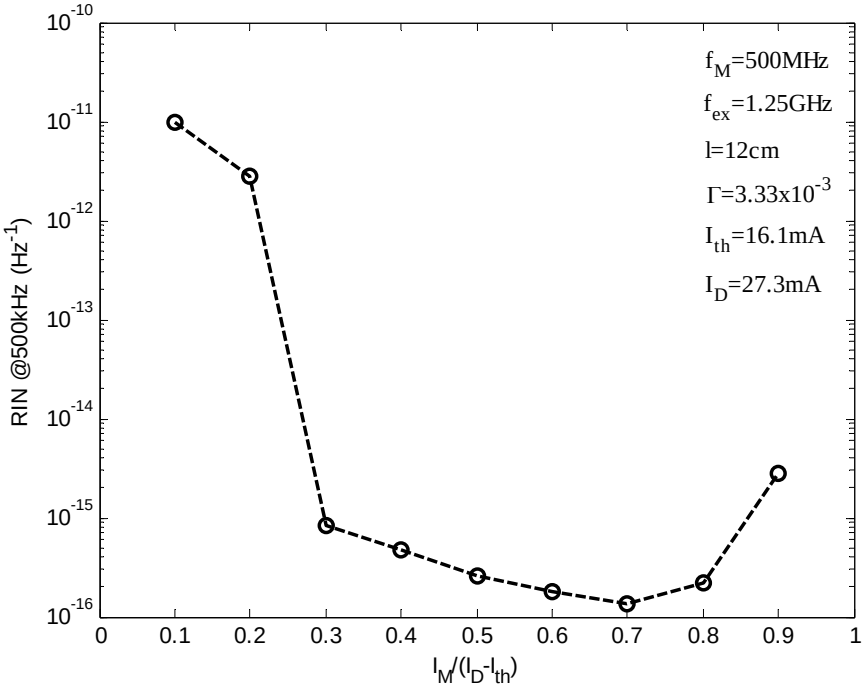

Fig. 4-11. Dependency of suppressed noise level with the modulation depth of HF current. HF modulation of more than 30% is required to suppress the OFB noise in this numerical example. Frequency of modulation chosen is 500MHz.

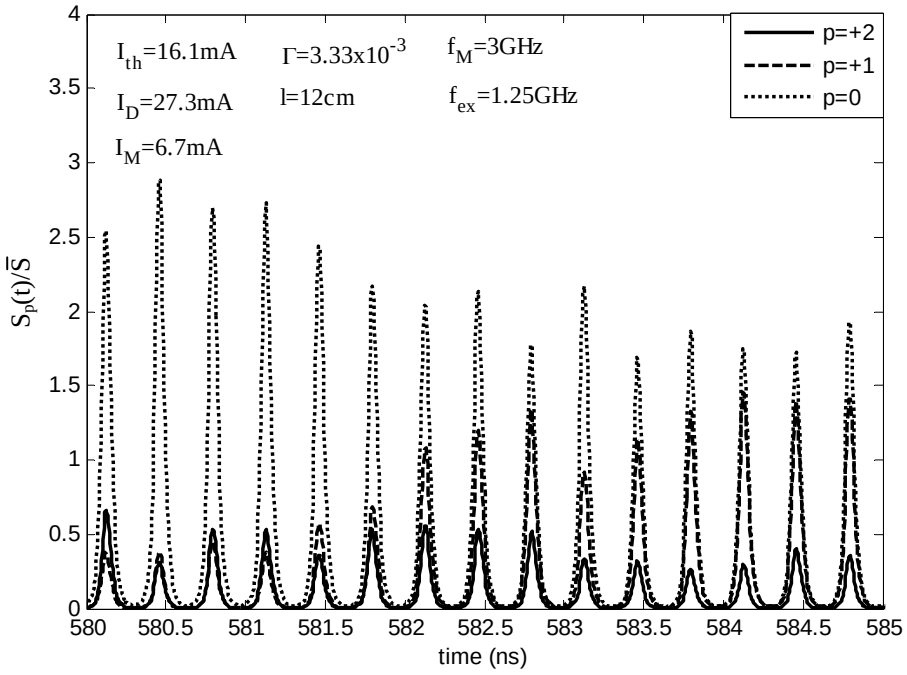

(a)

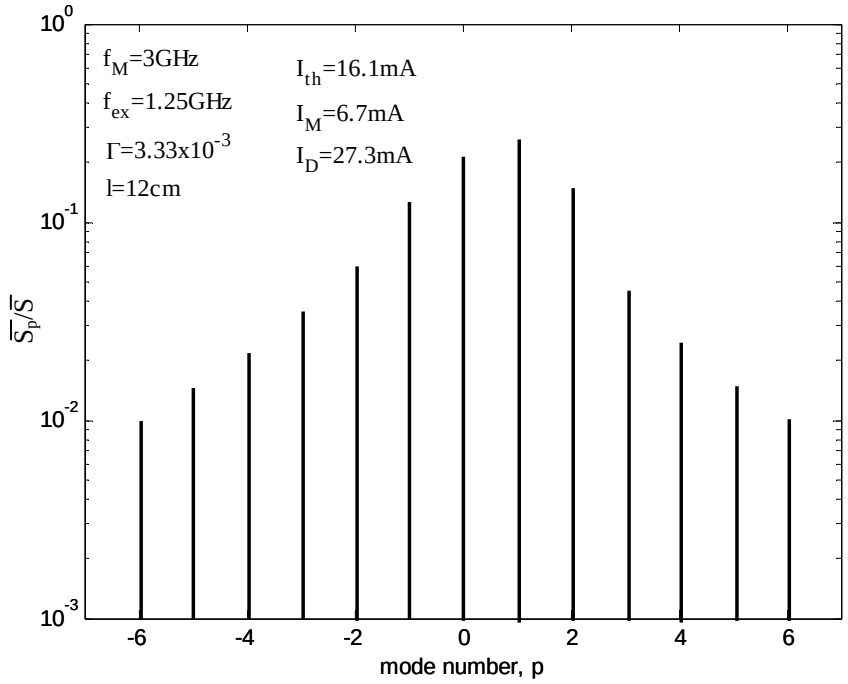

(b)

Fig. 4-12. (a) Temporal variations of all lasing modes in the case that feedback noise is reduced. (b) Longitudinal mode spectrum with the OFB and HF superposition. Lasing modes show stable multimode operation.

4-b. Mechanism of Noise Reduction

If we assume the superposition of HF current, that is, the injection current I is modulated with amplitude I_M and angular frequency $\Omega=2\pi f_M$ [see Eqn. 4-2] then we have

$$I = \tilde{I} + \frac{1}{2}\left(I_M e^{j\Omega t} + I_M^* e^{-j\Omega t}\right) \tag{4-19}$$

Corresponding to introduction of the modulation, variations of the electron number N and the photon number S_p are expressed as,

$$N = \tilde{N} + N_M e^{j\Omega t} + N_M^* e^{-j\Omega t} \tag{4-20}$$

$$S_p = \tilde{S}_p + S_{Mp} e^{j\Omega t} + S_{Mp}^* e^{-j\Omega t} \tag{4-21}$$

where $\tilde{N}$ and $\tilde{S}_p$ are slowly varying terms compared with Ω, and N_M and S_{Mp} are modulated terms. By substituting Eqn. (4-20) and (4-21) into (4-17), the variation in $\tilde{S}_p$ is given by,

$$\frac{d\tilde{S}_p}{dt} = \left\{\tilde{A}_p - B_p \tilde{S}_p - \left(D_{pq} + H_{pq}\right)\tilde{S}_q - G_{tho} + C_p\right\}\tilde{S}_p + K_p + F_{Sp}(t) \tag{4-22}$$

$$\text{with } K_p = \frac{a\xi}{V}\left\{\tilde{N} + N_M S_{Mp}^* + N_M^* S_{Mp}\right\} \tag{4-23}$$

Similar equations can be obtained for S_q.

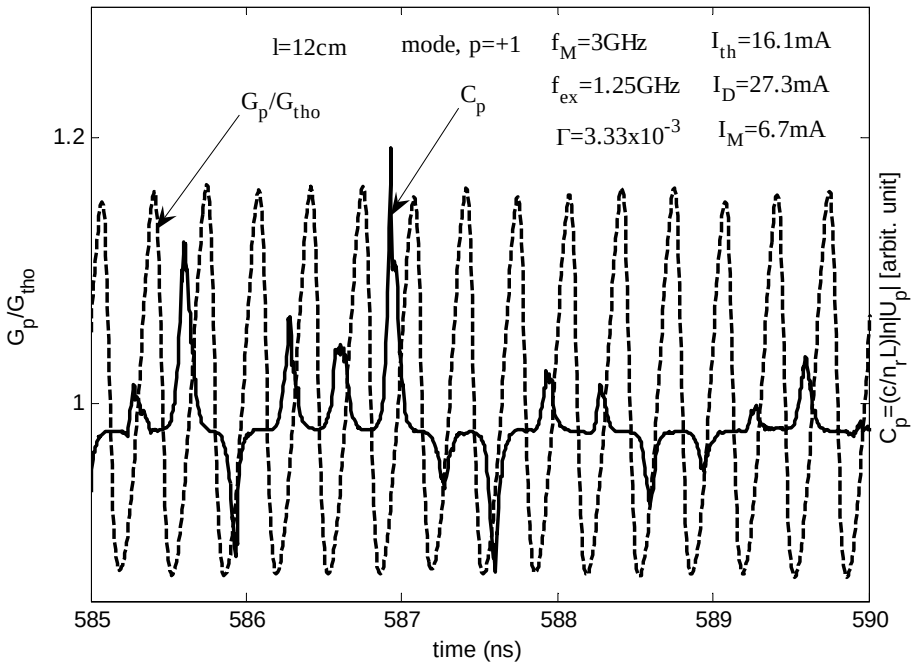

Fig. 4-13. Temporal variations of the gain G_p and the contribution of the OFB C_p with which the OFB noise is well suppressed. Variations of G_p and C_p are not synchronized.

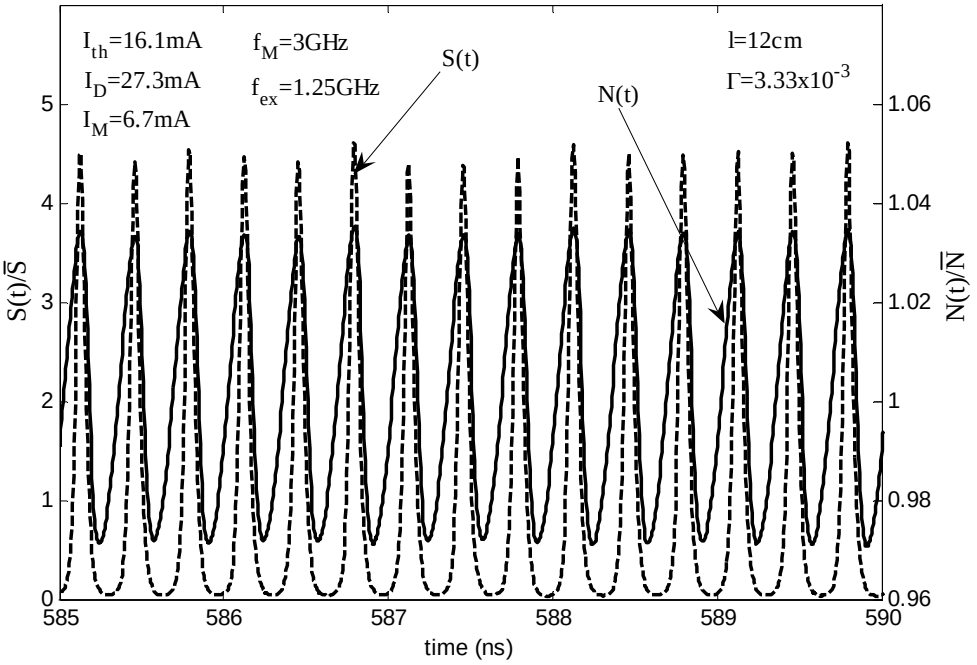

Fig. 4-14. Temporal variations of electron number and total photon number corresponding to Fig. 4-13. Variations of the electron number and the photon number are large enough and are in the same phase.

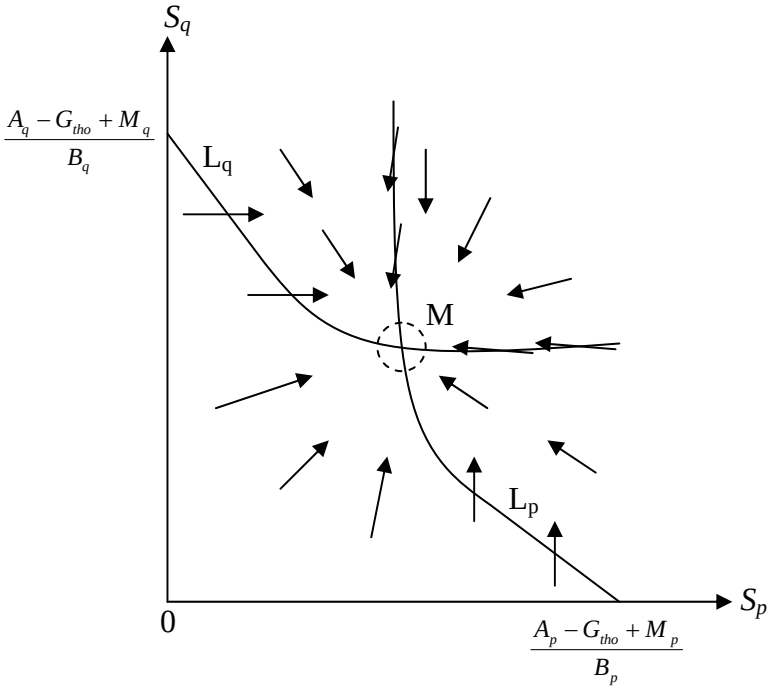

Fig. 4-15. Change to monostable state by inclusion of HF components in the lasing operation. The operating point *M* indicates a stable multimode operation of modes *p* and *q*.

Temporal variations of the gain G_p and the contribution of the OFB $C_p=(c/n_rL)\ln|U_p|$ shown in Fig. 4-13 is the case with which the OFB noise is well suppressed. We find that the variations of G_p and C_p are not synchronized for the phase difference between the feedbacked light and

emitting light, $\theta_p(t-\tau)-\theta_p(t)$ in Eqn. (3-99), has no fixed relation. Then, variations of the electron number N and the gain coefficient G_p are not disturbed by the OFB, resulting in sufficient variation of the photon number S_p as shown in Fig. 4-14. As the variations of the electron number and the photon number are large enough and the varying phases between them are same, the term K_p in (4-23) increases.

As found from Eqn. (4-23), the term K_p is increased by the HF modulation for variation of the electron number N_M and that of the photon number S_M are large enough and in same phase. With the increase of the term K_p, the lines L_p and L_q concave more strongly achieving a monostable state operation as shown in Fig. 4-15. The point M is an operating point at steady state, which indicates multimode operation of modes p and q. In this case of Fig. 4-15, the operating point slightly moves by the OFB, but never shows the mode hopping. The OFB noise is thus suppressed by the superposition of HF current [17], [26].

4-c. Condition Unable to Suppress Noise

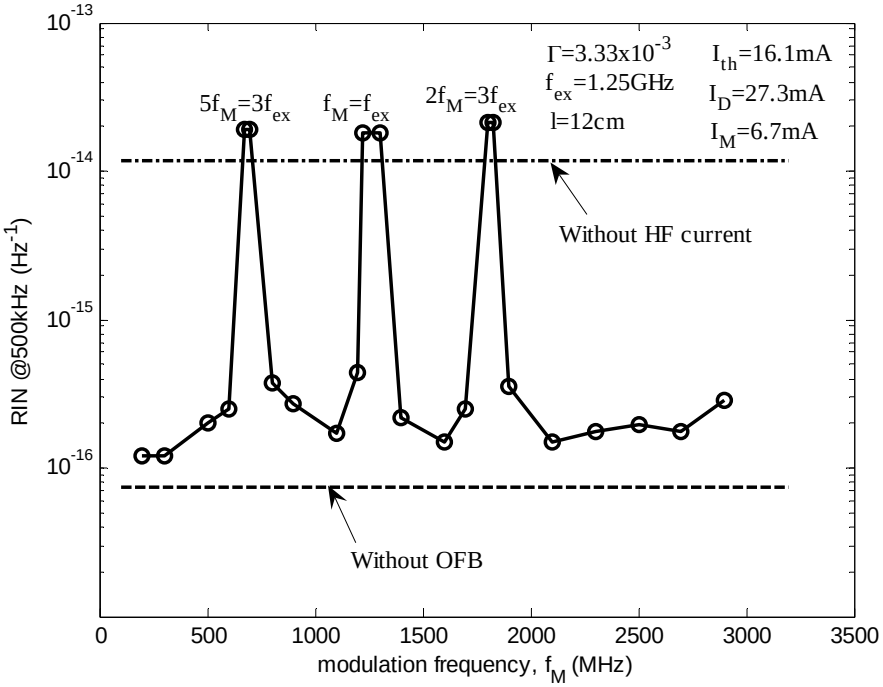

Fig. 4-16. Calculated data showing dependence of the RIN on modulation frequency of the superposed HF current. The feedback distance is L=12cm which corresponds to f_{ex}=1.25GHz.

Suppression of the OFB noise by the superposition of HF current is not always effective. Dependency of the modulation frequency f_M of the HF current for noise suppression is shown in Fig. 4-16. The feedback distance is L=12cm which corresponds f_{ex}=1.25GHz. The RIN is evaluated at the noise frequency of 500KHz. The dashed line indicates the RIN level with neither the OFB nor the superposition of HF current, that is, quantum noise level. The chain line is the RIN level with the OFB but without the HF current. The solid line is the RIN level with the superposition of HF

current. The modulation depth is $I_M/(I_D-I_{th})$=0.6 which must be large enough to suppress the OFB noise. The noise is reduced in wide range of the modulation frequency f_M. However, the RIN raises up when modulation frequency f_M of the superposed current coincides with a rational number of the round trip time period f_{ex}.

Fig. 4-17 shows experimental data of variations of the RIN at 1MHz with the modulation frequency f_M [26]. The feedback distance is l=21.4cm which corresponds to a round trip time period of f_{ex}=700MHz. The experimental data shows evidence that the OFB noise raises up when f_M and f_{ex} are in rational relations.

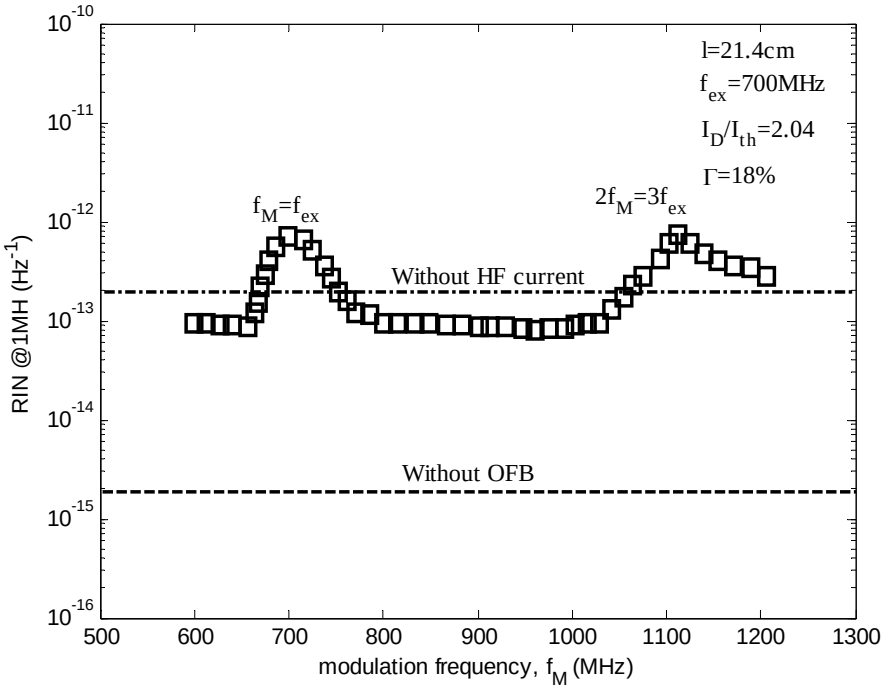

Fig. 4-17. Experimental data showing dependence of the RIN on modulation frequency of the superposed HF current [26]. The feedback distance is l=21.4cm which corresponds to f_{ex}=700MHz.

As discussed in the previous section, condition to suppress the OFB noise is that, variations of the electron number and the photon number become in the same phase. Temporal variations of the gain G_p and the contribution of the OFB $C_p=(c/n_rL)\ln|U_p|$ shown in Fig. 4-18 is the case of $5f_M=3f_{ex}$ with which the OFB noise is increased with mode hopping remained. We find that the variations of G_p and C_p are synchronized with f_M having almost 180^0 phase difference when $5f_M=3f_{ex}$. The phase difference $\theta_p(t-\tau)-\theta_p(t)$ is locked with the rational frequency of f_M [56] and works to reduce variation of G_p+C_p for variations of G_p and C_p are in inverse phase relation. Then the modulation of the photon number is reduced as found from (3-101) or (4-17).

Calculated values for the temporal variations of the electron number and the total photon number are shown in Fig. 4-19 is for the case of $5f_M=3f_{ex}$ with which the OFB noise is increased with mode hopping remained. Variation of the electron number and that of the photon number

have 90^0 phase difference. Also, amplitudes of the variations are small. Then the term K_p in Eqn. (4-23) cannot increase in this case.

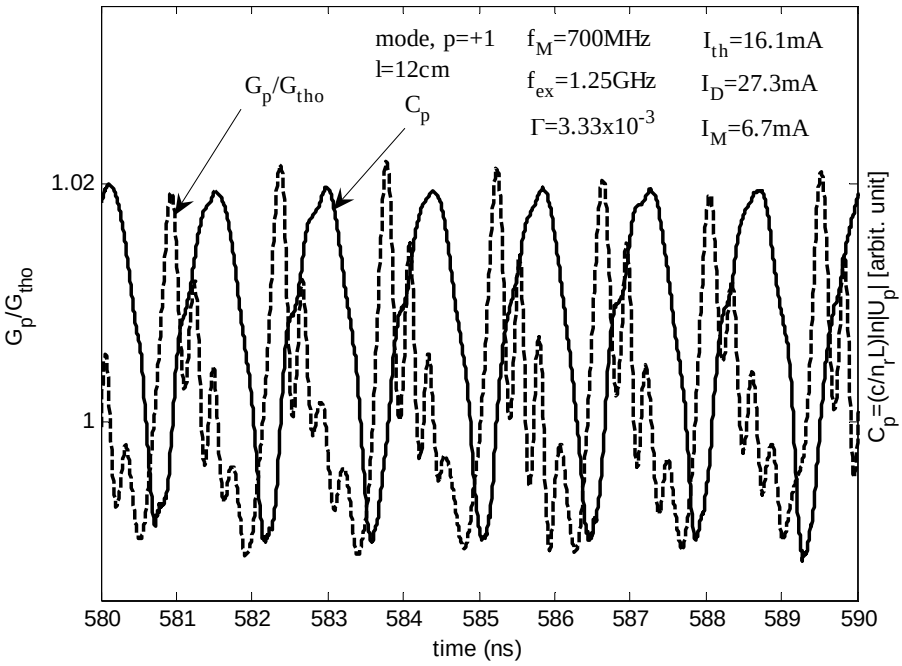

Fig. 4-18. Temporal variations of the gain G_p and the contribution of the OFB C_p for the case of $5f_M=3f_{ex}$ with which the OFB noise is increased with the mode hopping remained. Variations of G_p and C_p are are synchronized with f_M and have almost 180^0 phase difference.

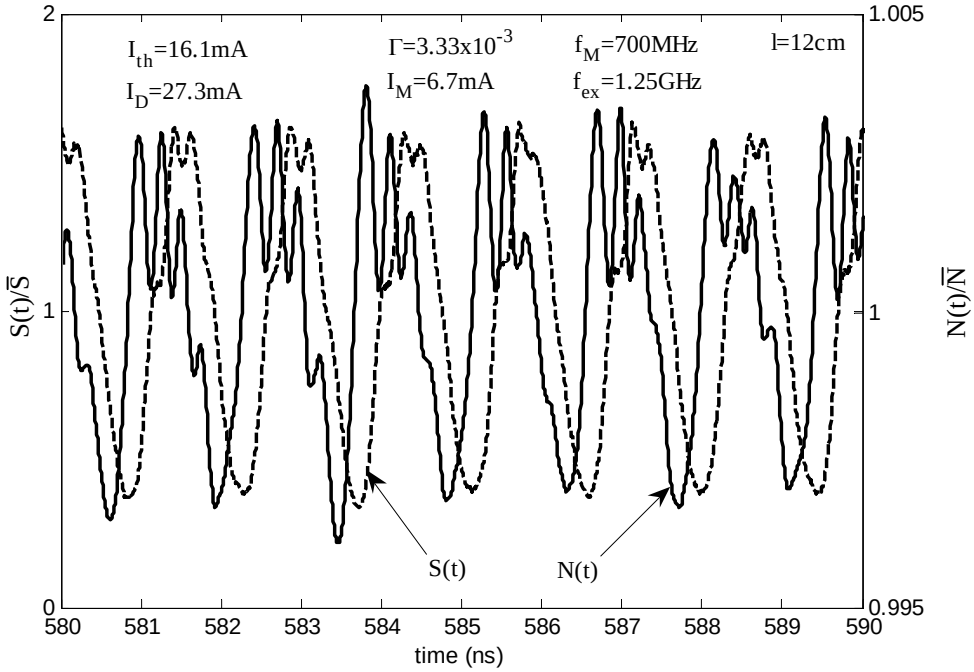

Fig. 4-19. Temporal variations of electron number and total photon number for the case of $5f_M=3f_{ex}$. Variation of the electron number and that of the photon number have 90^0 phase difference. Amplitudes of the variations are small.

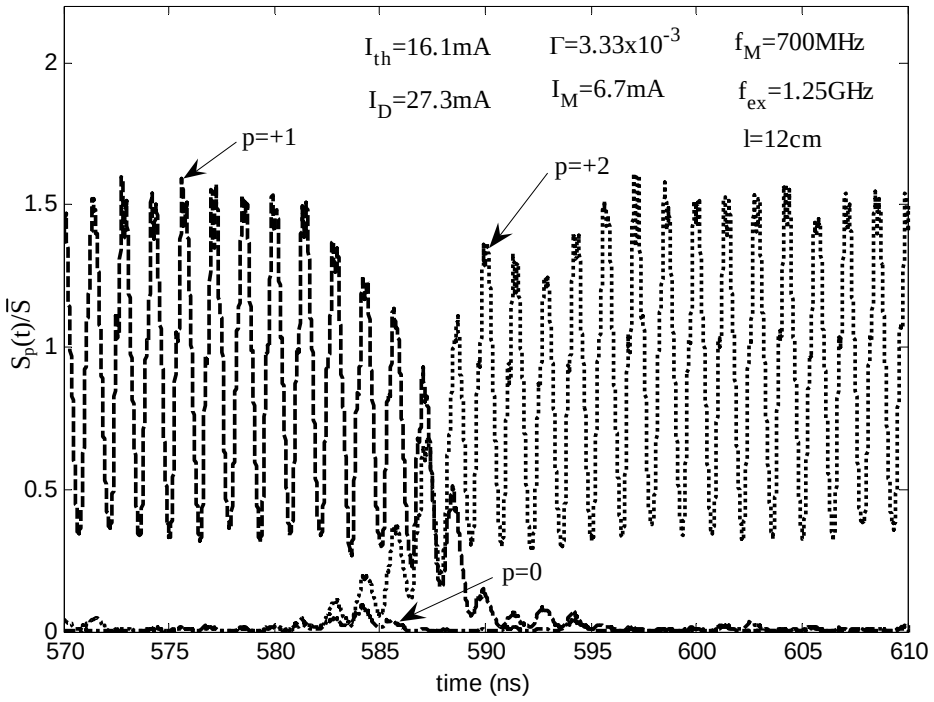

(a)

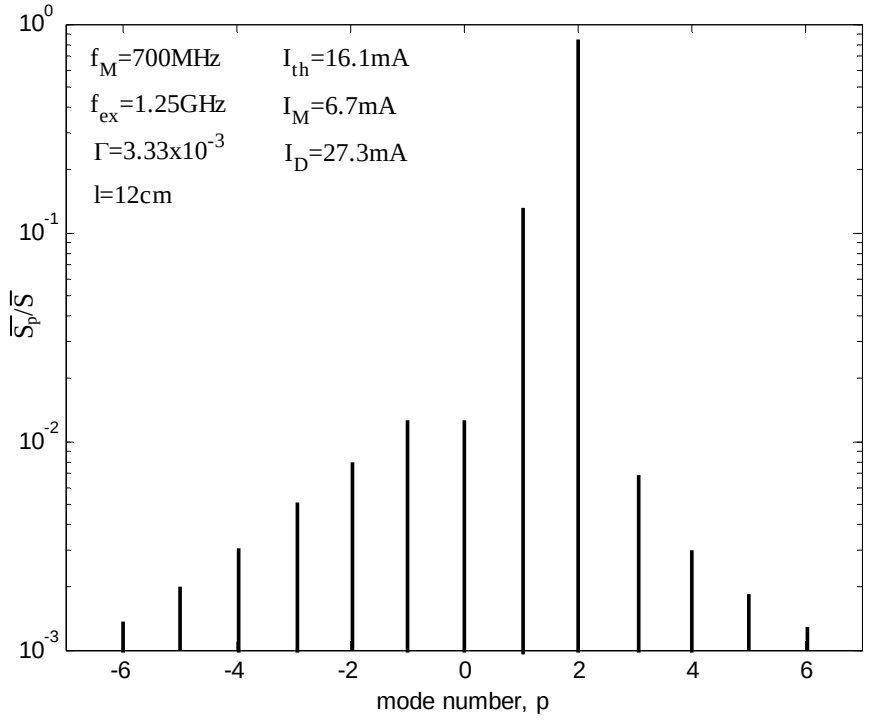

(b)

Fig. 4-20. (a) Temporal variations of all lasing modes in the case when the noise raises up with the condition $5f_M=3f_{ex}$. (b) Longitudinal mode spectrum corresponding to condition unable to reduce noise. The lasing modes show unstable mode hopping between p=+2 and p=+1.

Numerically calculated temporal variations and optical spectrum of the lasing modes are shown in Fig. 4-20 for the case that the OFB noise raises up with the condition $5f_M=3f_{ex}$. It seems from the spectra of the internal lasing modes that the laser operates in multimode but Fig. 4-20 (a) confirms unstable mode hopping between p=+2 and p=+1 and hence the noise still remains increased.

Chapter V: Conclusion

This chapter gives some concluding remarks on the whole thesis works, analysis and results. First we comment on optical feedback noise properties and then on the noise reduction mechanism by superposition of high frequency current injection.

Semiconductor lasers tend to be suffered by the optical feedback (OFB) noise caused by reflection of the output light at surface of the optical disc or the optical fiber. A simulation model giving generation of the OFB noise and its suppression by the superposition of HF current is shown in this dissertation.

We have proposed a new model to analyze generation of noise in semiconductor lasers under influence of the optical feedback (OFB) which is reflected from a surface of connecting optical device.

Newly introduced factors in this analysis are multimode properties and noise generating sources in the lasers. The self and mutual gain saturation effects among the lasing modes, phase delay on the feedbacked light and Langevin noise sources on the photon generation, its phase and carrier number fluctuations are taken into account in form of the rate equations. Mode competition phenomena among lasing modes in the solitary laser and optical phase delay between the feedbacked light and emitting light were counted in the model

Temporal variations of the photon numbers, the optical phases and the electron numbers were traced by numerical calculation. The noise has been expressed in terms of the RIN (relative intensity noise) by help of the fast Fourier transformation from the variant photon numbers.

The RIN is classified into two groups of the low frequency type and the flat type based on the noise frequency profile. Features of these two types of noise are well simulated by this model with good correspondence to the experimentally obtained data.

Detailed variations of the noise characteristics with the optical feedback ratio are given with discussion on the modal behavior. The highest OFB noise, that is, low frequency type noise is caused by the mode competition phenomena among lasing modes which is induced by the OFB. On the other hand, flat type noise is caused by the phase distortion effect between the internal reflected light and external feedbacked light.

Without any optical feedback the laser shows single mode operation with one dominant mode. But with increase of external OFB it first shows mode hopping phenomena between bi-stable states. The laser changes its operation to stable multimode without any mode hopping with further increase of the OFB.

Superposition of high frequency (HF) current is the most popularly used technique to suppress the OFB noise. However, noise suppression by the superposition of HF current does not work when the modulation

frequency of the HF current coincides with a rational number of the round trip time for the OFB.

The superposition of HF current works to modulate both the electron number N and the photon number S_p, which works to change the operating state from the bi-stable state to the monostable state, and stop the mode hopping resulting in suppression of the OFB noise. However, when the modulation frequency f_M of the superposed HF current coincides with a rational number of the returning period f_{ex} of the OFB, modulations of the electron number N and the photon number S_p are suppressed by the phase locking effect with undesirable phase relation, resulting in reduced modulation of N and S_p. Thus the noise suppression effect does not work under the condition $nf_M=mf_{ex}$.

References

[1] R.N. Hall, G.E. Fenner, J.D. Kingsley, T.J. Soltys and R.O. Carlson, "Coherent light emission from GaAs junctions", Phys. Rev. Lett., vol. 9, pp. 366-369, 1962.

[2] M. Yamada and Y. Suematsu, "A condition of single longitudinal mode operation in injection lasers with index-guiding structure", IEEE J. Quantum Electron., vol. QE-15, no. 8, pp. 743-749, 1979.

[3] R. Lang and K. Kobayashi, "External optical feedback effects on semiconductor injection laser properties", IEEE J. Quantum Electron., vol. QE-16, no. 3, pp. 347-355, 1980.

[4] M. Yamada and Y. Suematsu, "Analysis of gain suppression in undoped injection lasers", J. Appl. Phys., vol. 52, no. 4, pp. 2653-2664, 1981.

[5] M. Nakamura, K. Aiki, N. Chinone, R. Ito and J. Umeda, "Longitudinal mode behaviors of mode stabilized $Al_xGa_{1-x}As$ injection lasers", J. Appl. Phys., vol. 49, pp. 4644, 1978.

[6] Y. Yamamoto, "AM and FM quantum noise in semiconductor lasers–part I: theoretical analysis", IEEE J. Quantum Electron., vol. QE-19, no. 1, pp. 34-46, 1983.

[7] K. Vahala and A. Yariv, "Semiclassical theory of noise in semiconductor lasers–part II", IEEE J. Quantum Electron., vol. QE-19, no. 6, pp. 1102-1109, 1983.

[8] M. Yamada, "Transverse and longitudinal mode control in semiconductor injection lasers", IEEE J. Quantum Electron., vol. QE-19, no. 9, pp. 1365-1380, 1983.

[9] K. Stubkjaer and M.B. Small, "Feedback-induced noise in index-guided semiconductor lasers and its reduction by modulation", Electronics Letters, vol. 19, no. 10, pp. 388-389, 1983.

[10] P. Spano, S. Piazzolla and M. Tamburrini, "Theory of noise in semiconductor lasers in the presence of optical feedback", IEEE J. Quantum Electron., vol. QE-20, no. 4, pp. 350-357, 1984.

[11] K.E. Stubkjaer and M.B. Small, "Noise properties of semiconductor lasers due to optical feedback", IEEE J. Quantum Electron., vol. QE-20, no. 5, pp. 472-478, 1984.

[12] D. Marcuse, "Computer simulation of laser photon fluctuations: theory of single-cavity laser", IEEE J. Quantum Electron., vol. QE-20, no. 10, pp. 1139-1148, 1984.

[13] A. Ohishi, N. Chinone, M. Ojima and A. Arimoto, "Noise characteristics of high-frequency superposed laser diodes for optical disc systems", Electronics Letters, vol. 20, no. 20, pp. 821-822, 1984.

[14] M. Yamada, "Theory of mode competition noise in semiconductor injection lasers", IEEE J. Quantum Electron., vol. QE-22, no. 7, pp. 1052-1059, 1986.

[15] N. Schunk and K. Petermann, "Numerical analysis of the feedback regimes for a single-mode semiconductor laser with external feedback", IEEE J. Quantum Electron., vol. 24, no. 7, pp. 1242-1247, 1988.

[16] M. Yamada, "Theoretical analysis of nonlinear optical phenomena taking into account the beating vibration of the electron density in semiconductor lasers", J. Appl. Phys., vol. 66, no. 1, pp. 81-89, 1989.

[17] M. Yamada and T. Higashi, "Mechanism of the noise reduction method by superposition of high frequency current for semiconductor injection lasers", IEEE J. Quantum Electron., vol. 27, no. 3, pp. 380-388, 1991.

[18] G.R. Gray, A.T. Ryan, G.P. Agrawal and E.C. Gage, "Optical-feedback-induced chaos and its control in multimode semiconductor lasers", IEEE J. Quantum Electron., vol. 30, no. 3, pp. 668-678, 1994..

[19] H. Kakiuchida and J. Ohtsubo, "Characteristics of a semiconductor laser with external feedback", IEEE J. Quantum Electron., vol. 30, no. 9, pp. 2087-2096, 1994.

[20] K. Petermann, "External optical feedback phenomena in semiconductor lasers", IEEE J. Quantum Electron., vol. 1, no. 2, pp. 480-489, 1995.

[21] M. Yamada, A. Kanamori and S. Takayama, "Experimental evidence of mode competition phenomena on the feedback induced noise in semiconductor lasers", IEICE Trans. Electron., vol. E79-C, no. 12, pp. 1766-1768, 1996.

[22] K. Matsuoka, K. Saeki, E. Teraoka, M. Yamada and Y. Kuwamura, "Quantum noise and feed-back noise in blue-violet InGaN semiconductor lasers", IEICE Trans. Electron., vol. E89-C, no. 3, pp. 437-439, 2006.

[23] K.I. Kallimani and M.J. O'Mahony, "Relative intensity noise for laser diodes with arbitrary amounts of optical feedback", IEEE J. Quantum Electron., vol. 34, no. 8, pp. 1438-1446, 1998.

[24] Y. Takiguchi, Y. Liu and J. Ohtsubo, "Low-frequency fluctuation induced by injection-current modulation in semiconductor lasers with optical feedback", Optics Letters, vol. 23, no. 17, pp. 1369-1371, 1998.

[25] M. Ahmed, M. Yamada and M. Saito, "Numerical modeling of intensity and phase noise in semiconductor lasers", IEEE J. Quantum Electron., vol. 37, no. 12, pp. 1600-1610, 2001.

[26] M. Yamada, S. Yamamura and T. Okamoto, "Characterization of the feedback induced noise in semiconductor laser under superposition of high frequency current", IEICE Trans. Electron., vol. E84-C, no. 10, pp. 1588-1596, 2001.

[27] J.S. Lawrence and D.M. Kane, "Nonlinear dynamics of a laser diode with optical feedback systems subject to modulation", IEEE J. Quantum Electron., vol. 38, no. 2, pp. 185-192, 2002.

[28] C.S. Serrat, S. Prins and R. Vilaseca, "Dynamics and coherence of a multimode semiconductor laser with optical feedback in an intermediate-length external-cavity regime", Physical Review A, vol. 68, no. 053804, pp. 1-7, 2003.

[29] S.G. Abdulrhmann, M. Ahmed, T. Okamoto, W. Ishimori and M. Yamada, "An improved analysis of semiconductor laser dynamics under strong optical feedback", IEEE J. of Selected Topics in Quantum Electron., vol. 9, no. 5, pp. 1265-1274, 2003.

[30] M. Ahmed and M. Yamada, "Field fluctuations and spectral line shape in semiconductor lasers subjected to optical feedback", J. Appl. Phys., vol. 95, no. 12, pp. 7573-7583, 2004.

[31] M. Yamada, K. Saeki, E Teraoka and Y. Kuwamura, "Reduction of the intensity noise by electric positive and negative feedback in blue-violet InGaN semiconductor lasers", IEICE Trans. Electron., vol. E89-C, no. 6, pp. 858-860, 2006.

[32] M. Yamada, M. Huda, E. Teraoka and Y. Kuwamura, "Effective noise reduction by electric positive and negative feedback in semiconductor lasers", IEEE J. Quantum Electron., vol. 45, no. 10, pp. 1248-1254, 2009.

[33] M.C. Soriano, T. Berkvens, G. Van der Sande, G. Verschaffelt, J. Danckaert and I. Fischer, "Interplay of current noise and delayed optical feedback on the dynamics of semiconductor lasers", IEEE J. Quantum Electron., vol. 47, no. 3, pp. 368-374, 2011.

[34] S.M.S. Imran, M. Yamada and Y. Kuwamura, "A theoretical analysis of the optical feedback noise based on multimode model of semiconductor lasers", IEEE J. Quantum Electron., vol. 48, no. 4, pp. 521-527, 2012.

[35] M. Ahmed, N.Z. El-Sayed and H. Ibrahim, "Chaos and noise control by current modulation in semiconductor lasers subject to optical feedback", The European Physical Journal D, vol. 66, no. 141, pp. 1-10, 2012.

[36] S.M.S. Imran and M. Yamada, "Numerical analysis of suppression effects on optical feedback noise by superposition of high frequency current in semiconductor lasers", IEEE J. Quantum Electronics, vol. 49, no. 2, pp. 196-204, 2013.

[37] D. Lenstra and J.S. Cohen, "Feedback noise in single-mode semiconductor lasers", Proceedings of the SPIE, vol. 1376, pp. 245-258, 1991.

[38] L.A. Coldren and S.W. Corzine, "Diode lasers and photonic integrated circuits", John Wiley & Sons, 1995.

[39] J.E. Kitching, "Quantum noise reduction in semiconductor lasers using dispersive optical feedback", PhD thesis, California Institute of Technology, California, 1995.

[40] H. Haken, "Light – Volume 2: Laser light dynamics", NH Publishing, 1985.

[41] M. Ahmed, "Longitudinal mode competition in semiconductor lasers under optical feedback: regime of short external cavity", Opt. Laser Technol., vol. 41, pp. 53-63, 2009.

[42] W.W. Chow and S.W. Koch, "Semiconductor laser-fundamentals: physics of the gain materials", Springer-Verlag Berlin Heidelberg, 1999.

[43] T. Suhara, "Semiconductor laser fundamentals", Marcel Dekker Inc., 2004.

[44] D.E. McCumber, "Intensity fluctuations in the output of cw laser oscillators", Physics Review, vol. 141, pp. 306-322, 1966.

[45] M. Yamada, "Intensity noise in semiconductor lasers", International Journal of Optoelectronics, vol. 10, no. 5, pp. 409-415, 1995.

[46] M. Yamada and M. Suhara, "Analysis of excess noise induced by optical feedback in semiconductor lasers based on mode competition theory", Trans. IEICE, vol. E73, pp. 77-82, 1990.

[47] H.C. Casey and M.B. Panish, “Heterostructure Lasers (Part A and B)”, New York: Academic, 1978.

[48] H. Kressel and J.K. Bulter, “Semiconductor Lasers”, New York: Academic, 1977.

[49] Y. Suematsu and A.R. Adams, “Handbook of semiconductor lasers and photonic integrated circuits”, Chapman & Hall, 1994.

[50] O. Hirota and Y. Suematsu, “Noise properties of injection lasers due to reflected waves”, IEEE J. Quantum Electron., vol. 15, no. 3, pp. 142-149, 1979.

[51] D. Lenstra, B.H. Verbeed and A.J. Den Boef, “Coherence collapse in single-mode semiconductor lasers due to optical feedback”, IEEE J. Quantum Electron., vol. QE-21, no. 6, pp. 674-679, 1985.

[52] H. Olesen, B. Tromborg and J.H. Osmundsen, “Nonlinear dynamics and spectral behavior for an external cavity laser”, IEEE J. Quantum Electron., vol. 22, no. 6, pp. 762-773, 1986.

[53] D. Lasaosa, M. Vega-Leal and C. Fananas, “Improved time-resolved simulation of amplitude and phase fluctuations in semiconductor laser light”, Journal of Opt. Quant. Electron., vol. 40, pp. 367-372, 2008.

[54] D.B. Thomas, W. Luk, P.H.W. Leong and J.D. Villasenor, “Gaussian random number generators”, ACM Comput. Surv., vol. 39, no. 4, Article 11, 2007.

[55] M. Ahmed, M. Yamada and S. Abdulrhmann, “A multimode simulation model of mode-competition low-frequency noise in semiconductor lasers”, Fluctuation and Noise Letters, vol. 1, no. 3, pp. L163-L170, 2001.

[56] P. Bak, T. Bohr and M.H. Jensen, “Mode-locking and the transition to chaos in dissipative systems”, Phys. Scripta, vol. T9, pp. 50-58, 1985.

Appendix-A

Threshold Gain Level G_{th}

From the classical Maxwell's equations we get Eqn. (3-7) as,

$$\nabla^2\vec{E} - \mu_0\sigma\frac{\partial\vec{E}}{\partial t} - \mu_0\varepsilon_0\varepsilon_r\frac{\partial^2\vec{E}}{\partial t^2} = \mu_0\frac{\partial^2\vec{P}}{\partial t^2} \tag{A-1}$$

The laser polarization $\vec{P}$ is introduced with the laser susceptibility χ as,

$$\vec{P} = \varepsilon_0\chi\vec{E} \tag{A-2}$$

From Eqn. (A-1) we get a wave equation for the main component E (E_x or E_y) of the electric field as,

$$\nabla^2 E - \mu_0\varepsilon(x,y)\frac{\partial^2 E}{\partial t^2} = \mu_0\left(\sigma\frac{\partial E}{\partial t} + \varepsilon_0\chi\frac{\partial^2 E}{\partial t^2}\right) \tag{A-3}$$

Electric field in the form of traveling wave propagating along the z direction can be expressed as,

$$E = \sum_p E_p(z)T(x,y)\exp\left[j\left(\omega_p t - \beta_p z\right)\right] + c.c. \tag{A-4}$$

where p is mode number

$E_p(z)$ is amplitude which varies with the propagation

ω_p is angular frequency

$\beta_p = \sqrt{\mu_0\varepsilon_0\varepsilon_r}\,\omega_p$ is propagation constant

$T(x,y)$ is a normalized field distribution function in the transverse plane such that

$$\int_{-\infty}^{+\infty}\int_{-\infty}^{+\infty}\left|T(x,y)\right|^2 dx.dy = 1 \tag{A-5}$$

From Eqn. (A-4) we get,

$$\frac{\partial E}{\partial z} = \exp\left[j\left(\omega_p t - \beta_p z\right)\right]\frac{\partial E_p(z)}{\partial z} + E_p(z)\exp\left[j\left(\omega_p t - \beta_p z\right)\right]\left(-j\beta_p\right)$$

$$\Rightarrow \frac{\partial^2 E}{\partial z^2} = \exp\left[j\left(\omega_p t - \beta_p z\right)\right]\left(-j\beta_p\right)\frac{\partial E_p(z)}{\partial z} + \exp\left[j\left(\omega_p t - \beta_p z\right)\right]\frac{\partial^2 E_p(z)}{\partial z^2}$$

$$+ E_p(z)\exp\left[j\left(\omega_p t - \beta_p z\right)\right]\left(-j\beta_p\right)^2 + \exp\left[j\left(\omega_p t - \beta_p z\right)\right]\left(-j\beta_p\right)\frac{\partial E_p(z)}{\partial z}$$

$$= \left[\frac{\partial^2 E_p(z)}{\partial z^2} - 2j\beta_p\frac{\partial E_p(z)}{\partial z} - \beta_p^2 E_p(z)\right]\exp\left[j\left(\omega_p t - \beta_p z\right)\right] \tag{A-6}$$

$$\frac{\partial E}{\partial t} = E_p(z)\exp\left[j\left(\omega_p t - \beta_p z\right)\right]\left(j\omega_p\right) \tag{A-7}$$

$$\Rightarrow \frac{\partial^2 E}{\partial t^2} = E_p(z)\exp\left[j\left(\omega_p t - \beta_p z\right)\right]\left(j\omega_p\right)^2 \qquad \text{(A-8)}$$

From Eqn. (A-2) we get,

$$\vec{P} = \varepsilon_0 \chi \vec{E} = \varepsilon_0 \chi E_p(z)\exp\left[j\left(\omega_p t - \beta_p z\right)\right]$$

$$\Rightarrow \frac{\partial \vec{P}}{\partial t} = \varepsilon_0 \chi E_p(z)\exp\left[j\left(\omega_p t - \beta_p z\right)\right]\left(j\omega_p\right)$$

$$\Rightarrow \frac{\partial^2 \vec{P}}{\partial t^2} = \varepsilon_0 \chi E_p(z)\exp\left[j\left(\omega_p t - \beta_p z\right)\right]\left(j\omega_p\right)^2 \qquad \text{(A-9)}$$

Using Eqn. (A-1) and (A-6)-(A-9) we obtain,

$$\frac{\partial^2 E_p(z)}{\partial z^2} - 2j\beta_p \frac{\partial E_p(z)}{\partial z} - \beta_p^2 E_p(z) - j\omega_p \mu_0 \sigma E_p(z) + \mu_0 \varepsilon_0 \varepsilon_r \omega_p^2 E_p(z) = -\mu_0 \varepsilon_0 \chi \omega_p^2 E_p(z)$$

$$\Rightarrow -2j\beta_p \frac{\partial E_p(z)}{\partial z} = j\omega_p \mu_0 \sigma E_p(z) - \mu_0 \varepsilon_0 \chi \omega_p^2 E_p(z)$$

[with the assumption $\left|\partial^2 E_p(z)/\partial z^2\right| << \beta_p\, \partial E_p(z)/\partial z$]

$$\Rightarrow \frac{\partial E_p(z)}{\partial z} = -\frac{j}{2}\frac{\omega_p \chi}{c n_r} E_p(z) - \frac{1}{2}\sqrt{\frac{\mu_0}{\varepsilon_0}}\frac{\sigma}{n_r} E_p(z) \qquad \text{(A-10)}$$

The possible solution of Eqn. (A-10) is,

$$E_p(z) = E_p(0)\exp\left(-\frac{j}{2}\frac{\omega_p \chi}{c n_r} z - \frac{1}{2}\sqrt{\frac{\mu_0}{\varepsilon_0}}\frac{\sigma}{n_r} z\right)$$

$$= E_p(0)\exp\left[-\frac{j}{2}\frac{\omega_p \chi}{c n_r}\left(\mathrm{Re}\{\chi\} + j\,\mathrm{Im}\{\chi\}\right) z - \frac{1}{2}\sqrt{\frac{\mu_0}{\varepsilon_0}}\frac{\sigma}{n_r} z\right]$$

$$= E_p(0)\exp\left[\frac{1}{2}\frac{\omega_p}{c n_r}\mathrm{Im}\{\chi\} z - \frac{1}{2}\sqrt{\frac{\mu_0}{\varepsilon_0}}\frac{\sigma}{n_r} z - \frac{j}{2}\frac{\omega_p}{c n_r}\mathrm{Re}\{\chi\} z\right] \qquad \text{(A-11)}$$

Now Eqn. (A-4) can be rewritten as,

$$\vec{E} = E_p(0)\exp\left[\frac{1}{2}\frac{\omega_p}{c n_r}\mathrm{Im}\{\chi\} z - \frac{1}{2}\sqrt{\frac{\mu_0}{\varepsilon_0}}\frac{\sigma}{n_r} z - \frac{j}{2}\frac{\omega_p}{c n_r}\mathrm{Re}\{\chi\} z + j\left(\omega_p t - \beta_p z\right)\right]$$

$$\approx E_p(0)\exp\left[\frac{1}{2}\frac{\omega_p}{c n_r}\mathrm{Im}\{\chi\} z - \frac{1}{2}\sqrt{\frac{\mu_0}{\varepsilon_0}}\frac{\sigma}{n_r} z + j\left(\omega_p t - \beta_p z\right)\right]$$

$$\left[\varepsilon_r >> \mathrm{Re}\{\chi\} \Rightarrow \beta_p >> \frac{1}{2}\frac{\omega_p}{c n_r}\mathrm{Re}\{\chi\}\right]$$

$$\Rightarrow \vec{E} = E_p(0)\exp\left[\frac{1}{2}\left(\frac{n_r}{c} g - k\right) z + j\left(\omega_p t - \beta_p z\right)\right] \qquad \text{(A-12)}$$

where $k = \sqrt{\frac{\mu_0}{\varepsilon_0}}\frac{\sigma}{n_r}$ is the internal loss coefficient and

$g \approx \frac{\omega_p}{n_r^2}\mathrm{Im}\{\chi\}$ is the threshold gain coefficient.

The forward traveling wave propagating along z-direction is represented by

$$E_p^{(+)}(z) = E_p^{(+)}(0)\exp\left[\frac{1}{2}\left(\frac{n_r}{c}g - k\right)z + j\left(\omega_p t - \beta_p z\right)\right] \tag{A-13}$$

and the backward traveling wave is,

$$E_p^{(-)}(z) = E_p^{(-)}(L)\exp\left[\frac{1}{2}\left(\frac{n_r}{c}g - k\right)(L - z) + j\left(\omega_p t - \beta_p\{L - z\}\right)\right] \tag{A-14}$$

where $E_p^{(+)}(0)$ and $E_p^{(-)}(L)$ are amplitudes of the forward and backward propagating waves at z=0 and z=L, respectively. The boundary conditions at the mirrors are,

$$E_p^{(-)}(L) = \sqrt{R_b}E_p^{(+)}(L) \tag{A-15}$$

$$E_p^{(-)}(0) = \sqrt{R_f}E_p^{(-)}(0) \tag{A-16}$$

From Eqn. (A-13)-(A-15) we obtain,

$$E_p^{(-)}(L)\exp\left[\frac{1}{2}\left(\frac{n_r}{c}g - k\right)(L - L) + j\left(\omega_p t - \beta_p\{L - L\}\right)\right]$$

$$= \sqrt{R_b}E_p^{(+)}(0)\exp\left[\frac{1}{2}\left(\frac{n_r}{c}g - k\right)L + j\left(\omega_p t - \beta_p L\right)\right]$$

$$\Rightarrow E_p^{(-)}(L) = \sqrt{R_b}E_p^{(+)}(0)\exp\left[\frac{1}{2}\left(\frac{n_r}{c}g - k\right)L - j\beta_p L\right] \tag{A-17}$$

From Eqn. (A-13), (A-14), (A-16) and (A-17) we get,

$$E_p^{(+)}(0)\exp\left[\frac{1}{2}\left(\frac{n_r}{c}g - k\right).0 + j\left(\omega_p t - \beta_p.0\right)\right]$$

$$= \sqrt{R_b}E_p^{(-)}(L)\exp\left[\frac{1}{2}\left(\frac{n_r}{c}g - k\right)L + j\left(\omega_p t - \beta_p L\right)\right]$$

$$\Rightarrow E_p^{(+)}(0) = \sqrt{R_f}\sqrt{R_b}E_p^{(+)}(0)\exp\left[\left(\frac{n_r}{c}g - k\right)L - 2j\beta_p L\right]$$

$$\Rightarrow \exp\left[\left(\frac{n_r}{c}g - k\right)L\right] = \frac{1}{\sqrt{R_f R_b}}$$

$$\Rightarrow \left(\frac{n_r}{c} g - k \right) L = \ln \frac{1}{\sqrt{R_f R_b}} = \frac{1}{2} \ln \frac{1}{R_f R_b}$$

$$\Rightarrow g = \frac{c}{n_r} \left[k + \frac{1}{2L} \ln \frac{1}{R_f R_b} \right]$$

$$\Rightarrow G_{th} = \frac{c}{n_r} \left[k + \frac{1}{2L} \ln \frac{1}{R_f R_b} \right] \qquad \text{(A-18)}$$

Appendix-B

First & Second Order Density Matrix Elements

Dynamic equation of the density matrix in a semiconductor laser has been given as,

$$\frac{d\rho}{dt} = \frac{1}{j\hbar}[(H_0 - RE), \rho] - \frac{1}{2}\left[\left(\rho - \tilde{\tilde{\rho}}\right)\Gamma_{in} + \Gamma_{in}\left(\rho - \tilde{\tilde{\rho}}\right)\right] - \frac{1}{2}\left[(\rho - \tilde{\rho})\Gamma_s + \Gamma_s(\rho - \tilde{\rho})\right] + \Lambda \quad \text{(B-1)}$$

where H_0 is the principle Hamiltonian

R is the dipole moment that picks up a spatial component in the same direction with the electric field E

$\tilde{\rho}$ is the electron distribution at thermal equilibrium

$\tilde{\tilde{\rho}}$ is the electron distribution at quasi thermal equilibrium

Γ_s is an operator giving the spontaneous emission

Γ_{in} is an operator for the intraband relaxation effect

Λ is an operator that describes the current injection.

When we consider RE coherent phase is included; but in case of only E no phase information is involved. So the density matrix elements can be written with the perturbation term RE as,

$$\langle b|\rho|b\rangle = \rho_{bb} = \rho_{bb}^{(0)} + \rho_{bb}^{(2)}\left(R^2E^2\right) + \ldots \quad \text{(B-2)}$$

$$\langle a|\rho|b\rangle = \rho_{ab} = \rho_{ab}^{(1)}(RE) + \rho_{ab}^{(3)}\left(R^3E^3\right) + \ldots \quad \text{(B-3)}$$

Here, the diagonal element ρ_{bb} of the density matrix indicates occupation probability of the electron at the energy level in the conduction band $|b\rangle$ and the off diagonal element ρ_{ab} indicates the polarization in which the electron spreads over the energy level in the valence band $|a\rangle$ and that in the conduction band $|b\rangle$.

Now for each power order of RE we have the following relations,

$$\frac{d\rho_{bb}^{(0)}}{dt} = \frac{\tilde{\tilde{\rho}}_b - \rho_{bb}^{(0)}}{\tau_b} + \frac{\tilde{\rho}_b - \rho_{bb}^{(0)}}{\tau_s} + \Lambda_b \quad \text{(B-4)}$$

$$\frac{d\rho_{bb}^{(2l)}}{dt} = \frac{E}{j\hbar}\left(\rho_{ba}^{(2l-1)}R_{ab} - \rho_{ab}^{(2l-1)}R_{ba}\right) - \rho_{bb}^{(2l)}\left(\frac{1}{\tau_b} + \frac{1}{\tau_s}\right) \text{ for } l=1,2,3,\ldots \quad \text{(B-5)}$$

$$\frac{d\rho_{ab}^{(2l+1)}}{dt} = \left(j\omega_{ba} - \frac{1}{\tau_{in}}\right)\rho_{ab}^{(2l+1)} + R_{ab}\frac{E}{\hbar}j\left(\rho_{bb}^{(2l)} - \rho_{aa}^{(2l)}\right) \text{ for } l=0,1,2,\ldots \quad \text{(B-6)}$$

where τ_s is the electron lifetime whose value is in the order of 10^{-9}s and τ_b is the intraband relaxation time in the order of 10^{-13}s.

From Eqn. (B-6), dynamic equation of the first order density matrix elements can be written as,

$$\frac{d\rho_{ab}^{(1)}}{dt} = \left(j\omega_{ba} - \frac{1}{\tau_{in}} \right) \rho_{ab}^{(1)} + j\left(\rho_{bb}^{(0)} - \rho_{aa}^{(0)} \right) R_{ab} \frac{1}{\hbar} \sum_{p=-\infty}^{+\infty} E_p \exp\left(j\omega_m t \right) \qquad \text{(B-7)}$$

Let, $\rho_{ab}^{(1)} = u(t) \exp\left[\left(j\omega_{ba} - \frac{1}{\tau_{in}} \right) t \right]$

$$\Rightarrow \frac{d\rho_{ab}^{(1)}}{dt} = \frac{\partial u}{\partial t} \exp\left[\left(j\omega_{ba} - \frac{1}{\tau_{in}} \right) t \right] + \left(j\omega_{ba} - \frac{1}{\tau_{in}} \right) u(t) \exp\left[\left(j\omega_{ba} - \frac{1}{\tau_{in}} \right) t \right]$$

$$\Rightarrow \frac{\partial u}{\partial t} = j\left(\rho_{bb}^{(0)} - \rho_{aa}^{(0)} \right) \frac{R_{ab}}{\hbar} \sum_p E_p \exp\left[\left\{ j\left(\omega_p - \omega_{ba} \right) + \frac{1}{\tau_{in}} \right\} t \right]$$

$$\Rightarrow u(t) = j\left(\rho_{bb}^{(0)} - \rho_{aa}^{(0)} \right) \frac{R_{ab}}{\hbar} \sum_p \frac{E_p \exp\left[\left\{ j\left(\omega_p - \omega_{ba} \right) + \frac{1}{\tau_{in}} \right\} t \right]}{j\left(\omega_p - \omega_{ba} \right) + \frac{1}{\tau_{in}}} \qquad \text{(B-8)}$$

Hence, the first order density matrix element becomes

$$\rho_{ab}^{(1)} = j\left(\rho_{bb}^{(0)} - \rho_{aa}^{(0)} \right) \frac{R_{ab}}{\hbar} \sum_p \frac{E_p \exp\left(j\omega_p t \right)}{j\left(\omega_p - \omega_{ba} \right) + \frac{1}{\tau_{in}}} \qquad \text{(B-9)}$$

Now from Eqn. (B-5), dynamic equation of the second order density matrix element can be written as,

$$\frac{d\rho_{bb}^{(2)}}{dt} = \left(\rho_{ba}^{(1)} R_{ab} - \rho_{ab}^{(1)} R_{ba} \right) \frac{1}{j\hbar} \sum_q E_q \exp\left(j\omega_q t \right) - \rho_{bb}^{(2)} \left(\frac{1}{\tau_b} + \frac{1}{\tau_s} \right)$$

$$= -\frac{1}{\hbar^2} \left(\rho_{bb}^{(0)} - \rho_{aa}^{(0)} \right) \left| R_{ba} \right|^2 \sum_p \sum_q \left\{ \frac{E_p^* E_q \exp\left\{ j\left(\omega_q - \omega_p \right) t \right\}}{j\left(\omega_{ba} - \omega_p \right) + \frac{1}{\tau_{in}}} \right.$$

$$\left. + \frac{E_p E_q \exp\left\{ j\left(\omega_p + \omega_q \right) t \right\}}{j\left(\omega_p - \omega_{ba} \right) + \frac{1}{\tau_{in}}} \right\} - \rho_{bb}^{(2)} \left(\frac{1}{\tau_b} + \frac{1}{\tau_s} \right)$$

$$= -\frac{1}{\hbar^2}\left(\rho_{bb}^{(0)} - \rho_{aa}^{(0)}\right)\left|R_{ba}\right|^2 \sum_p \sum_q \left\{ \frac{E_p^* E_q \exp\left\{j\left(\omega_q - \omega_p\right)t\right\}}{j\left(\omega_{ba} - \omega_p\right) + \frac{1}{\tau_{in}}} + c.c. \right\} \quad \text{(B-9)}$$

$$- \rho_{bb}^{(2)}\left(\frac{1}{\tau_b} + \frac{1}{\tau_s}\right)$$

Let, $\rho_{bb}^{(2)} = u(t)\exp\left\{-\left(\frac{1}{\tau_b} + \frac{1}{\tau_s}\right)t\right\}$

$$\Rightarrow \frac{d\rho_{bb}^{(2)}}{dt} = \frac{\partial u}{\partial t}\exp\left\{-\left(\frac{1}{\tau_b} + \frac{1}{\tau_s}\right)t\right\} - \left(\frac{1}{\tau_b} + \frac{1}{\tau_s}\right)u(t)\exp\left\{-\left(\frac{1}{\tau_b} + \frac{1}{\tau_s}\right)t\right\}$$

$$\Rightarrow \frac{\partial u}{\partial t} = -\frac{1}{\hbar^2}\left(\rho_{bb}^{(0)} - \rho_{aa}^{(0)}\right)\left|R_{ba}\right|^2 \sum_p \sum_q \left\{ \frac{E_p E_q^* \exp\left[\left\{j\left(\omega_p - \omega_q\right) + \left(\frac{1}{\tau_b} + \frac{1}{\tau_s}\right)\right\}t\right]}{j\left(\omega_p - \omega_{ba}\right) + \frac{1}{\tau_{in}}} + c.c. \right\}$$

$$\Rightarrow u(t) = -\frac{1}{\hbar^2}\left(\rho_{bb}^{(0)} - \rho_{aa}^{(0)}\right)\left|R_{ba}\right|^2$$

$$\sum_p \sum_q \frac{E_p E_q^* \exp\left[\left\{j\left(\omega_p - \omega_q\right) + \left(\frac{1}{\tau_b} + \frac{1}{\tau_s}\right)\right\}t\right]}{\left\{j\left(\omega_p - \omega_{ba}\right) + \frac{1}{\tau_{in}}\right\}\left\{j\left(\omega_p - \omega_q\right) + \left(\frac{1}{\tau_b} + \frac{1}{\tau_s}\right)\right\}} \quad \text{(B-10)}$$

Now the second order density matrix element becomes,

$$\rho_{bb}^{(2)} = -\frac{1}{\hbar^2}\left(\rho_{bb}^{(0)} - \rho_{aa}^{(0)}\right)\left|R_{ba}\right|^2$$

$$\sum_p \sum_q \left[\frac{E_p E_q^* \exp\left\{j\left(\omega_p - \omega_q\right)t\right\}}{\left\{j\left(\omega_p - \omega_{ba}\right) + \frac{1}{\tau_{in}}\right\}\left\{j\left(\omega_p - \omega_q\right) + \left(\frac{1}{\tau_b} + \frac{1}{\tau_s}\right)\right\}} + c.c. \right] \quad \text{(B-11)}$$

Appendix-C

Derivation of Dynamic Equation for Carrier Numbers

Variation of electron density has been written in Eqn. (3-46) as,

$$\frac{dN}{dt} = -\sum_p \sum_q \frac{\varepsilon_0 \kappa}{\hbar} \left\{ \left[(1 + j\alpha)N - N_g - b(\lambda_p - \lambda_0)^2 \right] E_p E_q^* \exp\left[j(\omega_p - \omega_q)t \right] + c.c. \right\} - \frac{N}{\tau_s} + \frac{I}{eV} \tag{C-1}$$

Mode numbers p and q shown in Eqn. (C-1) mean to scan all possible modes in the laser. However, for simple discussion we can restrict these modes to specific two modes p and q here. Therefore, let

$$\Omega = \omega_q - \omega_p \tag{C-2}$$

Then Eqn. (C-1) can be simply written in terms of carrier numbers as,

$$\begin{aligned} \frac{dN}{dt} = & -\frac{1}{V} \frac{\varepsilon_0 \kappa}{\hbar} \left[\left\{ (1 + j\alpha)N - N_g - bV(\lambda_p - \lambda_0)^2 \right\} \left\{ |E_p|^2 + E_p E_q^* \exp(-j\Omega t) \right\} \right. \\ & \left. + \left\{ (1 + j\alpha)N - N_g - bV(\lambda_q - \lambda_0)^2 \right\} \left\{ |E_q|^2 + E_q E_p^* \exp(j\Omega t) \right\} + c.c. \right] \\ & - \frac{N}{\tau_s} + \frac{I}{e} \\ \approx & -\frac{1}{V} \frac{2\varepsilon_0 \kappa}{\hbar} \left[\left\{ N - N_g - bV(\lambda_p - \lambda_0)^2 \right\} |E_p|^2 + \left\{ N - N_g - bV(\lambda_q - \lambda_0)^2 \right\} |E_q|^2 \right] \\ & - \frac{N}{\tau_s} + \frac{I}{e} \end{aligned}$$

If electric field is expressed as standing wave in the cavity with the spatial distribution function as given in Eqn. (3-41), we have

$$\frac{dN}{dt} = -\frac{1}{V} \frac{2\varepsilon_0 \kappa}{\hbar} \sum_p \left\{ N - N_g - bV(\lambda_p - \lambda_0)^2 \right\} |\overline{E}_p|^2 |\Phi_p(\vec{r})|^2 - \frac{N}{\tau_s} + \frac{I}{e} \tag{C-3}$$

By taking spatial integration over the active region and using quantization of the lasing field introduced in Eqn. (3-49), we get

$$\begin{aligned} \frac{dN}{dt} &= -\frac{1}{V} \frac{2\varepsilon_0 \kappa}{\hbar} \xi \sum_p \frac{\hbar \omega_p}{2\varepsilon} \left\{ N - N_g - bV(\lambda_p - \lambda_0)^2 \right\} S_p - \frac{N}{\tau_s} + \frac{I}{e} \\ &= -\frac{1}{V} \xi \sum_p \frac{\kappa \omega_p}{n_r^2} \left\{ N - N_g - bV(\lambda_p - \lambda_0)^2 \right\} S_p - \frac{N}{\tau_s} + \frac{I}{e} \\ &= -\sum_p \frac{a\xi}{V} \left\{ N - N_g - bV(\lambda_p - \lambda_0)^2 \right\} S_p - \frac{N}{\tau_s} + \frac{I}{e} \\ &= -\sum_p A_p S_p - \frac{N}{\tau_s} + \frac{I}{e} \end{aligned} \tag{C-4}$$

where coefficient a, known as gradient of the gain peak, is defined as

$$a \equiv \frac{\kappa \omega_p}{n_r^2} \tag{C-5}$$

and A_p is the first order linear gain coefficient as introduced in (3-25).

Appendix-D

Varying Electron Density & Field Spatial Distribution

The spatial distribution of electric field with cavity length L is given by,

$$\Phi_p(\vec{r}) = \sqrt{\frac{2}{L}} T(x,y)\cos(\beta_p z) \tag{D-1}$$

where $T(x,y)$ indicates the two-dimensional field distribution in the transverse cross-section in a cavity with width W and thickness d.

Assuming that the field is well confined in the lateral x-direction in Fig. 2-1 and penetrates into the cladding region along the thickness y-direction, we can write

$$\begin{aligned}\iiint |\Phi_p(\vec{r})|^2 dxdydz &= \frac{2}{L}\int_0^L \int_{-d/2}^{d/2}\int_{-W/2}^{W/2} |T(x,y)|^2 \cos^2(\beta_p z)dxdydz \\ &= \frac{2}{L}\int_0^L \xi\cos^2(\beta_p z)dz\end{aligned} \tag{D-2}$$

where $\xi = \int_{-d/2}^{d/2}\int_{-W/2}^{W/2} |T(x,y)|^2 dxdy$ is the confinement factor.

For different modes p and q, assuming same initial phase

$$\begin{aligned}&\Phi_p(\vec{r})\Phi_q^*(\vec{r})\exp\{j(\omega_p-\omega_q)t\} \\ &= \frac{2}{L}|T(x,y)|^2\cos(\beta_p z)\cos(\beta_q z)\exp\{j(\omega_p-\omega_q)t\} \\ &= \frac{2}{L}|T(x,y)|^2\frac{1}{2}\{\cos[(\beta_p-\beta_q)z]+\cos[(\beta_p+\beta_q)z]\}\exp\{j(\omega_p-\omega_q)t\} \\ &\approx \frac{1}{L}|T(x,y)|^2\cos\{(\beta_p-\beta_q)z\}\exp\{j(\omega_p-\omega_q)t\}\end{aligned} \tag{D-3}$$

Wavelength of $\cos[(\beta_p+\beta_q)z]$ is very short compared to diffusion length and hence been neglected here.

Now we recall the equation for varying electron density caused by the beating effect given in Eqn. (3-65) as,

$$N = \overline{N} + \{N_1\cos[(\beta_p-\beta_q)z]\exp[j(\omega_p-\omega_q)t] + c.c.\}$$

$$\begin{aligned}\Rightarrow \frac{dN}{dt} &= j(\omega_p-\omega_q)N_1\cos[(\beta_p-\beta_q)z]\exp[j(\omega_p-\omega_q)t] + c.c. \\ &= -\frac{a}{2}\{[(1+j\alpha)N - N_g - b(\lambda_p-\lambda_0)^2]\sqrt{S_pS_q}\Phi_p(\vec{r})\Phi_q^*(\vec{r}) \\ &\qquad \exp[j(\omega_p-\omega_q)t] + c.c.\} - \frac{N}{\tau_s} + \frac{I}{eV}\end{aligned}$$

$$\Rightarrow \frac{dN}{dt} = -a\left\{\left[N_0 - N_g - b\left(\lambda_p - \lambda_0\right)^2\right]\sqrt{S_p S_q}\,\Phi_p(\vec{r})\Phi_q^*(\vec{r})\exp\left[j\left(\omega_p - \omega_q\right)t\right]\right.$$
$$\left. + N_1\cos\left[\left(\beta_p - \beta_q\right)z\right]\exp\left[j\left(\omega_p - \omega_q\right)t\right]\left[S_p\left|\Phi_p(\vec{r})\right|^2 + S_q\left|\Phi_q(\vec{r})\right|^2\right]\right\}$$
$$- \frac{N_0}{\tau_s} - \frac{N_1}{\tau_s}\cos\left[\left(\beta_p - \beta_q\right)z\right]\exp\left[j\left(\omega_p - \omega_q\right)t\right] + \frac{I}{eV}$$
$$= \left[-a\left\{\left[N_0 - N_g - b\left(\lambda_p - \lambda_0\right)^2\right]\sqrt{S_p S_q}\,\frac{1}{L}\left|T(x,y)\right|^2 + \frac{N_1}{L}\left|T(x,y)\right|^2\left(S_p + S_q\right)\right\}\right.$$
$$\left. - \frac{N_1}{\tau_s}\right]\cos\left[\left(\beta_p - \beta_q\right)z\right]\exp\left[j\left(\omega_p - \omega_q\right)t\right]$$

$$\Rightarrow N_1\left[j\left(\omega_p - \omega_q\right) + \frac{1}{\tau_s} + \frac{a}{L}\left|T(x,y)\right|^2\left(S_p + S_q\right)\right] =$$
$$-a\left[N_0 - N_g - b\left(\lambda_p - \lambda_0\right)^2\right]\sqrt{S_p S_q}\,\frac{1}{L}\left|T(x,y)\right|^2$$

$$\Rightarrow N_1 \approx \frac{-\frac{a}{L}\left[N_0 - N_g - b\left(\lambda_p - \lambda_0\right)^2\right]\sqrt{S_p S_q}\left|T(x,y)\right|^2}{j\left(\omega_p - \omega_q\right) + \frac{1}{\tau_s} + \frac{a}{L}\left(S_p + S_q\right)\left|T(x,y)\right|^2} \qquad \text{(D-4)}$$

The parameter $T(x,y)$ in Eqn. (3-66) and (D-1) can be defined as

$$T(x,y) = \sqrt{\frac{2}{W}}\cos\left(\frac{x}{W}\pi\right) \qquad \text{(D-5)}$$

$$\int_{-W/2}^{W/2}\left|T(x,y)\right|^2 dx = \int_{-W/2}^{W/2}\frac{2}{W}\cos^2\left(\frac{x}{W}\pi\right)dx = \frac{1}{W}\int_{-W/2}^{W/2}\left\{1 + \cos\left(\frac{2x}{W}\pi\right)\right\}dx = 1 \qquad \text{(D-6)}$$

$$\int_{-W/2}^{W/2}\left|T(x,y)\right|^4 dx = \frac{4}{W^2}\int_{-W/2}^{W/2}\cos^4\left(\frac{x}{W}\pi\right)dx$$
$$= \frac{1}{W^2}\int_{-W/2}^{W/2}\left\{1 + \cos^2\left(\frac{2x}{W}\pi\right)\right\}^2 dx$$
$$= \frac{1}{W^2}\int_{-W/2}^{W/2}\left\{1 + 2\cos\left(\frac{2x}{W}\pi\right) + \cos^2\left(\frac{2x}{W}\pi\right)\right\}dx$$
$$= \frac{1}{W^2}\int_{-W/2}^{W/2}\left\{1 + 2\cos\left(\frac{2x}{W}\pi\right) + \frac{1}{2} + \frac{1}{2}\cos\left(\frac{4x}{W}\pi\right)\right\}dx$$
$$= \frac{3}{2W} \qquad \text{(D-7)}$$

$$\int_{-d/2}^{d/2}\left|T(x,y)\right|^2 dy = \xi \qquad \text{(D-8)}$$

$$\int_{-d/2}^{d/2}\left|T(x,y)\right|^4 dy \approx \frac{\xi^2}{d} \qquad \text{(D-9)}$$

Combining Eqn. (D-7) and (D-9) gives,

$$\int_{-d/2}^{d/2}\int_{-W/2}^{W/2}\left|T(x,y)\right|^4 dxdy = \frac{3\xi^2}{2dW} \tag{D-10}$$

$$\begin{aligned}
\left|\Phi_p(\vec{r})\Phi_q(\vec{r})\right|^2 &= \frac{4}{L^2}\left|T(x,y)\right|^4 \cos^2\left(\beta_p z\right)\cos^2\left(\beta_q z\right) \\
&= \frac{4}{L^2}\left|T(x,y)\right|^4 \frac{1}{2}\left[1+\cos\left(2\beta_p z\right)\right]\frac{1}{2}\left[1+\cos\left(\beta_q z\right)\right] \\
&= \frac{1}{L^2}\left|T(x,y)\right|^4 \left\{1+\cos\left(2\beta_p z\right)+\cos\left(2\beta_q z\right)+\cos\left(2\beta_p z\right)\cos\left(2\beta_q z\right)\right\} \\
&= \frac{1}{L^2}\left|T(x,y)\right|^4 \left\{1+\cos\left(2\beta_p z\right)+\cos\left(2\beta_q z\right)\right. \\
&\qquad \left. +\frac{1}{2}\left[\cos\left\{2\left(\beta_p-\beta_q\right)z\right\}+\cos\left\{2\left(\beta_p+\beta_q\right)z\right\}\right]\right\}
\end{aligned}$$

$$\begin{aligned}
\int\left|\Phi_p(\vec{r})\Phi_q(\vec{r})\right|^2 d^3\vec{r} &= \int_x\int_y\left|T(x,y)\right|^4 dxdy \times \frac{1}{L^2}\int_0^L\left\{1+\cos\left(2\beta_p z\right)+\cos\left(2\beta_q z\right)\right. \\
&\qquad \left. +\frac{1}{2}\left[\cos\left\{2\left(\beta_p-\beta_q\right)z\right\}+\cos\left\{2\left(\beta_p+\beta_q\right)z\right\}\right]\right\}dz \\
&\approx \frac{3\xi^2}{2dW}.\frac{1}{L}\left(1+\frac{1}{2}\delta_{pq}\right)
\end{aligned} \tag{D-11}$$